

Technical Report

# CAUCHARI JV PROJECT

Jujuy Province, Argentina

## UPDATED MINERAL RESOURCE ESTIMATE

Prepared for:



by:

Frits Reidel, CPG



Effective Date: April 19, 2019

## TABLE OF CONTENTS

|          |   |           |
|----------|---|-----------|
| <b>1</b> | <b>SUMMARY .....</b>  | <b>6</b>  |
| 1.1.     | Terms of reference .....  | 6         |
| 1.2.     | Property description and ownership .....  | 6         |
| 1.3.     | Physiography, climate and access .....  | 6         |
| 1.4.     | Exploration and drilling .....  | 7         |
| 1.5.     | Geology and mineralization .....  | 8         |
| 1.5.1.   | Geology .....   | 8         |
| 1.5.2.   | Mineralization .....  | 8         |
| 1.6.     | Status of exploration, development and operations .....                                   | 9         |
| 1.7.     | Brine resource estimate .....   | 9         |
| 1.8.     | Conclusions and recommendations .....   | 11        |
| <b>2</b> | <b>INTRODUCTION .....</b>   | <b>12</b> |
| 2.1.     | Terms of reference .....  | 12        |
| 2.2.     | Sources of Information .....  | 12        |
| 2.3.     | Units .....   | 13        |
| <b>3</b> | <b>RELIANCE ON OTHER EXPERTS .....</b>  | <b>14</b> |
| <b>4</b> | <b>PROPERTY LOCATION AND DESCRIPTION .....</b>  | <b>15</b> |
| 4.1.     | Location .....  | 15        |
| 4.2.     | Exploration and exploitation licenses .....   | 15        |
| 4.2.1.   | Licenses & coordinate system .....  | 15        |
| 4.2.2.   | Expenditure commitments for Minas .....   | 18        |
| 4.2.3.   | The Cauchari tenement package .....   | 18        |
| 4.2.4.   | Surface rights and legal access .....   | 18        |
| 4.3.     | Environmental liabilities .....   | 19        |
| 4.4.     | Permit status .....   | 20        |
| 4.5.     | Royalties .....   | 20        |
| 4.6.     | Ownership of the Cauchari JV .....  | 20        |
| 4.7.     | Other Significant Factors and Risks .....   | 20        |
| <b>5</b> | <b>ACCESSIBILITY, CLIMATE, LOCAL RESOURCES, INFRASTRUCTURE AND<br/>PHYSIOGRAPHY .....</b> | <b>21</b> |
| 5.1.     | Accessibility, local resources and infrastructure .....                                   | 21        |
| 5.2.     | Local population centers and accommodation .....  | 21        |
| 5.3.     | Physiography .....  | 21        |
| 5.4.     | Climate .....   | 24        |
| 5.4.1.   | Rainfall .....  | 25        |
| 5.4.2.   | Temperature .....   | 26        |
| 5.4.3.   | Wind .....  | 27        |
| 5.4.4.   | Evaporation .....   | 27        |
| 5.5.     | Vegetation .....  | 27        |
| 5.5.1.   | Low lying areas in the vicinity of water .....  | 27        |
| 5.5.2.   | Mixed steppes .....   | 28        |
| 5.5.3.   | Bushy steppes .....   | 28        |
| <b>6</b> | <b>HISTORY .....</b>  | <b>29</b> |
| 6.1.     | Historical mining and exploration activities .....  | 29        |
| 6.2.     | History of Cauchari JV ownership .....  | 29        |
| 6.3.     | 2009-2011 SAS exploration on Cauchari .....   | 29        |

|              |   |           |
|--------------|---|-----------|
| <b>7</b>     | <b>GEOLOGICAL SETTING AND MINERALIZATION .....</b>                        | <b>30</b> |
| 7.1.         | Regional geology .....  | 30        |
| 7.1.1.       | Jurassic-Cretaceous .....   | 30        |
| 7.1.2.       | Late Cretaceous to Eocene .....   | 30        |
| 7.1.3.       | Oligocene to Miocene Volcanism .....                                      | 30        |
| 7.1.4.       | Oligocene to Miocene Sedimentation .....                                  | 31        |
| 7.1.5.       | Pliocene-Quaternary .....   | 31        |
| 7.2.         | Local geology .....   | 32        |
| 7.2.1.       | Archibarca fan unit .....   | 36        |
| 7.2.2.       | West Fan unit .....   | 37        |
| 7.2.3.       | East Fan unit .....   | 38        |
| 7.2.4.       | Lower Sand unit .....   | 39        |
| 7.2.5.       | Clay unit .....   | 40        |
| 7.2.6.       | Halite unit .....   | 41        |
| 7.3.         | Mineralization .....  | 42        |
| <b>8</b>     | <b>DEPOSIT TYPE.....</b>  | <b>45</b> |
| 8.1.         | General .....   | 45        |
| 8.2.         | Hydrogeology .....  | 46        |
| 8.3.         | Drainable Porosity .....  | 47        |
| 8.4.         | Permeability .....  | 48        |
| <b>9</b>     | <b>EXPLORATION .....</b>  | <b>49</b> |
| 9.1.         | Geophysical Surveys - 2009 .....  | 49        |
| 9.2.         | Gravity Survey - 2009 .....   | 49        |
| 9.2.1.       | Data acquisition .....  | 49        |
| 9.2.2.       | Data processing .....   | 49        |
| 9.2.3.       | Gravity data modelling .....  | 53        |
| 9.3.         | Audio Magnetotelluric Survey - 2009 .....                                 | 53        |
| 9.3.1.       | <b>Data acquisition</b> .....   | 53        |
| 9.3.2.       | Data processing and modelling .....                                       | 54        |
| 9.3.3.       | <b>Model output and interpretation</b> .....                              | 54        |
| 9.4.         | Gravity Survey - 2016 .....   | 55        |
| 9.5.         | TEM Survey - 2018 .....   | 55        |
| <b>10</b>    | <b>DRILLING.....</b>  | <b>56</b> |
| 10.1.        | Overview .....  | 56        |
| <b>10.2.</b> | <b>Exploration drilling .....</b>   | <b>56</b> |
| <b>10.3.</b> | <b>Production well drilling .....</b>                                     | <b>60</b> |
| <b>10.4.</b> | <b>Pumping tests .....</b>  | <b>60</b> |
| 10.4.1.      | 48-hr pumping tests .....   | 60        |
| 10.4.2.      | 30-day pumping tests .....  | 60        |
| <b>11</b>    | <b>SAMPLE PREPARATION, ANALYSES AND SECURITY.....</b>                     | <b>62</b> |
| 11.1.        | Sampling methods .....  | 62        |
| 11.1.1.      | Core sample collection, handling and transportation .....                 | 62        |
| 11.1.2.      | <b>Drainable porosity sample preparation, handling and security</b> ..... | 62        |
| 11.1.3.      | <b>Brine sample preparation, handling and security</b> .....              | 62        |
| 11.2.        | <b>Drainable porosity analysis and quality control results</b> .....      | 63        |
| 11.2.1.      | <b>British Geological Survey - 2011</b> .....                             | 63        |
| 11.2.2.      | <b>GeoSystems Analyses – 2017/8</b> .....                                 | 64        |
| 11.2.3       | <b>Drainable porosity quality control - 2017/8</b> .....                  | 65        |

|              |  |            |
|--------------|--|------------|
| <b>11.3.</b> | <b>Brine analysis and quality control results</b>                        | <b>67</b>  |
| 11.3.1.      | Analytical methods   | 67         |
| 11.3.2.      | Analytical quality control - 2011 Program                                | 68         |
| 11.3.3.      | Analytical quality control - 2017/18 program                             | 70         |
| 11.3.4.      | Precision (Duplicates)   | 73         |
| 11.3.5.      | Accuracy (Standards)   | 73         |
| 11.3.6.      | Contamination (Blanks)   | 75         |
| <b>12</b>    | <b>DATA VERIFICATION</b>   | <b>76</b>  |
| <b>13</b>    | <b>MINERAL PROCESSING AND METALLURGICAL TESTING</b>                      | <b>77</b>  |
| <b>14</b>    | <b>MINERAL RESOURCE ESTIMATES</b>  | <b>78</b>  |
| 14.1         | Overview   | 78         |
| 14.2         | Resource model boundary and domains                                      | 78         |
| 14.3         | Specific yield   | 79         |
| 14.4         | Brine Concentration  | 80         |
| 14.5         | Resource Category  | 81         |
| 14.5.1       | CIM definitions  | 81         |
| 14.5.2       | Resource category definition   | 82         |
| 14.6         | Resource modeling methodology and construction                           | 83         |
| 14.6.1       | Overview   | 83         |
| 14.6.2       | Exploratory data analysis  | 84         |
| 14.6.3       | Variography  | 86         |
| 14.6.4       | Kriging estimation of Li and K concentrations                            | 90         |
| 14.7         | Grade estimate   | 92         |
| 14.8         | Resource estimate  | 94         |
| <b>15</b>    | <b>MINERAL RESERVE ESTIMATES</b>   | <b>95</b>  |
| <b>16</b>    | <b>MINING METHODS</b>  | <b>96</b>  |
| <b>17</b>    | <b>RECOVERY METHODS</b>  | <b>97</b>  |
| <b>18</b>    | <b>PROJECT INFRASTRUCTURE</b>  | <b>100</b> |
| <b>19</b>    | <b>MARKETING STUDIES AND CONTRACTS</b>                                   | <b>101</b> |
| <b>20</b>    | <b>ENVIRONMENTAL STUDIES, PERMITTING, AND SOCIAL OR COMMUNITY IMPACT</b> | <b>102</b> |
| 20.1.        | Environmental studies  | 102        |
| 20.2.        | Project permitting   | 102        |
| 20.3.        | Social and community requirements  | 102        |
| <b>21</b>    | <b>CAPITAL AND OPERATING COSTS</b>                                       | <b>103</b> |
| <b>22</b>    | <b>ECONOMIC ANALYSIS</b>   | <b>104</b> |
| <b>23</b>    | <b>ADJACENT PROPERTIES</b>   | <b>105</b> |
| 23.1.        | General comments   | 105        |
| 23.2.        | Salas de Jujuy – Olaroz lithium project                                  | 105        |
| 23.3.        | LAC exploration and development work in Salar de Cauchari                | 105        |
| <b>24</b>    | <b>ADDITIONAL RELEVANT INFORMATION</b>                                   | <b>106</b> |
| <b>25</b>    | <b>INTERPRETATION AND CONCLUSIONS</b>                                    | <b>107</b> |
| <b>26</b>    | <b>RECOMMENDATIONS</b>   | <b>109</b> |
| <b>27</b>    | <b>REFERENCES</b>  | <b>110</b> |
| <b>28</b>    | <b>DATE AND SIGNATURE PAGE - CERTIFICATE of AUTHOR</b>                   | <b>112</b> |

## TABLE OF FIGURES

|  |    |
|--|----|
| Figure 4.1 Location map of the Cauchari JV .....   | 16 |
| Figure 4.2 Location map of the Cauchari JV mining properties   | 17 |
| Figure 5.1 Project location, access and infrastructure.....  | 22 |
| Figure 5.2 Physiographic and morphotectonic features of the Central Andes.....   | 23 |
| Figure 5.3 The Cauchari and Olaroz drainage basin.....   | 24 |
| Figure 7.1 Generalized structural evolution of the Puna basins .....   | 32 |
| Figure 7.2 Structural section between Olaroz Salar and Salinas Grandes Salar .....   | 32 |
| Figure 7.3 Published geology of Salar de Cauchari .....  | 34 |
| Figure 7.4 Stratigraphic units in the Cauchari basin and their correlation across different published geological maps .....              | 35 |
| Figure 7.5 W-E section looking north through the Cauchari JV geological model.....   | 36 |
| Figure 7.6 W-E section looking north, showing the progressive inter-fingering of the Archibarca fan with the Clay and Halite units ..... | 37 |
| Figure 7.7 Sandy gravels with some clay from the Archibarca fan (CAU07R) .....   | 37 |
| Figure 7.8 W-E section look north between boreholes CAU16D and CAU10R.....   | 38 |
| Figure 7.9 ravel from CAU16D (264.5-268m) with sub-rounded green quartzites.....   | 38 |
| Figure 7.10 Section showing the interpreted geometry of the East Fan unit .....  | 39 |
| Figure 7.11 Section with the interpreted geometry of the Lower Sand unit .....   | 39 |
| Figure 7.12 Example of the Lower Sand unit (CAU12D: 389 m).....  | 40 |
| Figure 7.13 N-S section (looking NW) showing the distributions of the Clay and Halite units .....  | 40 |
| Figure 7.14 Example of the Clay unit (CAU12D: 177.5-179m).....   | 41 |
| Figure 7.15 NE-SW section looking west, showing the distribution of Halite and Clay units .....  | 41 |
| Figure 7.16 Example of the Halite unit .....   | 42 |
| Figure 8.1 Model showing the difference between mature and immature salars.....  | 46 |
| Figure 9.1 Location of the Cauchari gravity (yellow) and AMT (red) lines .....   | 51 |
| Figure 9.2 Gravimeter base station .....   | 52 |
| Figure 9.3 GPS base station .....  | 52 |
| Figure 9.4 Interpretation of the Cauchari north gravity line (looking north).....  | 54 |
| Figure 9.5 Resistivity profile for Cauchari north AMT line .....   | 55 |
| Figure 10.1 Location map of boreholes.....   | 59 |
| Figure 11.1 Comparison between GSA RBR and Core Labs Centrifuge by lithology .....   | 66 |
| Figure 11.2 Comparison between GSA RBR @120 mbar and Core Labs centrifuge by lithology.....  | 66 |
| Figure 11.3 Results of ionic balance analyses (2011).....  | 70 |
| Figure 14.1 Schematic showing the block model domains.....   | 79 |
| Figure 14.2 Normal probability plot of Sy grouped by lithology.....  | 80 |
| Figure 14.3 Resources category classification .....  | 83 |
| Figure 14.4 Lithium Box-plot .....   | 85 |
| Figure 14.5 Potassium Box-plot .....   | 85 |
| Figure 14.6 Archibarca variogram model fitted with the corresponding experimental variogram .....  | 87 |
| Figure 14.7 Clay-Halite variogram model fitted with the corresponding experimental variogram .....                                       | 87 |
| Figure 14.8 West Fan variogram model fitted with the corresponding experimental variogram .....  | 88 |
| Figure 14.9 Archibarca variogram model fitted with the corresponding experimental variogram .....  | 89 |
| Figure 14.10 Clay-Halite variogram model fitted with the corresponding experimental variogram .....                                      | 89 |
| Figure 14.11 West Fan variogram model fitted with the corresponding experimental variogram .....   | 89 |
| Figure 14.12 Li concentration distribution .....   | 91 |
| Figure 14.13 K concentration distribution .....  | 91 |
| Figure 14.14 NW-SE section looking West through the resource model showing the lithium grade .....                                       | 93 |
| Figure 17.1 Schematic of the lithium recovery process for the Cauchari JV Project .....  | 97 |
| Figure 17.2 General process diagram.....   | 98 |

## TABLE OF TABLES

|  |     |
|--|-----|
| Table 1.1 Maximum, average and minimum elemental concentrations of the Cauchari brine.....                                   | 8   |
| Table 1.2 Specific yield (Sy) values applied in the resource model.....  | 9   |
| Table 1.3 Cauchari JV Project Lithium and Potassium Resources estimate (April 19, 2019).....                                 | 10  |
| Table 1.4 Cauchari JV Project Mineral Resources expressed as LCE and potash .....  | 10  |
| Table 4.1 Surface rights of Cauchari JV tenements .....  | 19  |
| Table 5.1 Average monthly rainfall (mm) .....  | 26  |
| Table 5.2 Average monthly temperature (°C) .....   | 26  |
| Table 5.3 Average monthly wind velocity (km/hr).....   | 27  |
| Table 5.4 Olaroz - average monthly evaporation (mm) .....  | 27  |
| Table 7.1 AAL internal classification used for core logging .....  | 33  |
| Table 7.2 Lithology of the units in the Cauchari geological model.....   | 36  |
| Table 7.3 Section showing the interpreted geometry of the East Fan unit .....  | 39  |
| Table 7.3 Maximum, average and minimum elemental concentrations of the Cauchari brine .....                                  | 42  |
| Table 7.5 Average values (g/L) of key components and ratios for the Cauchari brine .....                                     | 43  |
| Table 7.6 Comparison of brine composition of various salars (weight %) .....   | 44  |
| Table 8.1 Results of drainable porosity analyses .....   | 47  |
| Table 8.2 ummary of estimated permeability values .....  | 48  |
| Table 9.1 Bulk rock density values used in the gravity interpretation .....  | 53  |
| Table 10.1 Cauchari summary borehole information (2011-2018) .....   | 58  |
| Table 10.2 CAU07 and CAU11 pumping test results .....  | 61  |
| Table 11.1 Physical and hydraulic test work on core samples – 2017/8 .....   | 64  |
| Table 11.2 Summary of the drainable porosity statistics by laboratory methods.....   | 65  |
| Table 11.3 List of analyses requested from the University of Antofagasta and Alex Stewart Argentina SA<br>Laboratories ..... | 68  |
| Table 11.4 Standards analysis results from ASA Mendoza (2011) .....  | 69  |
| Table 11.5 Duplicate analysis results (2011) .....   | 69  |
| Table 11.5 Results of standards analysis by NorLab (2017/18).....  | 71  |
| Table 7.2 Results of duplicate analyses by ASAMen (2017/18).....   | 73  |
| Table 7.2 Results of duplicate analyses by Norlab (2017/18) .....  | 73  |
| Table 11.9 Performance of STD-4G and STD-7G Standards. Norlab (2017/18).....   | 75  |
| Table 11.10 Performance of STD-500, STD-400 and STD-200 Standards. Norlab (2017/18).....                                     | 75  |
| Table 14.1 Distribution of specific yield (Sy) in the resource model .....   | 80  |
| Table 14.2 Univariate statistics of Li concentrations (mg/L) for each lithological unit.....                                 | 85  |
| Table 14.3 Univariate statistics of K concentrations (mg/L) for each lithological unit .....                                 | 86  |
| Table 14.4 Parameters for the calculation of the experimental variograms.....  | 90  |
| Table 14.5 Cauchari JV Project Lithium and Potassium Resources estimate (April 19, 2019).....                                | 94  |
| Table 14.6 Cauchari JV Project Mineral Resources expressed as LCE and potash .....   | 94  |
| Table 25.1 Average values of key components of the Cauchari brine composition (g/L) .....                                    | 107 |
| Table 25.2 Cauchari JV Project Lithium and Potassium Resources estimate (April 19, 2019).....                                | 108 |
| Table 25.3 Cauchari JV Project Mineral Resources expressed as LCE and potash .....   | 108 |

# 1 SUMMARY

## 1.1. Terms of reference

The Cauchari JV Project (herein “Cauchari JV” or the “Project”) in Jujuy Province in Northern Argentina is operated by Advantage Lithium Corporation (TSX-V: AAL) and which holds an indirect 75% stake in the Project. AAL retained FloSolutions to prepare this Technical Report for the Project. The objective of this report is to prepare an updated estimate of brine resources based on exploration work carried out between 2011 and December 2018 on the AAL mineral properties in Salar de Cauchari. Resource estimates are for lithium and potassium contained in brine.

This report has been prepared in conformance with the requirements of National Instrument 43-101 Standards of Disclosure for Mineral Projects and the associated Companion Policy 43-101CP and Form 43-101F1 of the Canadian Securities Administrators and the associated Best Practice Guidelines for Industrial Minerals and Mineral Processing as issued by the Canadian Institute of Mining and Metallurgy. The Report also includes technical judgment of appropriate additional technical parameters to accommodate certain specific characteristics of minerals hosted in liquid brine as outlined in CIM Best Practice Guidelines for Resource and Reserve Estimation for Lithium Brines and as discussed by Houston (Houston et al, 2011).

## 1.2. Property description and ownership

The Cauchari JV is located in the Puna, 230 km west of the city of San Salvador de Jujuy in Jujuy Province of northern Argentina. The Project is at an altitude of 3,900 masl and sits just to the south of paved Hwy. 52 that connects with the international border with Chile (80 km to the west) and the major mining center of Calama and the ports of Antofagasta and Mejillones in northern Chile, both major ports for the export of mineral commodities and import of mining equipment.

The Cauchari JV tenements cover 27,772 ha and consist of 22 minas which were applied for on behalf of South American Salars (SAS). There is an agreement between the vendors of these tenements and SAS. SAS is a joint venture company with the beneficial owners being Advantage Lithium with a 75% interest and La Frontera with a 25% stake. La Frontera is an Argentine company 85% owned by Orocobre Ltd and 15% owned by Argentine shareholders S. Rodriguez and M. Peral. La Frontera holds a 1% gross royalty on the Cauchari JV.

AAL acquired a 75% indirect ownership in the Cauchari JV by incurring exploration expenditures of USD 5 million in the Project and issuing 46,325,000 and 8,175,000 common shares of the Company, respectively, to Orocobre and Peral. Orocobre will have rights of first refusal on brine production (and may enter into an offtake agreement in respect of such brine production). The Project is operated by AAL and managed through a joint venture committee to which Orocobre appoints two members.

## 1.3. Physiography, climate and access

The physiography of the Project area on the Puna Plateau is characterized by north-south trending basins and ranges with canyons cutting through the Western and Eastern Cordilleras. There are numerous volcanic centers in the Puna. Dry salt lakes (salars) occur within many of the closed basins which have internal (endorheic) drainage. Inflow to these salars is in the form of summer rainfall, surface water runoff and groundwater inflows. Discharge is through evaporation. The Cauchari drainage basin covers some 6,000 km<sup>2</sup> with the nucleus of the Salar covering approximately 250 km<sup>2</sup>. A

large Archibarca alluvial fan is present on the western side of Salar de Cauchari. The eastern side of the Salar hosts smaller alluvial fans entering the basin. The Tocomar River enters from the south into the Cauchari basin and flows north towards the nucleus of the Salar. Hot springs are reported in the head water of the river in the southeastern extent of the basin.

The climate in the Project area is severe and can be described as typical of a continental, cold, high altitude desert, with resultant scarce vegetation. Daily temperature variations may exceed 25°C. Solar radiation is intense, especially during the summer months of October through March, leading to high evaporation rates. The rainy season is between the months of December to March. Occasional flooding can occur in the Salar during the wet season and may limit access to parts of the Salar until water evaporates. The climatic conditions are attractive for solar evaporation processes as demonstrated by the FMC (now Livent) and Orocobre lithium operations.

The Project site is reached by paved and unpaved roads from either Salta or Jujuy. The distance between San Salvador de Jujuy, the capital city of Jujuy Province, and the Project is approximately 230 km and takes about 4 hrs by car. The access from Jujuy is via Hwy RN 9 for approximately 60 km to the town of Purmamarca, from there via Hwy RN 52 for a further 150 km, passing the village of Susques to RP 70 along the west side of Cauchari (approximately 70 km east of the international border with Chile at Paso Jama). The Cauchari JV is accessed directly from RP 70.

#### 1.4. Exploration and drilling

Three drilling campaigns have been carried out for the Project between 2011 and 2018. The first program in 2011 by SAS (Phase I) covered the SE Sector of the Project area, the second and third campaigns (Phase II and III) by AAL covered both the NW and SE Sectors of the Project area. The work carried out during the three drilling campaigns can be summarized as follows:

- Exploration drilling on a general grid basis to allow the estimation of “in-situ” brine resources. The drilling methods were selected to allow for 1) the collection of continuous core to prepare “undisturbed” samples from specified depth intervals for laboratory porosity analyses and 2) the collection of depth-representative brine samples at specified intervals. The 2011 campaign included five (5) diamond core holes CAU01 through CAU05 and one rotary hole (CAU06). The second and third campaigns in 2017/8 included twenty (20) diamond core holes (CAU12 through CAU29).
- Brine sample collection during the drilling programs consisted of bailed and packer samples in the diamond holes, and packer and pumped samples in the rotary holes. A total of 1,946 brine samples (including 540 QA/QC samples) were analyzed by Norlabs (Jujuy, Argentina) as the primary laboratory and by Alex Steward Assayers (Mendoza, Argentina) and the University of Antofagasta (Chile) as secondary QA/QC laboratories. Additional brine QA/QC analyses were carried out on centrifuged samples collected by the Geosystems Analysis laboratory in Tucson, AZ.
- HQ core was retrieved during the diamond core drilling from which some 415 primary undisturbed samples were prepared for laboratory drainable porosity and other physical parameter determinations by GeoSystems Analysis (GSA) in Tucson, AZ. Laboratory QA/QC porosity analyses (30) were undertaken by Corelabs in Houston, TX and Daniel B Stephens & Associates laboratories (DBSA) in Albuquerque, NM.



- The 2017/8 campaign included five rotary holes (CAU07 through CAU11) which were drilled and completed as test production wells to carry out pumping tests and additional selective brine sampling. Six nested monitoring wells were installed adjacent to CAU07 and CAU11 for use during the long-term pumping tests as part of the Phase III program.
- Initial short-term (48 hour) pumping tests were carried out on CAU07 through CAU11 during 2017. Long-term pumping tests (30 day) with subsequent recovery were carried out on CAU07 and CAU11.
- A number of geophysical surveys have been carried out since 2011 in the Project area to further define basin geometry, continuity of lithological units, and to define the brine / fresh water interface along the perimeter of the Salar. These geophysical surveys included gravity, TEM, VES and AMT methods.

## 1.5. Geology and mineralization

### 1.5.1. Geology

Based on the drilling campaigns carried out in the Salar between 2011 and 2018, six major geological units were identified and correlated from the logging of drill cuttings and undisturbed core to a general depth of over 600 m. No borehole has reached bedrock. Salar de Cauchari is a mixed style salar, with a halite nucleus in the center of the Salar overlain with up to 50 m of fine grained (clay) sediments. The halite core is interbedded with clayey to silty and sandy layers. The Salar is surrounded by relative coarse grained alluvial and fluvial sediments. These fans demarcate the perimeter of the actual Salar visible in satellite images and at depth extend towards the center of the Salar where they form the distal facies with an increase in sand and silt. At depth (between 300 m and 600 m) a deep sand unit has been intercepted in several core holes in the SE Sector of the Project area.

### 1.5.2. Mineralization

The brines from Salar de Cauchari are solutions nearly saturated in sodium chloride with an average concentration of total dissolved solids (TDS) of 290 g/L. The average density is 1.18 g/cm<sup>3</sup>. Components present in the Cauchari brine are: K, Li, Mg, Ca, Cl, SO<sub>4</sub>, HCO<sub>3</sub> and B. Table 1.1 shows a breakdown of the principal chemical constituents in the brine including maximum, average, and minimum values, based on the 546 brine samples that were collected and analyzed from the exploration boreholes during the 2011 and 2017/8 drilling programs.

**Table 1.1 Maximum, average and minimum elemental concentrations of the Cauchari brine**

| Analyte  | Li   | K     | B     | Na      | Ca    | Mg    | SO <sub>4</sub> | Density           |
|----------|------|-------|-------|---------|-------|-------|-----------------|-------------------|
| Units    | mg/L | mg/L  | mg/L  | mg/L    | mg/L  | mg/L  | mg/L            | g/cm <sup>3</sup> |
| Maximum  | 956  | 8,202 | 2,528 | 135,362 | 1,681 | 2,640 | 62,530          | 1.23              |
| Mean     | 512  | 4,349 | 941   | 105,721 | 504   | 1,323 | 18,930          | 1.19              |
| Minimum  | 157  | 101   | 621   | 101     | 175   | 314   | 101             | 1.07              |
| Std.Dev. | 144  | 1,186 | 487   | 16,033  | 212   | 412   | 8,561           | 0.03              |

## 1.6. Status of exploration, development and operations

AAL has contracted Tier-1 global engineering consultancy Worley Parsons to complete a Preliminary Feasibility Study for the Project by Q3 2019, with the evaluation of production scenarios of up to 30 ktpa of lithium carbonate. The Phase III drilling and testing program was completed in December 2018 and this Technical Report provides an updated resource estimate based on the results of all drilling and testing programs carried out for the Project to date. Estudios y Servicios Ambientales SRL (Ambiental), a major Argentine environmental consultancy, with extensive experience in salars and Northern Argentina, has been contracted to oversee the completion of an Environmental Impact Statement (EIA) for the Project by Q3 2019.

## 1.7. Brine resource estimate

The brine resource estimate was determined by defining the aquifer geometry, the drainable porosity or specific yield (Sy) of the hydrogeological units in the Salar, and the concentration of the elements of economic interest, lithium and potassium. The resource estimate is limited to the AAL mining concessions in Salar de Cauchari and covers an area of 117.7 km<sup>2</sup>.

The resource model domain is constrained by the following factors:

- The top of the model coincides with the brine level in the Salar as measured in a number of monitoring wells and further interpreted by TEM and SEV geophysical profiles.
- The lateral boundaries of the model domain are limited to the area of the Cauchari tenements where they flank the neighboring LAC concessions and by the brine / fresh water interface along the eastern and western limits of the Salar as interpreted from boreholes information and TEM and SEV profiles.
- The bottom of the model coincides with a surface created from the bottom of the boreholes. Locally, a deeper resource volume has been defined in the Lower Sand as defined by boreholes CAU11R, CAU12D, CAU13D and CAU19D.

The specific yield values used to develop the resource estimate are based on results of the logging and hydrogeological interpretation of recovered core of 25 diamond boreholes, results of drainable porosity analyses carried out on 301 primary undisturbed samples by GSA with additional measurements made by DBSA, Corelabs and with additional data available from the British Geological Survey (BGS) in 2011. Table 1.2 shows the drainable porosity values assigned to the different geological units for the resource model.

**Table 1.2 Specific yield (Sy) values applied in the resource model**

| Geological Unit | Average |
|-----------------|---------|
| Halite          | 0.05    |
| East Fan        | 0.03    |
| West Fan        | 0.11    |
| Archibarca Fan  | 0.12    |
| Clay            | 0.03    |
| Lower Sand      | 0.14    |

The distributions of lithium and potassium concentrations in the model domain are based on a total of 546 brine analyses mentioned in Section 1.5.2 above. The boreholes within the resource area are appropriately spaced at a borehole density of one bore per 4 km<sup>2</sup>

The resource estimate for the Project was developed using the Stanford Geostatistical Modeling Software (SGeMS) and the geological model as a reliable representation of the local lithology. The author was closely involved with the block model development; all results have been reviewed and checked at various stages and are believed to be valid and appropriate for this resource estimate. Table 1.3 shows the Measured, Indicated and Inferred Lithium and Potassium Resources for the Cauchari JV Project.

**Table 1.3 Cauchari JV Project Lithium and Potassium Resources estimate (April 19, 2019)**

|  | Measured (M)   |                  | Indicated (I)  |                  | M+I            |                  | Inferred       |                  |
|--|----------------|------------------|----------------|------------------|----------------|------------------|----------------|------------------|
| <b>Aquifer volume (km<sup>3</sup>)</b> | 10             |                  | 21             |                  | 31             |                  | 11             |                  |
| <b>Mean specific yield</b>             | 6.6%           |                  | 5.9%           |                  | 6.1%           |                  | 5.6%           |                  |
| <b>Brine volume (km<sup>3</sup>)</b>   | 0.6            |                  | 1.2            |                  | 1.9            |                  | 0.6            |                  |
| <b>Brine volume (km<sup>3</sup>)</b>   | Li             | K                | Li             | K                | Li             | K                | Li             | K                |
| <b>Mean grade (g/m<sup>3</sup>)</b>    | 35             | 291              | 26             | 238              | 29             | 255              | 27             | 225              |
| <b>Mean concentration (mg/l)</b>       | 527            | 4,438            | 452            | 4,145            | 476            | 4,238            | 473            | 3,867            |
| <b>Resource (tonnes)</b>               | <b>345,000</b> | <b>2,800,000</b> | <b>550,000</b> | <b>5,000,000</b> | <b>900,000</b> | <b>7,800,000</b> | <b>290,000</b> | <b>2,400,000</b> |

Notes to Table 1.3:

- CIM definitions were followed for mineral resources.
- The Qualified Person for this Mineral Resource estimate is Frits Reidel, CPG.
- No cut-off concentrations have been applied to the resource estimate
- Numbers may not add due to rounding.

Table 1.4 shows the Mineral Resource of the Cauchari JV Project expressed as lithium carbonate equivalent (LCE) and potash (KCl).

**Table 1.4 Cauchari JV Project Mineral Resources expressed as LCE and potash (tonnes)**

|                         | Measured (M) | Indicated (I) | M+I        | Inferred  |
|-------------------------|--------------|---------------|------------|-----------|
| Lithium Carbonate (LCE) | 1,850,000    | 2,950,000     | 4,800,000  | 1,500,000 |
| Potash (KCl)            | 5,400,000    | 9,600,000     | 14,900,000 | 4,600,000 |

Notes to Table 1.4:

- Lithium is converted to lithium carbonate (Li<sub>2</sub>CO<sub>3</sub>) with a conversion factor of 5.32.
- Potassium is converted to potash with a conversion factor of 1.91.
- Numbers may not add due to rounding.

It is the opinion of the author that the Salar geometry, brine chemistry composition and the specific yield of the Salar sediments have been adequately characterized to support the resource estimates for the Project herein.

## 1.8. Conclusions and recommendations

Based on the analyses and interpretation of the results of the exploration work carried out on the Cauchari JV between 2011 and 2018, the following concluding statements are prepared:

- The entire Cauchari JV area within the NW and SE Sectors has been covered by exploratory drilling at an approximate borehole density of one exploration borehole per 4 km<sup>2</sup>; it is the opinion of the author that such borehole density is appropriate for the Mineral Resource estimate described herein. AAL has additional properties south of the resource which have not been subject to any drilling and which have potential to host lithium brine.
- The results of the drilling (25 diamond core holes and 6 rotary boreholes), 8 pumping tests and the analysis of 1,047 primary brine samples identify distinct brine composition and grade at specific depth intervals, showing a relatively uniform distribution of lithium bearing brines throughout the Project area to a depth of 600 m.
- It is the opinion of the author that the Salar geometry, brine chemistry composition and the specific yield of the Salar sediments have been adequately defined to support the Measured, Indicated and Inferred Resource estimate described in Table 1.3.
- It is recommended that a three-dimensional groundwater flow and transport model is constructed and calibrated for Salar de Cauchari to carry out simulations of future brine production scenarios and prepare a brine reserve estimate.
- It is recommended that the PFS for the Cauchari JV Project is completed as planned during 2019.
- Environmental baseline monitoring should be continued during 2019 as well as the completion of the EIA by Q3 2019.

## 2 INTRODUCTION

### 2.1. Terms of reference

The Cauchari Joint Venture (herein Cauchari JV or the “Project”) is operated by Advantage Lithium Corp. (TSX-V: AAL) and which hold a 75% stake in the Project. AAL retained FloSolutions to prepare this Technical Report for the Project in the province of Jujuy in the north of Argentina. The objective of this report is to prepare an estimate of brine resources based on exploration work carried out between 2011 and December 2018 on the mineral properties in Salar de Cauchari held through Argentine company South American Salars (SAS). Resource estimates are for lithium and potassium contained in brine.

This report has been prepared in conformance with the requirements of National Instrument 43-101 Standards of Disclosure for Mineral Projects and the associated Companion Policy 43-101CP and Form 43-101F1 of the Canadian Securities Administrators and the associated Best Practice Guidelines for Industrial Minerals and Mineral Processing as issued by the Canadian Institute of Mining and Metallurgy. The Report also includes technical judgment of appropriate additional technical parameters to accommodate certain specific characteristics of minerals hosted in liquid brine as outlined in CIM Best Practice Guidelines for Resource and Reserve Estimation for Lithium Brines and as discussed by Houston (Houston et al, 2011).

### 2.2. Sources of Information

Previous technical reports prepared for the Project include:

- Preliminary Economic Assessment of the Advantage Lithium Project, Jujuy Province, Argentina. NI 43-101 Technical Report prepared for Advantage Lithium Corp by Worley Parsons, dated August 31, 2018
- Lithium and Potassium Resources, Cauchari Project, NI 43-101 Technical Report prepared for Advantage Lithium Corp by Frits Reidel and Peter Ehren, dated June 27, 2018.
- Technical Report on the Cauchari Lithium Project Jujuy Province, Argentina. NI 43-101 Report Prepared for Advantage Lithium Corp by Murray Brooker and Peter Ehren. Effective 5<sup>th</sup> December, 2016, Amended 22 December, 2016.
- Technical Report on the Cauchari Project Jujuy Province, Argentina. NI 43-101 Report Prepared for Orocobre Limited. Prepared by Consulting Hydrogeologist John Houston. Effective April 30, 2010.

The author was provided full access to the AAL database including drill core and cuttings, drilling and testing results, brine chemistry and porosity laboratory analyses, aquifer testing results, geophysical surveys and all other information available from the work carried out on the Project between 2011 and 2018. The documentation reviewed, and other sources of information, are listed at the end of this report in Section 27 References.

The report was prepared by Frits Reidel, CPG, “qualified person” (QP) who is independent of AAL as such terms are defined by NI 43-101.. The author has relevant experience in the evaluation of brine deposits in South America and has been involved with exploration and development efforts of the Olaroz and Cauchari Salars since 2009. The author has been to the project area frequently since 2009.

Specifically, Frits Reidel visited the Cauchari JV area on numerous occasions during the Phase II and III Drilling Programs in 2017 and 2018.

## 2.3. Units

The metric (SI system) units of measure are used in this report unless otherwise noted.

### List of abbreviations

All currency in this report is US dollars (US\$) unless otherwise noted.

|                    |                             |                   |                                |
|--------------------|-----------------------------|-------------------|--------------------------------|
| μ                  | Micron                      | km <sup>2</sup>   | square kilometer               |
| °C                 | degree Celsius              | kPa               | Kilopascal                     |
| °F                 | degree Fahrenheit           | kVA               | kilovolt-amperes               |
| μg                 | Microgram                   | kW                | Kilowatt                       |
| A                  | Ampere                      | kWh               | kilowatt-hour                  |
| a                  | Annum                       | L                 | Litre                          |
| bbl                | Barrels                     | L/s               | litres per second              |
| Btu                | British thermal units       | M                 | Metre                          |
| C\$                | Canadian dollars            | M                 | mega (million)                 |
| cal                | Calorie                     | m <sup>2</sup>    | square metre                   |
| cfm                | cubic feet per minute       | m <sup>3</sup>    | cubic metre                    |
| cm                 | centimeter                  | Min               | Minute                         |
| cm <sup>2</sup>    | square centimeter           | MASL              | metres above sea level         |
| d                  | Day                         | Mm                | millimeter                     |
| dia.               | Diameter                    | Mph               | miles per hour                 |
| dmt                | dry metric tonne            | MVA               | megavolt-amperes               |
| dwt                | dead-weight ton             | MW                | Megawatt                       |
| ft                 | Foot                        | MWh               | megawatt-hour                  |
| ft/s               | foot per second             | m <sup>3</sup> /h | cubic metres per hour          |
| ft <sup>2</sup>    | square foot                 | opt, oz/st        | ounce per short ton            |
| ft <sup>3</sup>    | cubic foot                  | Oz                | Troy ounce (31.1035g)          |
| g                  | Gram                        | Ppm               | part per million               |
| G                  | giga (billion)              | Psia              | pound per square inch absolute |
| Gal                | Imperial gallon             | Psig              | pound per square inch gauge    |
| g/L                | gram per litre              | RL                | relative elevation             |
| g/t                | gram per tonne              | S                 | Second                         |
| gpm                | Imperial gallons per minute | St                | short ton                      |
| gr/ft <sup>3</sup> | grain per cubic foot        | Stpa              | short ton per year             |
| gr/m <sup>3</sup>  | grain per cubic metre       | Stpd              | short ton per day              |
| hr                 | hour                        | T                 | metric tonne                   |
| ha                 | hectare                     | Tpa               | metric tonne per year          |
| hp                 | horsepower                  | Tpd               | metric tonne per day           |
| in                 | inch                        | US\$              | United States dollar           |
| in <sup>2</sup>    | square inch                 | USg               | United States gallon           |
| J                  | joule                       | USgpm             | US gallon per minute           |
| k                  | kilo (thousand)             | V                 | Volt                           |
| kcal               | kilocalorie                 | W                 | Watt                           |
| kg                 | kilogram                    | Wmt               | wet metric tonne               |
| km                 | kilometre                   | yd <sup>3</sup>   | cubic yard                     |
| km/h               | kilometre per hour          | Yr                | Year                           |

### 3 RELIANCE ON OTHER EXPERTS

The preparation of a technical report of this nature requires multiple technical disciplines; the author has relied on other experts in items related to the legal status of mining properties, environmental affairs and topography.

**Legal** – For the purpose of this report, the author has relied on ownership information provided by AAL. This includes a report by independent lawyer, Santiago Saravia Frias for information regarding the legal status of the properties, the property (tenement) agreements, the surveyed limits of properties and permits, and surface property rights dated 31<sup>st</sup> August, 2018 and the previous report provided on March 14, 2017 and in addition to the certificate of ownership provided by the Jujuy Mines Department public notary on 22<sup>nd</sup> August 2018. These documents apply to information in Section 4 and related summaries in its entirety. The independent QPs have not investigated title or mineral rights of the Project and express no legal opinion as to the ownership status of the Cauchari Properties

**Environmental** – SAS representatives Miguel Peral and Silvia Rodriguez for information regarding permits held by the company and the environmental reporting status of the Project. This refers to information in Sections 4 and 20.

**Topography** - The author also has relied on the topographic information provided by AAL.

## 4 PROPERTY LOCATION AND DESCRIPTION

### 4.1. Location

The Cauchari JV is located in the Puna region of Jujuy Province in northern Argentina as shown in Figure 4.1. The Project is at an altitude of 3,900 masl and is located 230 km west of the city of San Salvador de Jujuy, the capital of the Jujuy Province.

The Project site sits just to the south of paved Hwy. 52 that passes through the international border with Chile, approximately 80 km west (Jama Pass) and continues on to the major mining center of Calama and the ports of Antofagasta and Mejillones in northern Chile, both major ports for the export of mineral commodities and import of mining equipment.

### 4.2. Exploration and exploitation licenses

#### 4.2.1. Licenses & coordinate system

The location of the SAS licenses is shown in Figure 4.2, with property (tenement or claim) information presented in Table 4.1. Tenement co-ordinates (and all other co-ordinates used in this report) are given in the Argentine coordinate system, which uses the Gauss Krueger Transverse Mercator projection and the Argentine Posgar 94 datum. The properties are located in Argentine GK Zone 3.

Two tenement types exist in the Argentine mining regulations. Cateos (Exploration Permits) are licenses that allow the holder to explore the tenement for a period of time that is proportional to its size. An Exploration Permit of 1 unit (500 hectares) is granted for a period of 150 days. For each additional unit (500 hectares) the period is extended by 50 days. The maximum allowed permit size is 20 units (10,000 hectares) and which is granted for a period of 1,100 days. The period begins 30 days after granting of the permit.

A relinquishment must be made after the first 300 days, and a second one after 700 days. The applicant should pay a canon fee of \$1,600 Argentine pesos per unit (500 hectares) and submit an exploration work plan and environmental impact assessment.

Minas (Mining/exploitation Permits) are licenses which allow the holder to exploit the property (tenement) subject to regulatory environmental approval. Minas are of unlimited duration, providing the property holder meets its obligations under the Mining Code. These include:

- Paying the annual rent (canon) payments;
- Completing a survey of the property boundaries;
- Submitting a mining investment plan; and
- Meeting the minimum investment commitment.



Figure 4.1 Location map of the Cauchari JV

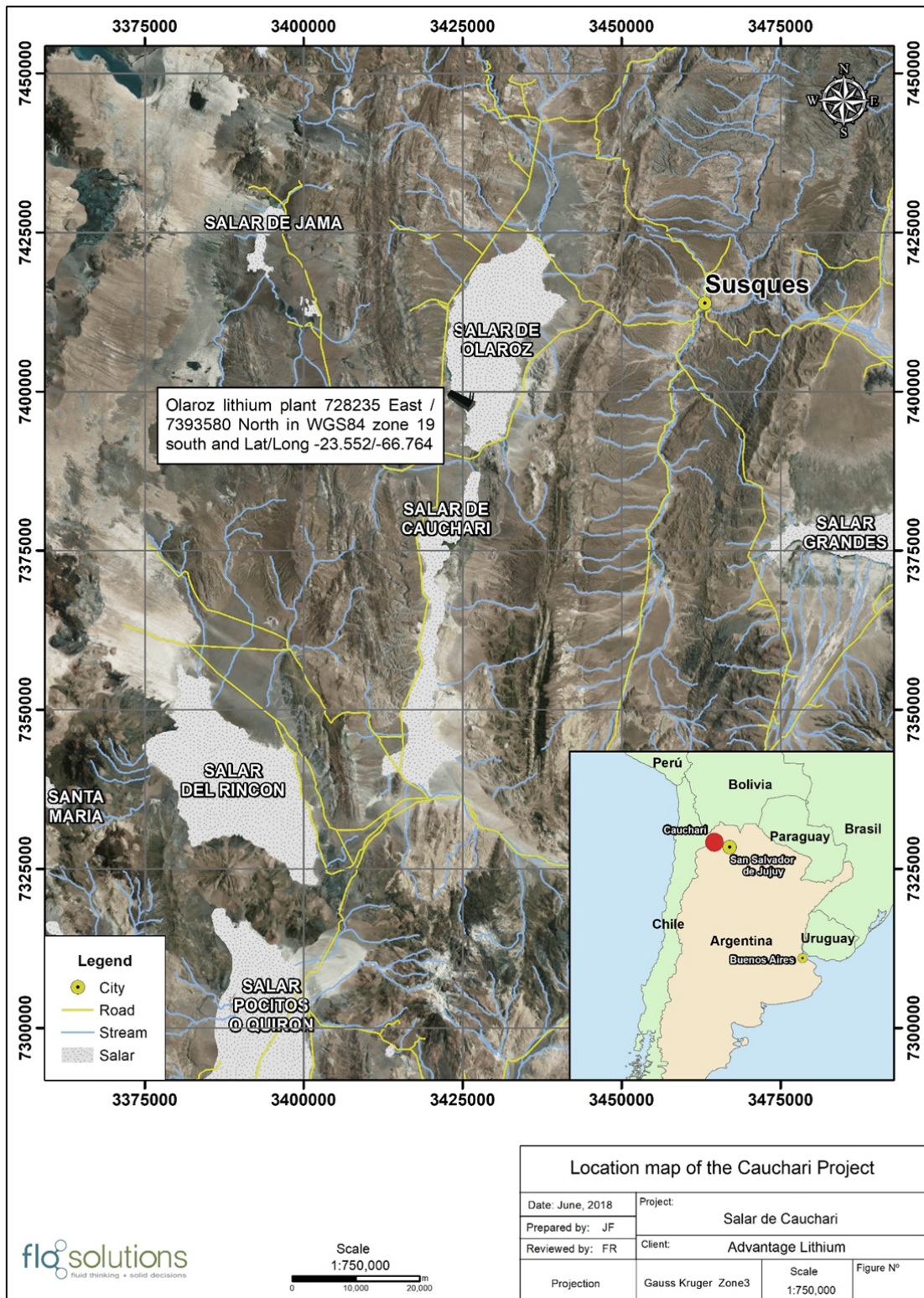
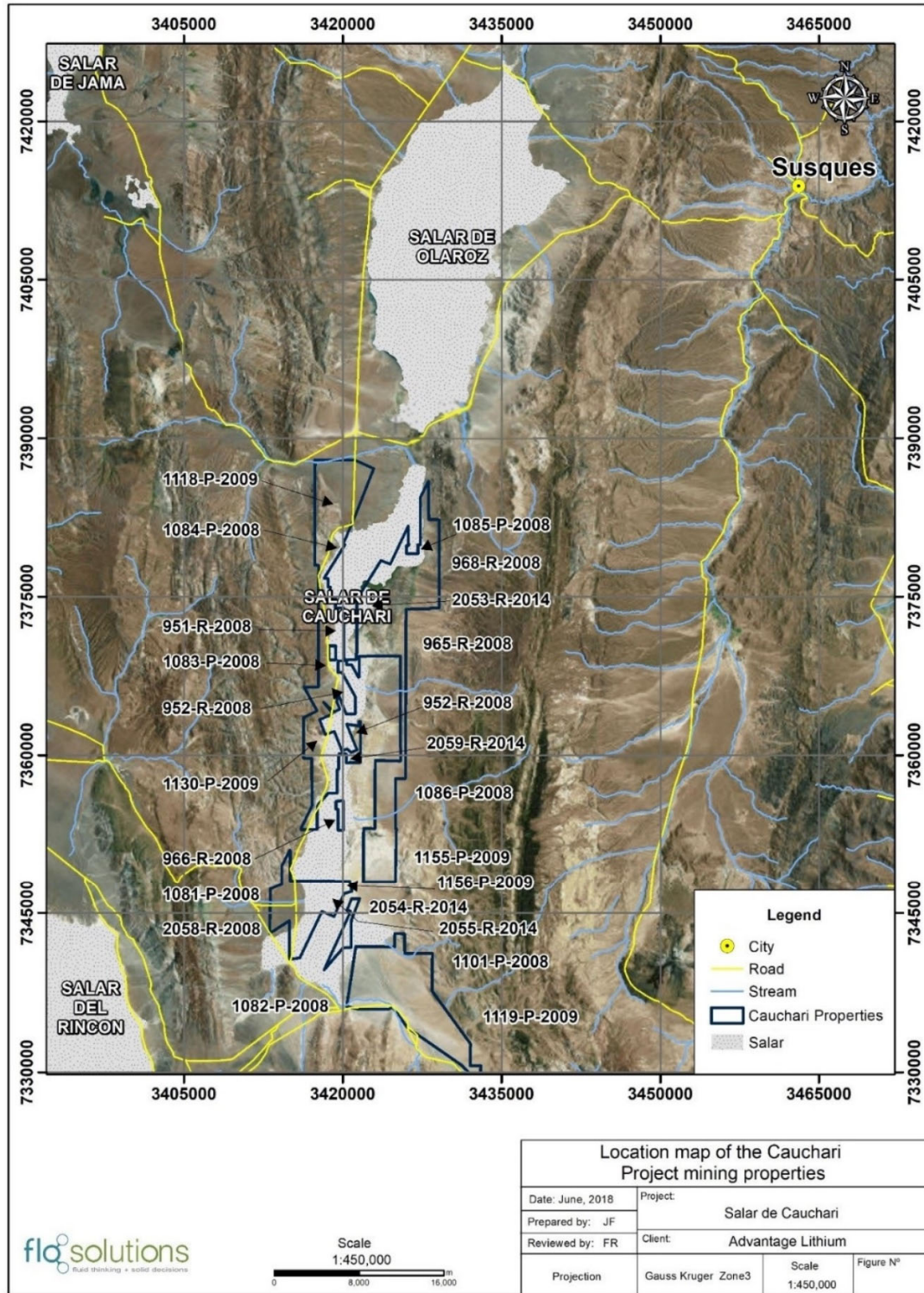


Figure 4.2 Location map of the Cauchari JV mining properties



#### 4.2.2. Expenditure commitments for Minas

The Cauchari properties are now all held as applications for minas.

- The investment commitment is 300 times the annual rent payment, to be spent over a five year period and payable within five years of the filing of a capital investment plan.
- During each of the first two years the amount of the investment shall not be less than 20% and the rest of the investment (60 %) freely distributed during the remaining three years.
- The annual tenement tax varies according to the mineral commodity. For brines it is \$3,200 Argentine pesos/yr per 100 hectares.

Mining properties (of both types) must specify the type of mineral the holder is seeking to explore and exploit. The canon fees are dependent on the class of minerals applied for. Properties cannot be over-staked by new properties specifying different minerals; adding a new mineral species to a properties file is a relatively straightforward procedure and may require payment of a different canon fee.

All Cauchari properties are in the process of being granted as minas/exploitation permits, replacing the Cateos previously held by SAS. Provided that the title holder fulfils the legal requirements, in due time the pertinent exploitation licence/property should be granted. Independent legal review has confirmed the property obligations have been met and that the properties are in good standing.

Expenditure commitments for individual properties are listed in Table 4.1.

#### 4.2.3. The Cauchari tenement package

The Cauchari tenements cover approximately 27,772 hectares in the province of Jujuy. These consist of 22 minas which were applied for on behalf of SAS. There is an agreement between the vendors of these properties (tenements) and SAS. The legal report prepared by independent Argentine registered lawyer Mr Santiago Saravia Frias (dated 12 August, 2016) showed that these properties were originally owned by Silvia Rodriguez and are in the legal process of being transferred to SAS.

#### 4.2.4. Surface rights and legal access

Mineral rights, in general, have a nature of public benefit and are owned by the Provinces which grant exploration and exploitation concession rights for the development of mining projects. Surface rights are independently owned from mining rights and in the case of the Cauchari JV are owned by the communities of Catua, Termas de Tuzgle de Puesto Sey and/or Los Manantiales de Pastos Chicos. Table 4.1 shows the details of surface ownership in the Cauchari JV area. The owners of mineral exploration and exploitation concessions have certain obligations to the surface rights owners including the approval of an Environmental Impact Analyses (EIA) and possible other compensation measures to be agreed.

**Table 4.1 Surface rights of Cauchari JV tenements**

| Property           | Property Number | Property Area (ha) | Property Type & Expiry | Land owner (communities)  | Total Five Year Mining Investment (Argentine Pesos)t | Annual canon (rent) fee US\$ |
|--------------------|-----------------|--------------------|------------------------|---|--|------------------------------|
| Juan Pablo II      | 2055R 2014      | 495                | Mina - Perpetual       | Termas de Tuzgle de Puesto Sey  | 320,000  | 1,067                        |
| Juan XXIII         | 2054 R 2014     | 442                | Mina - Perpetual       | Termas de Tuzgle de Puesto Sey  | 320,000  | 1,067                        |
| Papa Francisco I   | 2053 R 2014     | 1,997              | Mina - Perpetual       | Termas de Tuzgle de Puesto Sey and Los Manantiales de Pastas Chicos.                        | 1,280,000  | 4,267                        |
| San Gabriel I      | 951R 2008       | 795                | Mina - Perpetual       | Catua, Termas de Tuzgle de Puesto sey and Los Manantiales de Pastas Chicos.                 | 512,000  | 1,707                        |
| San Joaquin I      | 952 R 2008      | 488                | Mina - Perpetual       | Catua and Termas de Tuzgle de Puesto Sey  | 320,000  | 1,067                        |
| San Francisco Sur  | 965 R 2008      | 1,345              | Mina - Perpetual       | Catua, Termas de Tuzgle de Puesto sey and Los Manantiales de Pastas Chicos.                 | 896,000  | 2,987                        |
| San Carlos Este    | 966 R 2008      | 118                | Mina - Perpetual       | Termas de Tuzgle de Puesto Sey  | 128,000  | 427                          |
| Francisco Norte    | 968 R 2008      | 700                | Mina - Perpetual       | Pastas Chicos   | 448,000  | 1,493                        |
| Georgina           | 1081 p 2008     | 1,247              | Mina - Perpetual       | Catua   | 832,000  | 2,773                        |
| Olapapatita I      | 1082 p 2008     | 1,422              | Mina - Perpetual       | The Province of Jujuy has established an encumbrance for solar energy in the whole tenement | 960,000  | 3,200                        |
| San Gabriel Sur    | 1083 p 2008     | 1,450              | Mina - Perpetual       | Catua, Termas de Tuzgle de Puesto Sey and Los Manantiales de Pastos Chicos.                 | 960,000  | 3,200                        |
| San Gabriel Norte  | 1084 p 2008     | 1,527              | Mina - Perpetual       | Cauta and Los Mantantiales de Pastos Chicos   | 1,024,000  | 3,413                        |
| San Francisco Este | 1085 p 2008     | 1,201              | Mina - Perpetual       | Termas de Tuzgle de Puesto Sey and Los Manantiales de Pastos Chicos.                        | 768,000  | 2,560                        |
| Sulfita            | 1086 p 2008     | 1,717              | Mina - Perpetual       | Termas de Tuzgle de Puesto Sey  | 1,152,000  | 3,840                        |
| Olapapatita II     | 1101 p 2008     | 2,484              | Mina - Perpetual       | The Province of Jujuy has established an encumbrance for solar energy in the whole tenement | 1,600,000  | 5,333                        |
| Olapapatita III    | 1119 p 2009     | 2,493              | Mina - Perpetual       | The Province of Jujuy has established an encumbrance for solar energy in the whole tenement | 1,600,000  | 5,333                        |
| San Gerardo        | 1118 p 2009     | 2,396              | Mina - Perpetual       | Catua, Termas de Tuzgle de Puesto Sey and Los Manantiales de Pastos Chicos.                 | 1,536,000  | 5,120                        |
| San Gerardo II     | 1130 p 2009     | 1,239              | Mina - Perpetual       | Catua Comunity  | 832,000  | 2,773                        |
| Antonito I         | 1155 p 2009     | 1,500              | Mina - Perpetual       | Termas de Tuzgle de Puesto Sey  | 960,000  | 3,200                        |
| Solitaria I        | 1156 p 2009     | 66                 | Mina - Perpetual       | Termas de Tuzgle de Puesto Sey  | 64,000   | 213                          |
| Mina San Gabriel X | 2059 R 2014     | 885                | Mina - Perpetual       | Termas de Tuzgle de Puesto Sey  | 576,000  | 1,920                        |
| Mina Juan Pablo I  | 2058 R 2014     | 1,765              | Mina - Perpetual       | Termas de Tuzgle de Puesto Sey  | 1,152,000  | 3,840                        |
| <b>Total</b>       |                 | <b>27,772</b>      |                        |   | <b>18,240,000</b>                                    | <b>60.800</b>                |

### 4.3. Environmental liabilities

The Cauchari tenements are not subject to any known environmental liabilities. There have been historical ulexite / borax mining activities adjacent to the Cauchari JV in the north of the Salar. These

mining operations are generally limited to within three meters of the surface and it is assumed that these borax workings will naturally reclaim when mining is halted due to wet season inflows.

#### 4.4. Permit status

Exploration and mining activities on cateos and minas are subject to regulatory approval of an environmental impact assessment (“EIA”) before initiating activities. The author understands that AAL obtained all approvals required for the drilling and testing programs in the Salar.

#### 4.5. Royalties

The Argentine federal government regulates ownership of mineral resources, although mineral properties are administered by the provinces. In 1993 the Federal Government established a limit of 3% on mining royalties to be paid to the provinces as a percentage of the “pit head” value of extracted minerals. AAL is expecting a 3% royalty payable to the Jujuy Province based on earnings before income and tax, if a brine mining operation is established.

#### 4.6. Ownership of the Cauchari JV

SAS is a joint venture company with the beneficial owners being Advantage Lithium with a 75% interest and La Frontera with a 25% stake. La Frontera is an Argentine company 85% owned by Orocobre Ltd and 15% owned by Argentine shareholders S. Rodriguez and M. Peral. La Frontera holds a 1% gross royalty on the Cauchari JV.

AAL acquired a 75% indirect ownership in the Cauchari JV by incurring exploration expenditures of US\$ 5 million in the Project and issuing 46,325,000 and 8,175,000 common shares of the Company, respectively, to Orocobre and Peral. Orocobre will have rights of first refusal on brine production (and may enter into an offtake agreement in respect of such brine production). The Project is operated by AAL and managed through a joint venture committee to which Orocobre appoints two members.

#### 4.7. Other Significant Factors and Risks

A number of normal risk factors are associated with the exploration and development of the Cauchari JV. These risks include, but are not limited to:

- Mining properties may not be renewed by the provincial authorities.
- Final environmental approvals may not be received from the necessary authorities.
- Obtaining all necessary licenses and permits on acceptable terms in a timely manner or at all.
- Changes in federal or provincial laws and their implementation may impact planned activities.
- Potential flooding in the Salar could temporarily delay planned exploration and development activities.
- The company may be unable to meet its obligations for expenditure and maintenance of property licenses.
- Activities on adjacent properties having an impact on the Cauchari JV.

## 5 ACCESSIBILITY, CLIMATE, LOCAL RESOURCES, INFRASTRUCTURE AND PHYSIOGRAPHY

### 5.1. Accessibility, local resources and infrastructure

The Project site is reached by paved and unpaved roads from either the Salta or Jujuy Provinces. The distance between San Salvador de Jujuy and the Project is approximately 230 km and takes about 4 hrs by car. The access from Jujuy is via Hwy RN 9 for approximately 60 km to the town of Purmamarca, from there Hwy RN 52 for a further 150 km, passing the village of Susques to RP 70 along the west side of Cauchari. The Cauchari JV is accessed directly from RP 70.

The Project is reached from the city of Salta, capital of Salta Province, via the town of Campo Quijano, then continuing along Hwy RN 51 through Quebrada del Toro, the town of San Antonio de los Cobres and a further 130 km to the junction with RP 70 on the west side of Salar de Cauchari. Total driving time from Salta to the Project is approximately 5 hours.

Both Jujuy and Salta have international airports with regular flights to Buenos Aires. The Project is located 20 km to the south of Orocobre's Olaroz lithium plant which has full infrastructure available including water, gas, and electricity. The Puna gas pipeline crosses to the north of Salar de Olaroz. Orocobre has constructed a connection to this pipeline for the Olaroz Project. A railway line connecting northern Argentina to Chile passes along the southern end of Salar de Cauchari, approximately 40 kilometers to the south of the Project site.

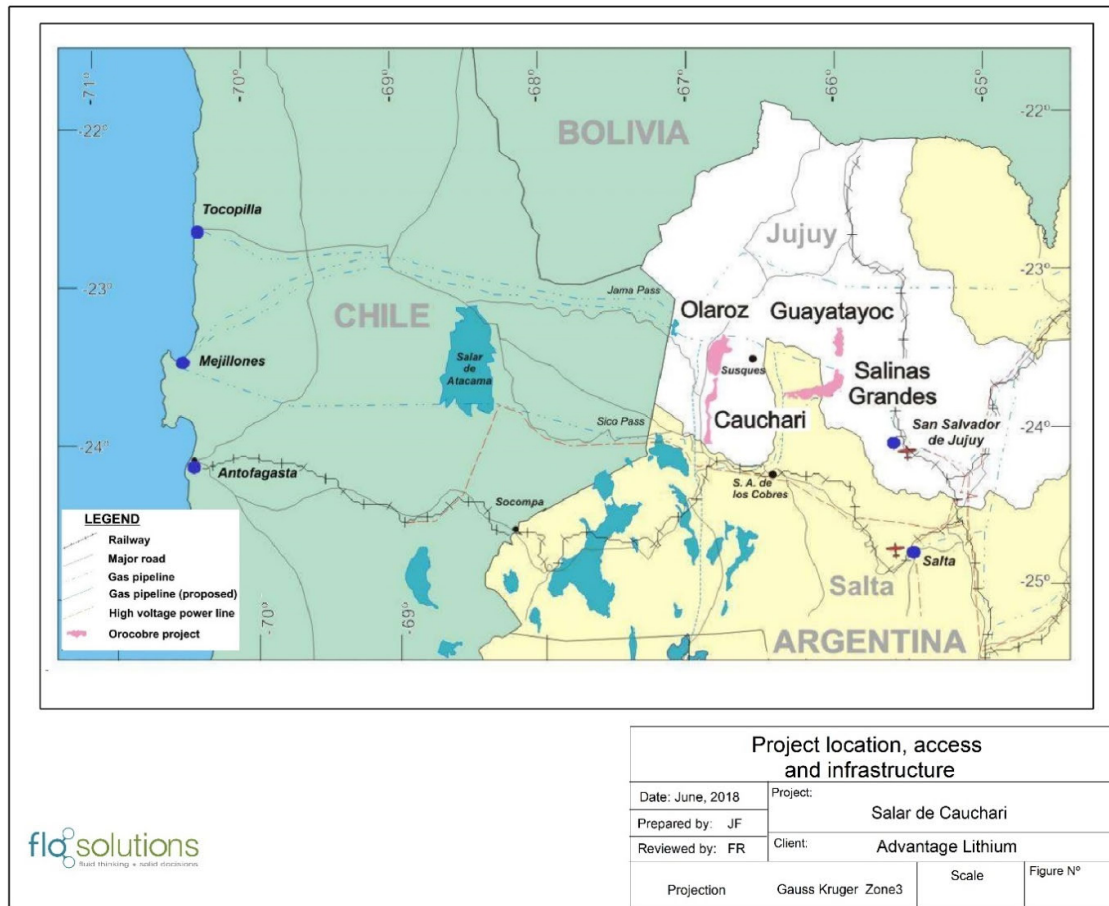
### 5.2. Local population centers and accommodation

There are a number of local villages within 50 kilometers of the Project site. These include: Catua 37 km southwest, Pastos Chicos and Puesto Sey to the east and Olaroz Chico 34 km north and Olacapato 50 km south. The regional administration is located in the town of Susques (population ~2,000) some 60 km northeast of the Project site. Susques has a regional hospital, petroleum and gas services, and a number of hotels. A year-round camp exists at the Project site and provides all services and accommodations for the on-going exploration program.

### 5.3. Physiography

The Altiplano-Puna is an elevated plateau within the central Andes (see Figure 5.2 below). The Puna covers part of the Argentinean provinces of Jujuy, Salta, Catamarca, La Rioja and Tucuman with an average elevation of 3,700 masl (Morlans, 1995; Kay et. al., 2008).

Figure 5.1 Project location, access and infrastructure

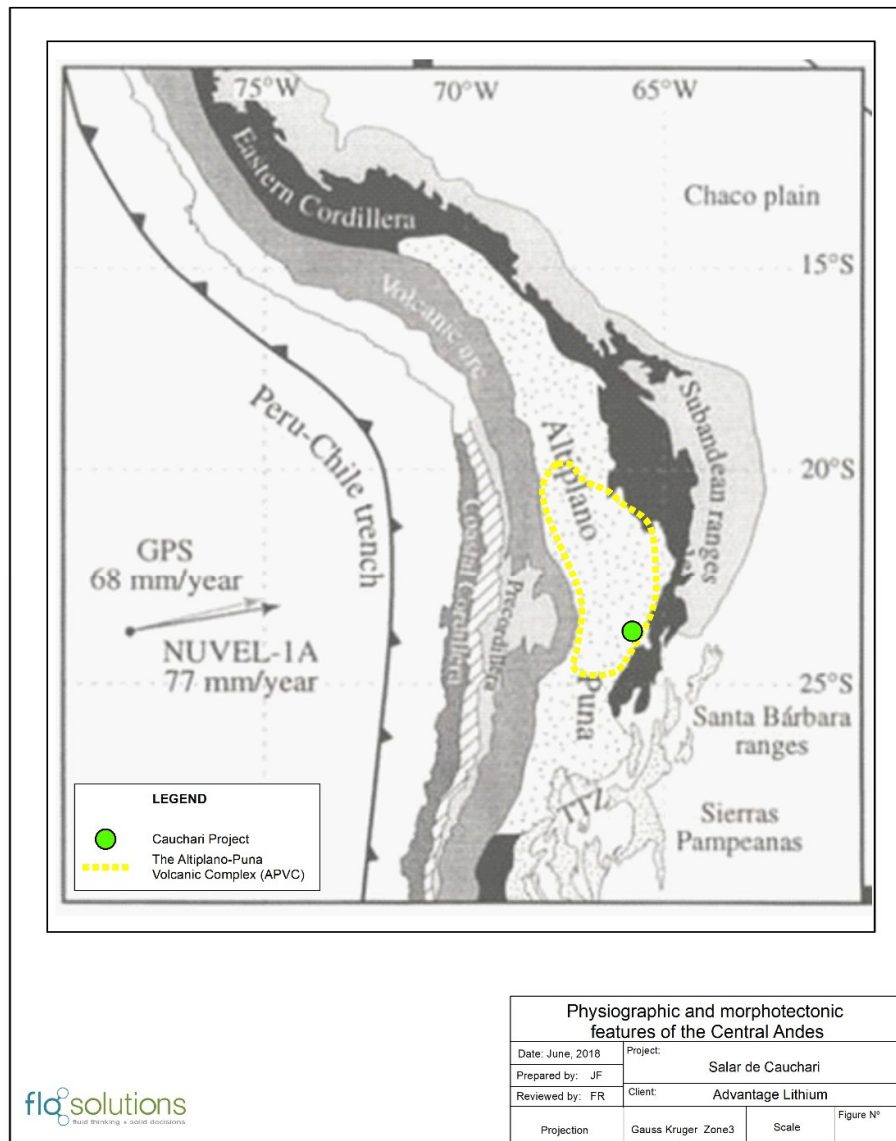


The Altiplano-Puna Volcanic Complex (APVC) is shown on Figure 5.2 and is associated with numerous stratovolcanoes and calderas. Investigations have shown that the APVC is underlain by an extensive magma chamber at 4-8 km depth (de Silva et al., 2006).

The physiography of the region is characterized by generally north-south trending basins and ranges, with canyons cutting through the Western and Eastern Cordilleras. There are numerous volcanic centers in the Puna, particularly in the Western Cordillera, where volcanic cones are present along the border of Chile and Argentina.

Dry salt lakes (salars) in the Puna occur within many of the closed basins (see Figure 5.2 below), which have internal (endorheic) drainage. Inflow to these salars is from summer rainfall, surface water runoff and groundwater inflows. Discharge is through evaporation.

Figure 5.2 Physiographic and morphotectonic features of the Central Andes

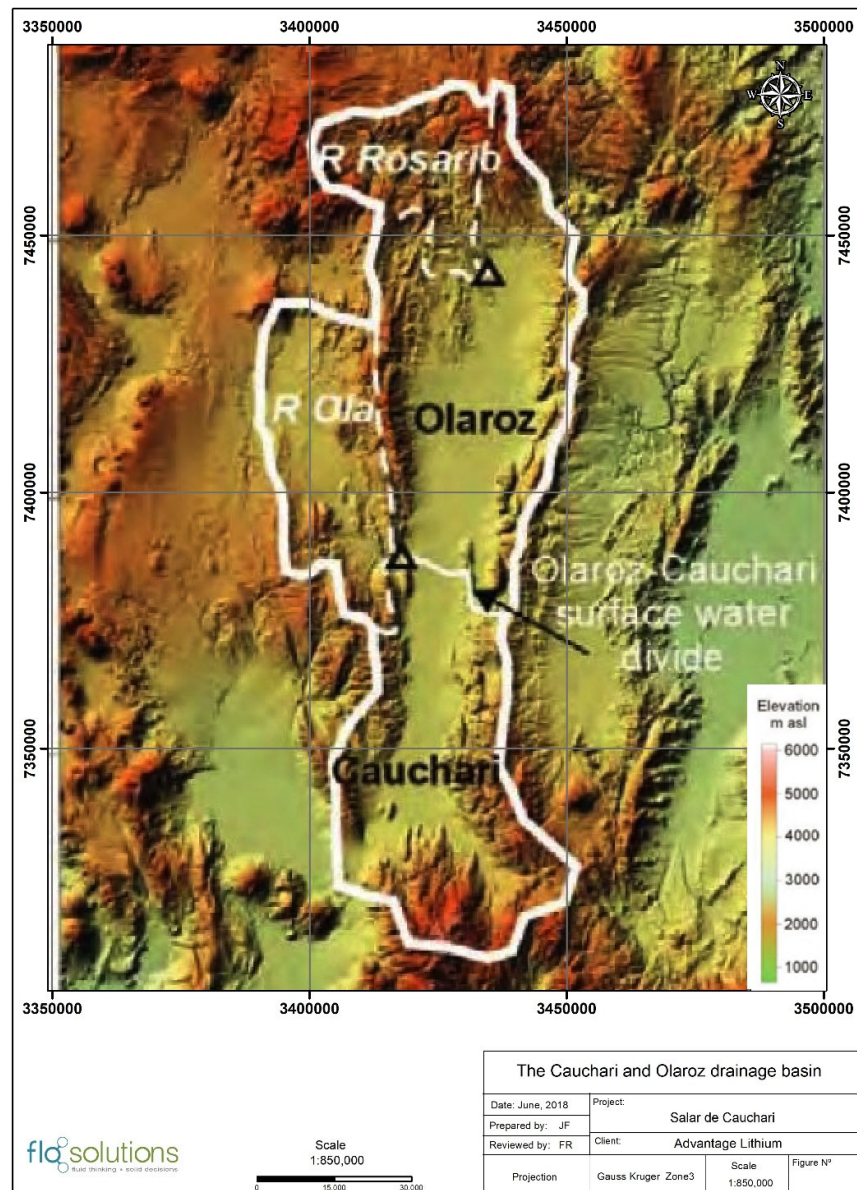


Key physiographic observations regarding the Cauchari salar include:

- The drainage divide between the Cauchari salar to the south and the Olaroz salar to the north is coincident with the international Hwy RN 52 crossing between these salars and continuing west to link Argentina to Chile at the Jama pass.
- The large Archibarca alluvial fan is present on the western side of Salar de Cauchari. The eastern side of the Salar hosts smaller alluvial fans entering the basin.
- The Tocomar River enters from the south into the Cauchari basin and flows north towards the nucleus of the Salar. Hot springs are reported in the head water of the river in the southeastern extent of the basin.
- The Cauchari drainage basin covers some 6,000 km<sup>2</sup> with the nucleus of the Salar covering approximately 250 km<sup>2</sup> as shown in Figure 5.3



Figure 5.3 The Cauchari and Olaroz drainage basin



## 5.4. Climate

The climate in the Project area is severe and can be described as typical of a continental, cold, high altitude desert, with resultant scarce vegetation. Daily temperature variations may exceed 25°C. Solar radiation is intense, especially during the summer months of October through March, leading to high evaporation rates. The rainy season is between the months of December to March. Occasional flooding can occur in the Salar during the wet season and may limit some mining activities.

Limited historical climate data are available for the Project and surrounding areas. Orocobre and Lithium Americas Corporation (LAC) operate weather stations in Salar de Olaroz and Cauchari, respectively since 2010. The climatic conditions are attractive for solar evaporation processes as demonstrated by the FMC and Orocobre lithium operations.

### 5.4.1. Rainfall

The rainy season is between the months of December to March when most of the annual rainfall occurs often in brief convective storms that originate from Amazonia to the northeast. The period between April and November is typically dry. Annual rainfall tends to increase towards the northeast, especially at lower elevations. Significant control on annual rainfall is exerted by ENSO (El Niño-Southern Oscillation) (Houston, 2006a) with significant yearly differences in rainfall linked to ENSO events.

Table 5.1 lists local rainfall data available from stations at the Olaroz pilot plant (20 km north), Susques (50 km northeast), Olacapato (50 km south), La Quaica (210 km north-northeast), Mina Pan de Azucar (140 km north-northeast) and Salar de Hombre Muerto (200 km south). Based on the historical data, location and elevation, Houston (2011) calculated that a mean long-term annual rainfall of 130 mm is probable for Salar de Olaroz. The Olaroz station shows an average annual precipitation of 49 mm over the 2008-2009 period (this data is incomplete; and actual rainfall is likely to be closer to 130 mm/yr as estimated by Houston in 2011). Considering the proximity of the Salar de Cauchari salar to Olaroz a similar rainfall would be expected.

Figure 5.4 Lines of iso-precipitation in Jujuy/Northern Salta

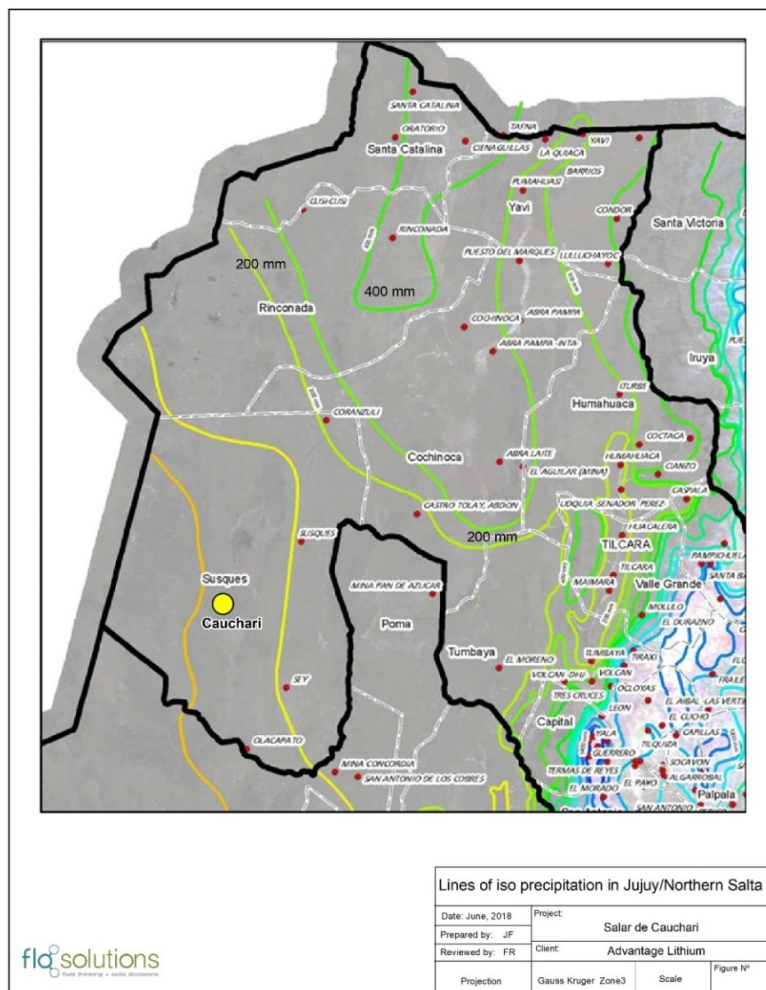


**Table 5.1 Average monthly rainfall (mm)**

| Olaroz project weather station, 30 km north of Project (3,900 masl) 2008-2016 |      |      |      |     |     |     |     |     |      |      |      |          |
|---|------|------|------|-----|-----|-----|-----|-----|------|------|------|----------|
| Jan   | Feb  | Mar  | Apr  | May | Jun | Jul | Aug | Sep | Oct  | Nov  | Dec  | Total mm |
| 19  | 15.5 | 9.4  | 0    | 0   | 0   | 0   | 0   | 0   | 0    | 0    | 5    | 48.9*    |
| Hombre Muerto salar, 180 km south of Project (4,000 masl) 2008-2009           |      |      |      |     |     |     |     |     |      |      |      |          |
| Jan   | Feb  | Mar  | Apr  | May | Jun | Jul | Aug | Sep | Oct  | Nov  | Dec  | Total mm |
| 8.7   | 17.1 | 25.2 | 0    | 0   | 0   | 0   | 0   | 0   | 2.4  | 4.2  | 17   | 74.6     |
| Susques, 50 km northeast of Project (3,675 masl) 1982-1990                    |      |      |      |     |     |     |     |     |      |      |      |          |
| Jan   | Feb  | Mar  | Apr  | May | Jun | Jul | Aug | Sep | Oct  | Nov  | Dec  | Total mm |
| 53.3  | 58.3 | 30.4 | 0.6  | 0   | 0   | 0   | 0   | 0   | 0.3  | 16   | 29.1 | 188.1    |
| La Quaica, 210 km north northeast of Project (3,442 masl) 1982-1990           |      |      |      |     |     |     |     |     |      |      |      |          |
| Jan   | Feb  | Mar  | Apr  | May | Jun | Jul | Aug | Sep | Oct  | Nov  | Dec  | Total mm |
| 80.3  | 72.6 | 52.4 | 11.8 | 0   | 0   | 0   | 0   | 0   | 12.8 | 35.2 | 73.9 | 339      |
| Mina Pan de Azucar, 140 km northeast of Project (3,690 masl) 1982-1990        |      |      |      |     |     |     |     |     |      |      |      |          |
| Jan   | Feb  | Mar  | Apr  | May | Jun | Jul | Aug | Sep | Oct  | Nov  | Dec  | Total mm |
| 100.6   | 100  | 66.4 | 19.7 | 0   | 0   | 0   | 0   | 0   | 6.7  | 76.3 | 87.9 | 457.6    |
| Olacapato, 50 km south of Project(3,820 masl) 1950-1990                       |      |      |      |     |     |     |     |     |      |      |      |          |
| Jan   | Feb  | Mar  | Apr  | May | Jun | Jul | Aug | Sep | Oct  | Nov  | Dec  | Total mm |
| 34  | 23   | 4    | 0    | 0   | 0   | 0   | 0   | 0   | 0    | 0    | 10   | 71       |

\* Incomplete data

#### 5.4.2. Temperature

Table 5.2 shows temperature data for stations around the Project including Susques and Olaroz. The Olaroz station shows average monthly temperatures throughout the year from 4°C in July to 14°C in February based on data collected between Dec 2012 and Aug 2016.

**Table 5.2 Average monthly temperature (°C)**

| Olaroz project (3,900 masl) Dec 2012 – Aug 2016                 |      |      |      |      |      |      |      |      |      |      |      |      |      |
|---|------|------|------|------|------|------|------|------|------|------|------|------|------|
| Month   | Jan  | Feb  | Mar  | Apr  | May  | Jun  | Jul  | Aug  | Sep  | Oct  | Nov  | Dec  |      |
| Mean  | 12.8 | 14.1 | 11.6 | 10.8 | 6.9  | 5.1  | 4.3  | 5.3  | 5.5  | 9.3  | 11.5 | 13.0 | 9.2  |
| Maximum   | 22.9 | 24.1 | 21.9 | 21.6 | 19.1 | 15.5 | 13.4 | 16.8 | 17.9 | 21.2 | 22.6 | 24.1 | 20.1 |
| Minimum   | 2.7  | 4.1  | 1.4  | -0.8 | -5.2 | -5.3 | -4.9 | -6.3 | -7.0 | -2.7 | 0.4  | 1.9  | -1.8 |
| Susques Temp, 50 km northeast of Project (3,675 masl) 1972-1996 |      |      |      |      |      |      |      |      |      |      |      |      |      |
| Mean*   | 11.3 | 11.2 | 10.5 | 8.1  | 4.9  | 3.0  | 2.5  | 4.6  | 6.6  | 8.9  | 10.4 | 11.1 | 7.8  |
| Other Jujuy and Puna area data                                  |      |      |      |      |      |      |      |      |      |      |      |      |      |
| Month   | Jan  | Feb  | Mar  | Apr  | May  | Jun  | Jul  | Aug  | Sep  | Oct  | Nov  | Dec  |      |
| La Quiaca   | 12.3 | 12.0 | 12.2 | 10.0 | 6.4  | 3.9  | 4.1  | 5.8  | 8.6  | 10.4 | 12.0 | 12.2 | 9.2  |
| Abra Laite  | 11.3 | 11.2 | 10.5 | 8.2  | 5.1  | 3.2  | 2.7  | 4.7  | 6.6  | 8.9  | 10.4 | 11.0 | 7.8  |
| Barrios   | 11.9 | 11.7 | 11.2 | 9.0  | 6.1  | 4.2  | 3.7  | 5.7  | 7.5  | 9.8  | 11.1 | 11.6 | 8.6  |
| Cangrejillos  | 11.6 | 11.5 | 10.2 | 7.5  | 4.0  | 1.6  | 1.1  | 3.3  | 5.4  | 7.8  | 10.1 | 11.4 | 7.1  |
| Castro Tolay Abdon  | 12.4 | 12.2 | 11.5 | 9.1  | 6.0  | 4.0  | 3.4  | 5.6  | 7.6  | 10.0 | 11.5 | 12.2 | 8.8  |
| Abra Pampa  | 11.8 | 11.8 | 11.5 | 10.6 | 6.5  | 4.0  | 3.9  | 6.1  | 8.5  | 10.5 | 11.8 | 12.2 | 8.0  |
| Susques   | 10.8 | 10.6 | 10.2 | 8.3  | 5.0  | 2.3  | 2.0  | 3.8  | 6.1  | 9.8  | 10.3 | 11.1 | 7.5  |
| Tres Cruces   | 10.3 | 10.2 | 9.7  | 8.5  | 5.4  | 3.3  | 3.1  | 5.1  | 7.4  | 9.0  | 10.5 | 10.7 | 7.8  |
| Cieneguillas  | 10.7 | 10.7 | 10.3 | 8.2  | 5.3  | 3.5  | 2.9  | 4.8  | 6.5  | 8.8  | 10.0 | 10.5 | 7.7  |
| Cochinoca   | 11.2 | 11.0 | 10.5 | 8.3  | 5.2  | 3.4  | 2.8  | 4.8  | 6.7  | 9.0  | 10.3 | 10.9 | 7.8  |
| Condor  | 10.0 | 10.0 | 9.6  | 7.5  | 4.5  | 2.8  | 2.1  | 4.1  | 5.8  | 8.0  | 9.3  | 9.8  | 7.0  |
| Coranzuli   | 9.1  | 9.1  | 8.6  | 6.4  | 3.3  | 1.6  | 0.9  | 3.0  | 4.8  | 6.9  | 8.3  | 8.9  | 5.9  |

The average annual temperature at Olaroz is approximately 9° C, with extremes between 25° C and -19° C across the year. Conditions are expected to be very similar at Cauchari.

### 5.4.3. Wind

Strong winds are frequent in the Puna, reaching speeds of over 100 km/hr on rare occasions at Olaroz, with an average of 15 km/hour. The wind during summer is generally pronounced after midday and usually calm during the night. During winter wind velocities are generally higher than the summer. Wind speed data for several stations in the Puna are presented in Table 5.3.

**Table 5.3 Average monthly wind velocity (km/hr)**

| Location   | Jan  | Feb  | Mar  | Apr  | May  | Jun  | Jul  | Aug  | Sep  | Oct  | Nov  | Dec  | Average |
|------------|------|------|------|------|------|------|------|------|------|------|------|------|---------|
| Purmamarca | 3.56 | 3.79 | 4.28 | 4.3  | 5.58 | 5.04 | 4.7  | 3.61 | 3.99 | 5.03 | 4.44 | 3.86 | 4.35    |
| Susques    | 2.37 | 3.38 | 4.73 | 4.62 | 6.6  | 4.38 | 1.68 | 3.61 | 4.09 | 4.44 | 2.32 | 2.62 | 3.74    |
| Olaroz     | 6.4  | 7.4  | 8.7  | 8.6  | 10.6 | 8.4  | 5.7  | 7.6  | 8.1  | 8.4  | 6.3  | 6.6  | 7.7     |

### 5.4.4. Evaporation

No evaporation measurements have been made at the Cauchari JV, however evaporation rates are expected to be similar to those at the Olaroz Project. Class A evaporation pans with both fresh water and brine have been monitored in Olaroz since 2008. Table 5.4 contains provisional monthly evaporation data from Olaroz. Evaporation rates reach a maximum in October before the wet season when increased cloud cover leads to a reduction in evaporation. The minimum evaporation rates are during the colder months between May and August.

Average annual evaporation (1992-2001) in Salar de Hombre Muerto at the El Fenix Camp (FMC) weather station was 2,710 mm (Houston 2010 b). Evaporation decreases with increasing elevation. The highest evaporation rates from natural soil surfaces are usually associated with the marginal areas of salars where water availability is greatest (Houston, 2006b).

**Table 5.4 Olaroz - average monthly evaporation (mm)**

| Density g/cc | Jan | Feb | Mar | Apr | May | Jun | Jul | Aug | Sep | Oct | Nov | Dec | Total |
|--------------|-----|-----|-----|-----|-----|-----|-----|-----|-----|-----|-----|-----|-------|
| 1            | 383 | 331 | 356 | 307 | 201 | 213 | 221 | 242 | 332 | 461 | 421 | 433 | 3,900 |
| 1.198        | 248 | 173 | 234 | 208 | 133 | 162 | 173 | 180 | 236 | 327 | 276 | 265 | 2,614 |

## 5.5. Vegetation

Due to the extreme weather conditions in the region, the predominant vegetation is of the high-altitude xerophytic type adapted to high levels of solar radiation, winds and severe cold. The vegetation is dominated by woody herbs of low height from 0.40 - 1.5 m, grasses, and cushion plants. With high salinity on its surface, the nucleus of the salar is devoid of vegetation.

To date no specific vegetation survey has been completed out in the Project area, although this is being carried out as part of the Project's environmental assessment. However it is possible to define a number of vegetation areas based on their physiography.

### 5.5.1. Low lying areas in the vicinity of water

These environments are characterized by having vegetation cover of 70-85 %, occupying small areas (1 km<sup>2</sup> maximum) associated with water-logged soils and more or less permanent bodies of water.

### 5.5.2. Mixed steppes

Different types of steppes are recognized and may consist of *Stipa sp.*, *Festuca sp.*, and *Panicum chloroleucum*.

### 5.5.3. Bushy steppes

Three different types are recognized, depending on the dominant bush species, such as rica-rica (*Acantholippia sp.*), tall tollillar (*Fabiana densa*) and short tollillar (*Fabiana sp.*).

## 6 HISTORY

### 6.1. Historical mining and exploration activities

Salars in the Puna have historically been exploited for salt (halite) and for borates (typically ulexite); Salar de Cauchari was no exception. Exploration and exploitation efforts were generally limited to the upper three meters of the salar surface. Historical production levels of borates were generally not documented and therefore are unknown. Lithium and potassium have not been exploited on the Project mineral properties.

Fabricaciones Militares (an Argentine government agency) carried out sampling of brines from the Argentine salars in the Puna during the 1970's. The presence of anomalous Li values was detected at that time when only salt and borates were exploited.

Initial evaluation of the mineral potential of salars in Northern Argentina was also documented by Igarzábal (1984) as part of the Instituto de Beneficios de Minerales (INBEMI) investigation carried out by the University of Salta. This investigation involved limited sampling of Li, K and other elements; Salar de Cauchari showed some of the highest lithium values of 0.092% Li (and 0.52% K).

### 6.2. History of Cauchari JV ownership

The following is an overview of the history of the ownership of the mineral properties that now comprise the Cauchari JV:

- Historic borate mining was carried out in the Cauchari salar by Borax Argentina, which is now owned by Orocobre.
- The Cauchari properties were acquired by Mr Miguel Peral and Mrs Silvia Rodriguez through direct property staking (not through third-party purchases).
- Peral and Rodriguez subsequently contributed these properties to the formation of South American Salars Pty Ltd (SAS) in return for a 15% ownership in this Australian registered company. SAS is majority owned by Orocobre (85%).
- Orocobre and SAS agreed to a joint venture with Advantage Lithium Corp (AAL) in November 2016 as described in detail in Section 4.6 above.

### 6.3. 2009-2011 SAS exploration on Cauchari

- Geochemical sampling in 2009 consisting of 134 brine samples from 105 pits showed that the northern part the Salar had the most elevated lithium concentrations.
- 2009 geophysical surveys undertaken by Orocobre in Cauchari consisted of three coincident gravity and AMT lines aimed at mapping the basin geometry and depth.
- Five diamond holes and one rotary hole were drilled in the SE Sector of the Cauchari JV to a maximum depth of 248 m in 2011. Drilling equipment did not perform as required, with two of the holes abandoned at <100 m depth and only one hole reaching the target depth for the program.
- An initial inferred resource of 470,000 t of lithium carbonate equivalent (LCE) was defined from the 2011 drilling program with a NI 43-101 technical report issued in December 2016 outlining the results of the previous exploration.

Exploration work by AAL under the joint venture agreement with Orocobre was started in 2017. This report contains the results of the 2017-2018 JV work.

## 7 GEOLOGICAL SETTING AND MINERALIZATION

### 7.1. Regional geology

Salar de Cauchari is located towards the center of the Puna Plateau. The Puna is an elevated plateau in northern Argentina which has been subject to uplift along thrust systems inverting earlier extensional faults. The Puna is host to numerous large ignimbrites and stratovolcanoes. A summary evolution of the Puna is shown in Figure 7.1, after Houston (2010b)

#### 7.1.1. Jurassic-Cretaceous

The Andes have been part of a convergent plate margin since the Jurassic with both a volcanic arc and associated sedimentary basins developed as a result of eastward dipping subduction. The early island arc is interpreted to have formed on the west coast of South America during the Jurassic (195-130 Ma), progressing eastward during the mid-Cretaceous (125-90 Ma) (Coira et al., 1982).

An extensional tectonic regime existed through the late Cretaceous, generating back-arc rifting and grabens (Salfity & Marquillas, 1994). Marine sediments of Jurassic to Cretaceous age underlie much of the Central Andes.

#### 7.1.2. Late Cretaceous to Eocene

During the late Cretaceous to the Eocene (~78-37 Ma), the volcanic arc migrated east to the position of the current Precordillera (Allmendinger et al, 1997). Significant crustal shortening occurred during the Incaic Phase (44-37 Ma), (Gregory-Wodzicki, 2000) forming a major north-south watershed, contributing to the formation of coarse clastic continental sediments.

Initiation of shortening and uplift in the Eastern Cordillera of Argentina around 38 Ma, contributed to forming a second north-south watershed, with the accumulation of coarse continental sediment throughout the Puna (Allmendinger et al., 1997).

#### 7.1.3. Oligocene to Miocene Volcanism

By the late Oligocene to early Miocene (20-25 Ma), the volcanic arc switched to its current location in the Western Cordillera. At the same time, significant shortening across the Puna on reverse faults led to the initiation of separated depo-centers (Figure 7.1). Major uplift of the Altiplano-Puna plateau began during the middle to late Miocene (10-15 Ma), perhaps reaching 2,500 m by 10 Ma, and 3,500 m by 6 Ma (Garzzone et al., 2006). Coutand et. al. (2001) interpret the reverse faults as being responsible for increasing the accommodation space in the basins by uplift of mountain ranges marginal to the Puna salar basins. This is confirmed by the seismic section across Olaroz to the north of Cauchari (Figure 7.1).

Late Miocene volcanism at 5-10 Ma in the Altiplano-Puna Volcanic Complex (APVC) between 21°-24° S (de Silva, 1989), erupted numerous ignimbrite sheets, with associated caldera subsidence, and the formation of andesitic to dacitic stratovolcanoes. This volcanic activity was often constrained by NW-SE trending crustal mega-fractures, which are particularly well displayed along the Calama-Olapato-El Toro lineament passing to the south of Salar de Cauchari (Salfity & Marquillas 1994; Chernicoff et al., 2002).

#### 7.1.4. Oligocene to Miocene Sedimentation

During the early to middle Miocene red bed sedimentation is common throughout the Puna, Altiplano and Chilean Pre-Andean Depression (Jordan & Alonso, 1987). This suggests continental sedimentation was dominant at this time. With thrust faulting, uplift and volcanism intensifying in the mid to late Miocene, sedimentary basins between the thrust sheets became isolated by the thrust bounded mountain ranges. At this stage the basins in the Puna developed internal drainages, bounded by major mountain ranges to the west and east.

Sedimentation in the basins consisted of alluvial fans forming from the uplifting ranges with progressively finer sedimentation and playa sands and mudflat sediments deposited towards the low energy centers of the basins. Alonso et al., (1991) note there has been extensive evaporitic deposition since 15 Ma, with borate deposition occurring for the past 7 to 8 Ma.

Hartley et al., (2005) suggest Northern Argentina has experienced a semi-arid to arid climate since at least 150 Ma as a result of its stable location relative to the Hadley circulation (marine current). Most moisture originating in Amazonia was blocked due to Andean uplift, resulting in increased aridity in the Puna since at least 10-15 Ma.

The high evaporation level, together with the reduced precipitation, has led to increased aridity and the deposition of evaporites in many of the Puna basins.

#### 7.1.5. Pliocene-Quaternary

During the Pliocene-Pleistocene tectonic deformation took place as shortening moved east from the Puna into the Santa Barbara fault system. Coincident with this change in tectonic activity climatic fluctuation occurred with short wetter periods alternating with drier periods.

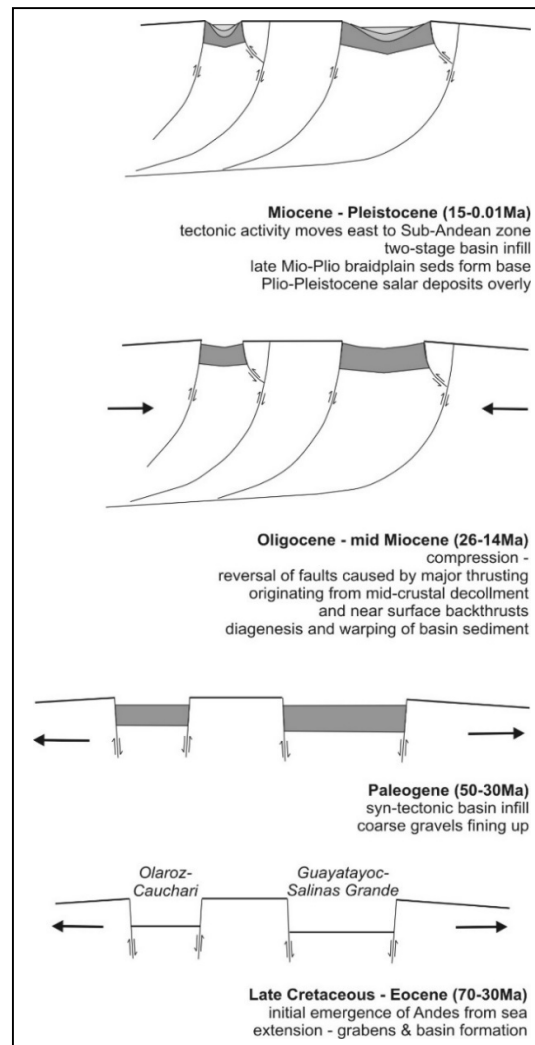
As a result of both, reduced tectonic activity in the Puna and the predominant arid conditions, reduced erosion led to reduced sediment accumulation in the isolated basins. However, both surface and groundwater inflows into the basins continued the leaching, dissolution transportation and concentration of minerals. Precipitation of salts and evaporites occurred in the center of basins where evaporation is the only means of water escaping from the hydrological system.

Evaporite minerals (halite, gypsum) occur disseminated within clastic sequences in the salar basins and as discrete evaporite beds. In some mature salars such as Salar de Hombre Muerto and Salar de Atacama thick halite sequences have formed.

Stratovolcanoes and calderas, with associated ignimbrite sheet eruptions, are located in the Altiplano and Puna extending as far south as Cerro Bonete and the Incapillo caldera. The Altiplano-Puna Volcanic Complex (APVC), located between the Altiplano (Bolivia) and Puna (Argentina), is associated with numerous of these stratovolcanoes and calderas. De Silva et al., (2006) have shown the APVC is underlain by an extensive magma chamber at 4-8 km depth.

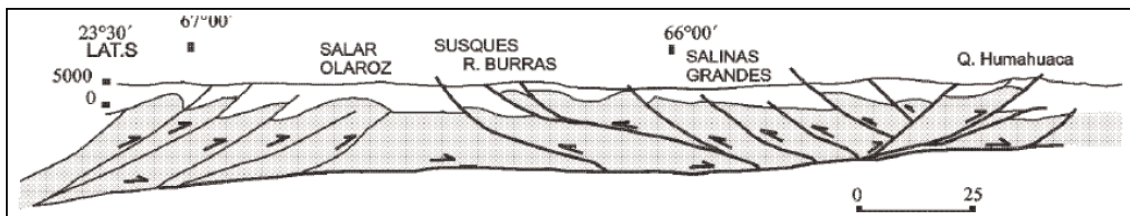


Figure 7.1 Generalized structural evolution of the Puna basins



Silicic magmas in the volcanoes Ojos de Salado (W of the Antofalla Salar), Tres Cruces and Cerro Bonete reflect crustal melting and melting in the thickening mantle wedge after the passage of the Juan Fernandez ridge. Volcanics of Pliocene to Quaternary age are present in the Project area.

Figure 7.2 Structural section between Olaroz Salar and Salinas Grandes Salar



## 7.2. Local geology

The published geological maps covering the Cauchari JV area are shown in Figure 7.3, with north-south trending belts of Ordovician and Cretaceous sediments forming the higher mountain ranges on the basin margins and younger Tertiary terrestrial sediments further within the basin, closer to the

Cauchari salar. A description of individual geological units in the Cauchari basin is provided in the stratigraphic column in Figure 7.4. The information obtained from the detailed logs of the boreholes drilled during the 2011 and 2017/8 campaigns was used to prepare the geological sections shown in Figures 7.5 and 7.6. The geological model is based on the interpretation of the logging that followed an internal classification system as in Table 7.1.

**Table 7.1 AAL internal classification used for core logging**

| CODE   |                  | DESCRIPTION   |
|--------|------------------|---|
| NR     | No Recovery      | Non-recovered material.   |
| GRA    | Gravel           | Gravel, coarse sediment with clasts over 4 mm.                                      |
| SND    | Sand             | Fine, medium to coarse sand with scarce to no matrix.                               |
| SNDMX  | Sand with Matrix | Sand layers with silt or clayey silt matrix.  |
| SNDHL  | Sand with Halite | Halite levels with sand interstitial or layers interbedded.                         |
| CLY    | Clay             | Clay, silty clays in general.   |
| CLYHL  | Clay with Halite | Clay with presence of crystalline halite in variable proportions.                   |
| SILT   | Silt             | Silt or clayey silt in general.   |
| SILTHL | Silt with Halite | Silt and clayey silt with presence of crystalline interstitial halite.              |
| HAL    | Halite           | Massive or granular crystalline halite with sparse proportions of clastic material. |

Six major lithological units were identified and are included in the geological conceptual model as shown in Figure 7.5.

Figure 7.3 Published geology of Salar de Cauchari

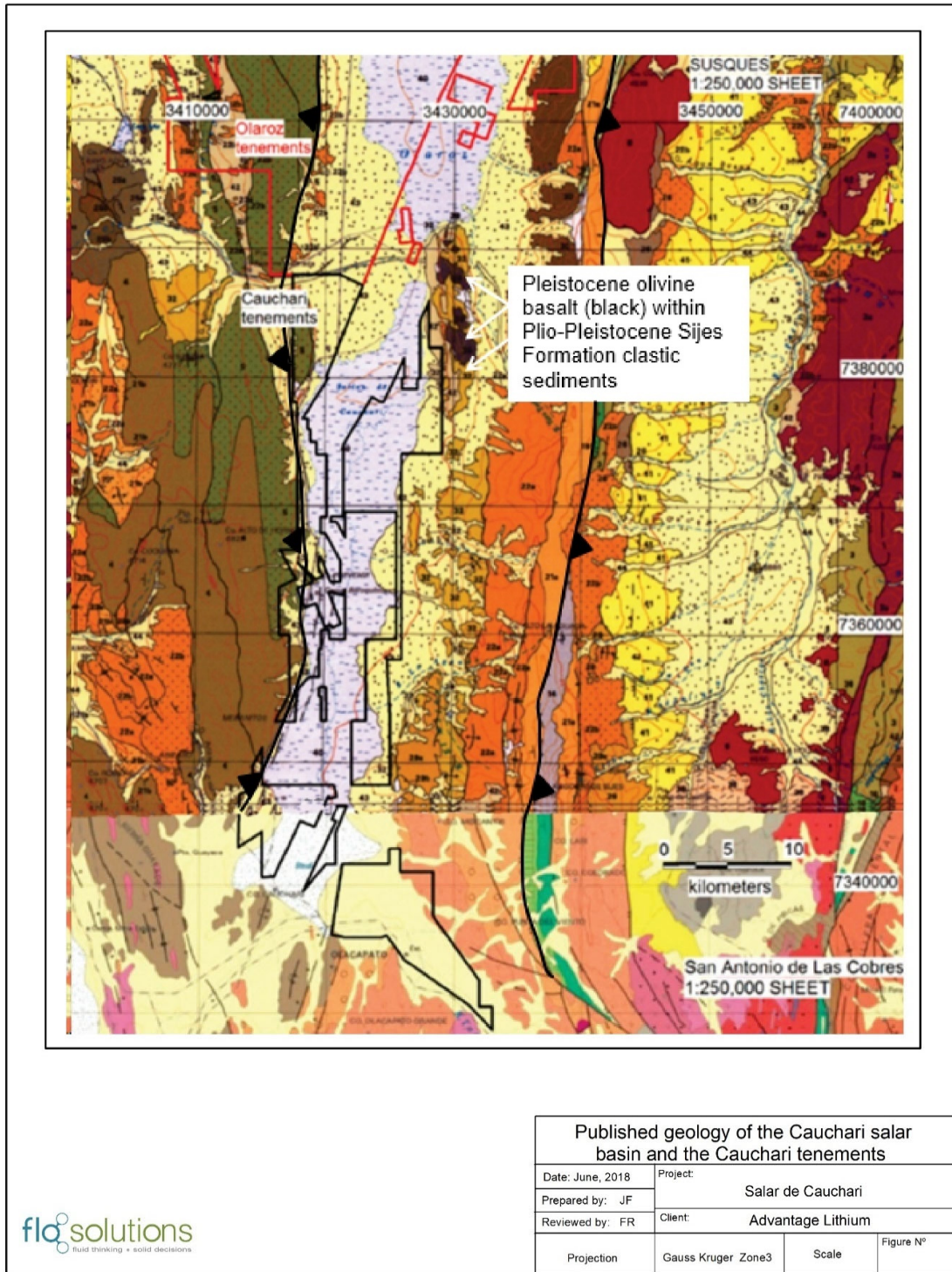


Figure 7.4 Stratigraphic units in the Cauchari basin and their correlation across different published geological maps

| Age period                                    | Ma                       | Rock types   | Geological environment                                     | Tectonic events  | 1:250,000 Map Sheet  |  |  |
|---|--------------------------|--|--|--|--|--|--|
|   |                          |  |  |  | Susques (2366-III)   | San Martín (2366A)   |  |
| Quaternary                                    | Holocene                 | Alluvial deposits, salars                                    | Closed basins, salars                                      | Post Quechua deformation   | Salar deposits, lacustrine, colluvial and alluvial sediments (40-44)                       | Salar deposits, lacustrine, colluvial and alluvial sediments (25-30)   |  |
|   | Pleistocene              | Alluvial, colluvial, lacustrine, ignimbrites                 | Closed basins, fan deposits, volcanic centres              | NE-SW shortening (from 0.2 Ma) due to strike-slip faulting continuing to present day   | Tuzgle ignimbrite (38-39)  | Alluvial and glacial deposits (5a, 25b, 26)  |  |
| Neogene                                       | Pliocene                 | Continental sediments +/- ignimbrites                        | Some volcanic complexes developed in continental sediments | Major volcanic centres and calderas 8-6 Ma   | Jama volcanic rocks (36-37). Andesite, dacite lavas, ignimbrites; Atana ignimbrite         | Mallar, Uquia and Jujuy Formations. Continental sediments - sandstone, conglomerate +/- mudstone (19, 22-24)   |  |
|   |                          | Andesitic to dacitic volcanics                               | Volcanic complexes in continental sediments                |  | Volcanic complexes (35)  | Start of thrusting, with WNW-ESE directed thrusting from 13-4 Ma   | Formations Oran (16 Ma - 0.25 Ma), Callegua, Formación Agua Negra. Continental sandstones, with clay interbeds (19, 20-21) |
|   |                          | Ignimbrites  |  | Coyaguayma & Casabindo dacite ignimbrites (33 & 34)  |  |  |  |
|   |                          | Continental sediments & tuffs                                |  | Sijas Formation (32) ~7-6.5 Ma sandstones, mudstones and tuffs   |  |  |  |
|   | Miocene                  | Continental sediments, tuffs, volcanic breccias              |  | Chimpa volcanic complex (31) andesites & dacites, lavas/ignimbrites. Pastos Chicos Fm ~10-7 Ma with unnamed tuff 9.5.  |  |  |  |
|   |                          | Dacite domes, pyroclastics, intrusives                       |  | Yungara dacite domes (30) & subvolcanics (SE side Claroz)  |  |  |  |
|   |                          | Rhyolitic, dacitic volcanic complexes, continental sediments |  | Volcanic complexes (23-29), Cerro Morado, San Pedro, Páirique, Cerro Bayo and Aguiliri, Pucara Formation. Andesite to dacite lavas, domes and ignimbrites. Susques Ignimbrite ~10 Ma |  |  |  |
|   |                          | Continental sediments  |  | Vichacera Superior (22b). Sandstones and conglomerates, with tuffs & ignimbrites   |  |  |  |
|   |                          |  |  | Vichacera Inferior (22a). Sandstones and interbedded claystones  |  |  |  |
|   |                          | 23.8   |  |  | End of Quechua phase event finished by 9-15 Ma, with associated folding                    |  |  |
| Paleogene                                     | Oligocene                | Continental sediments  | Red bed sequences  | Incaic Phase II - Compression, resulting in folding  | Rio Grande Fm Superior (21b). Red aeolian sandstones                                       |  |  |
|   | Eocene                   | Continental sediments, locally marine and limey              | Local limestone development, local marine sequences        |  | Rio Grande Fm Inferior (21a). Alternating coarse conglomerates and red sandstones          | Santa Barbara subgroup. (17) continental limy sandstones, siltstones, claystones   |  |
|   |                          | 55.8   |  |  |  | Balbuena subgroup (16). - see below  |  |
| <b>BASEMENT - PRE-TERTIARY UNITS (MARINE)</b> |                          |  |  |  |  |  |  |
| Mesozoic                                      | Cretaceous               | Continental sediments, locally marine and limey              |  | Peruvian phase - extension and deposition of marine sediments  | Balbuena Subgroup (19). Sandstones, calcareous sandstones, limestones, mudstones (Marine). | Balbuena subgroup (16). Continental/marine calcareous sandstones   |  |
|   |                          | Continental sediments  |  |  | Piruga Subgroup (16). Alluvial and fluvial sandstone & conglomerate                        | Piruga subgroup (15). Red sandstones, silty claystones and conglomerates   |  |
|   |                          |  |  |  | Granites, syenites, granodiorite (15, 17, 18)  | Granites, monzogranite (11-14)   |  |
| Paleozoic                                     | Carboniferous - Silurian | Marine sediments   | Marine platform and turbidite deposits                     | Isoclinal folding on NW/SE trending axes, extending to early Cretaceous  | Upper Paleozoic marine sediments (14)  | Machareti and Mandiyuti Groups (10). Sandstones, conglomeratic sandstones, siltstones and diamictites. Silurian Lipeon & Barite Formations (9). claystones and diamictites |  |
|   | Ordovician               | Marine sediments   | Marine delta and volcanic deposits/domes                   |  | Multiple Paleozoic intrusive suites (6-13)   | El Moreno Formation (8). Porphyritic dacite  |  |
|   |                          |  | Marine sediments   |  | Ordovician sandstones (3-5), volcanoclastic sediments & Ordovician turbidites              | Guayoc Chico Group (7) & Santa Victoria Groups (6). Marine sandstones, mudstones and limey units   |  |
|   | Cambrian                 |  |  |  | Meson Group (2). sandstones and mudstones  | Meson Group (5). Marine sandstones   |  |
| 540   |                          |  |  |  |  |  |  |
| PreCambrian                                   |                          | Schists, slate, phyllite                                     | Metamorphosed turbidites                                   |  | Puncoviscana Formation (1) turbidites  | Puncoviscana Formation (1) turbidites - metamorphosed and intruded by plutons  |  |

Figure 7.5 W-E section looking north through the Cauchari JV geological model.

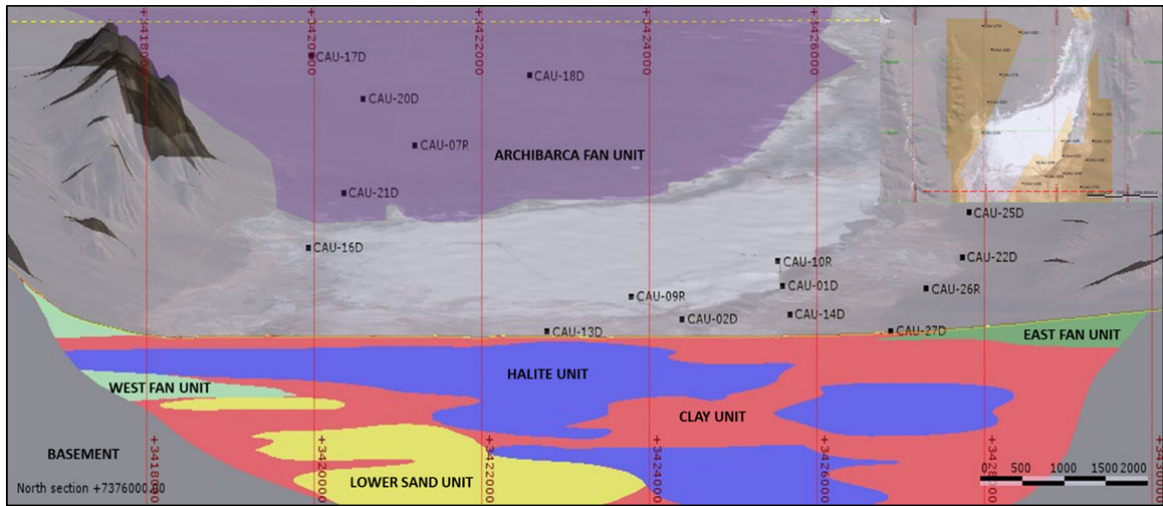


Table 7.2 provides a breakdown of the lithological composition of the units in the geological model for the Cauchari JV. A summary description of each of the geological units is provided hereafter.

Table 7.2 Lithology of the units in the Cauchari geological model

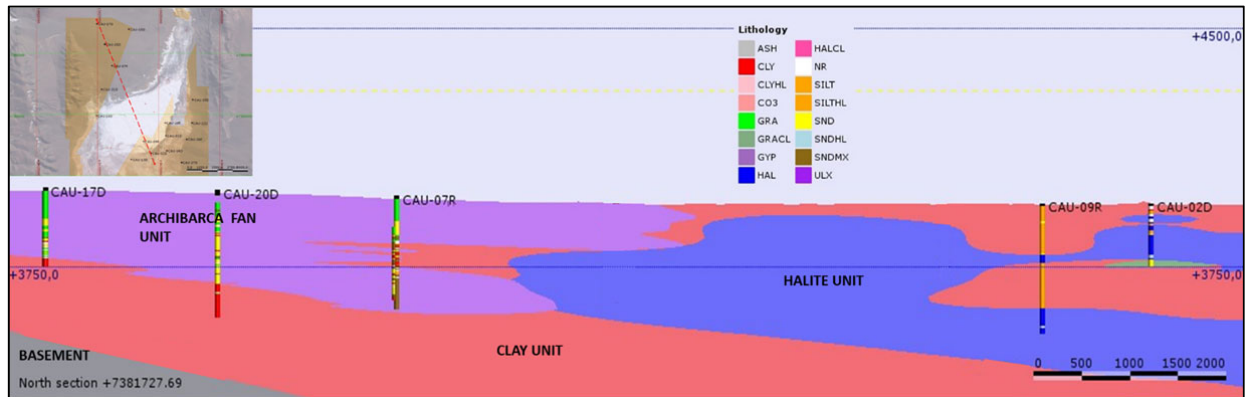
| UNIT/LITHO     | HAL    | CLY    | CLYHL | NR     | SND    | SNDHL | GRA    | SNDMX  | SILT   | SILTHL | ASH   | TOTAL  |
|----------------|--------|--------|-------|--------|--------|-------|--------|--------|--------|--------|-------|--------|
| CLAY           | 1.11%  | 68.77% | 3.73% | 3.09%  | 1.21%  | 0.12% | 0.01%  | 6.22%  | 10.70% | 5.01%  | 0.03% | 36.32% |
| HALITE         | 77.81% | 3.99%  | 9.70% | 1.63%  | 0.95%  | 2.95% |        | 0.69%  | 0.78%  | 1.51%  |       | 35.09% |
| ARCHIBARCA FAN |        | 3.02%  |       | 5.28%  | 31.76% |       | 34.09% | 24.45% | 1.00%  |        | 0.39% | 10.76% |
| EAST FAN       |        | 2.61%  |       | 4.50%  | 59.16% |       | 13.99% | 19.74% |        |        |       | 1.77%  |
| WEST FAN       | 0.03%  | 4.08%  |       | 19.87% | 36.01% |       | 10.98% | 28.95% | 0.07%  |        |       | 11.17% |
| LOWER SAND     | 0.58%  | 11.62% |       | 15.47% | 35.60% |       | 1.54%  | 35.20% |        |        |       | 4.89%  |
| TOTAL          | 27.74% | 27.78% | 4.76% | 5.32%  | 11.00% | 1.08% | 5.22%  | 10.44% | 4.28%  | 2.35%  | 0.05% |        |

### 7.2.1. Archibarca fan unit

The Archibarca alluvial fan constitutes the NW boundary to the salt deposits within the Salar de Cauchari and covers a surface area of around 23.8 km<sup>2</sup> within the AAL properties, extending north into properties owned by Orocobre. This unit is the surface divide between the Salar de Olaroz basin to the North and the Salar de Cauchari basin to the South.

The boreholes (CAU07R, CAU17D, CAU18D, CAU20D and CAU21D) drilled on the Archibarca fan intercepted coarse materials (sandy gravels and gravelly sand with coarse sand levels), overlapping and interfingering at greater than 200 m depth with saline / lacustrine deposits (Clay and Halite Unit) as shown in Figure 7.6. This suggests that the Archibarca fan unit overlies salar sediments above this depth.

**Figure 7.6 W-E section looking north, showing the progressive inter-fingering of the Archibarca fan with the Clay and Halite units**



The unit is characterized by a thick sequence of coarse sediments consisting of medium to coarse gravels which in turn are formed by clasts of gray quartzite and greenish-white clasts of quartz, basalts and graywackes transported downslope from the west. The clasts range from sub-angular to rounded with the presence of medium to coarse sand in variable proportions and with the presence of clay in some sandy and/or gravelly levels as shown in Figure 7.7. The alluvial fan gravel is commonly interbedded with thick layers of medium to coarse sand inter-fingered with levels of clay.

**Figure 7.7 Sandy gravels with some clay from the Archibarca fan (CAU07R)**



### 7.2.2. West Fan unit

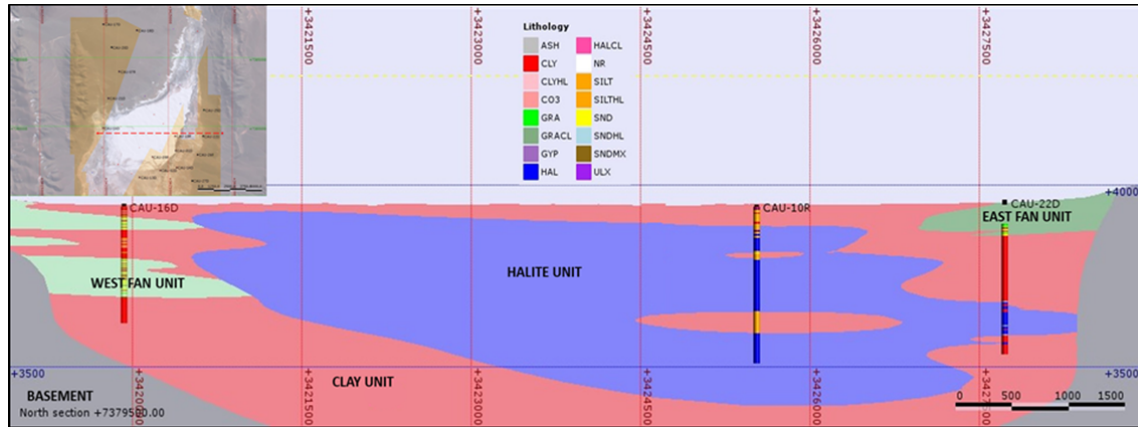
The piedmont developed at the base of the mountain range that constitutes the western boundary of Salar de Cauchari is dominated by a series of small alluvial fans that inter-finger with the saline / lacustrine sediments (Clay Unit) of the salar as shown in Figure 7.8.

Boreholes CAU16D and CAU15D were drilled along the western boundary of the Salar in the northern part of the West Fan. These boreholes intersected inter-fingering clayey levels (Clay unit) with thick intervals of sand and sandy silt with a few levels of sandy gravel.

Boreholes CAU23D, CAU24D, CAU28D and CAU29D were drilled in the southern part of the West Fan and intersect thick levels of sand, silty sand and gravel sequences at depth (200 m approx.)

interbedded with clay and halite levels (CAU24D). The sequence of coarse materials (sands and gravels) becomes thicker towards the south (CAU29D) where wide alluvial fans develop extending to the maximum depth of drilling (404 m in CAU29).

Figure 7.8 W-E section look north between boreholes CAU16D and CAU10R



The West Fan is dominated by fine to medium gray-green to dark green sands with abundant presence of gypsum crystals (Selenite), quartz and dark lithic material. The sands are interbedded with levels of medium to coarse gravel with sub-rounded clasts in a sandy matrix formed by the greenish quartzites and volcanic lithic material, with fragments from 1 to 8 cm in size as shown in Figure 7.9.

Figure 7.9 ravel from CAU16D (264.5-268m) with sub-rounded green quartzites



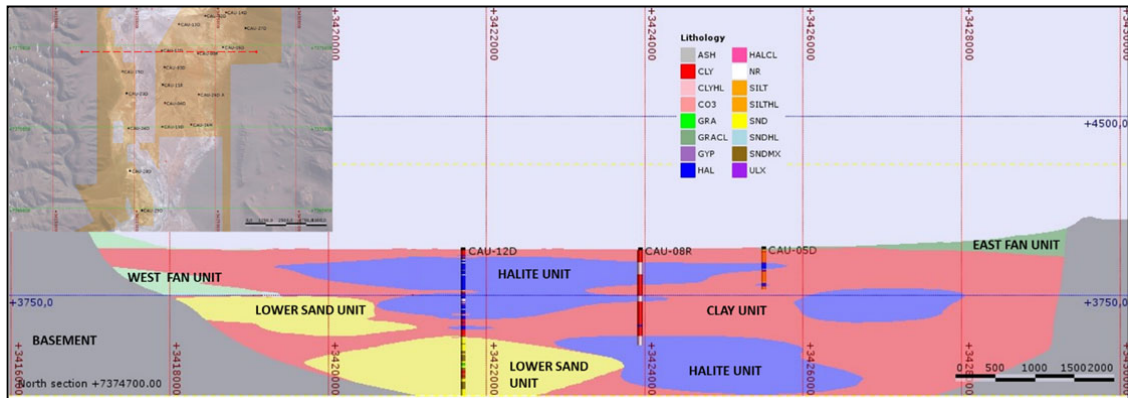
### 7.2.3. East Fan unit

To the eastern boundary of the Cauchari basin is dominated by a series of fluvial/alluvial fans with a variable extension. Boreholes CAU01D, CAU02D, CAU05D, CAU10D, CAU14D, CAU22D, CAU26D/A and CAU27D intercept 3 m to 20 m thick layers of alternating friable dark sands to massive cemented grits that are interpreted as distal facies of the fans seen along the eastern margin of the Salar.

The East Fan unit is much more restricted in thickness and areal extent than the sequences observed along the western margin (West Fan Unit) with shallow/thinner sequences that overlie lacustrine / saline deposits.

Figures 7.8 and 7.10 show overlapping sequences of the East Fan unit over the saline / lacustrine units along the eastern margin of the basin.

Figure 7.10 Section showing the interpreted geometry of the East Fan unit

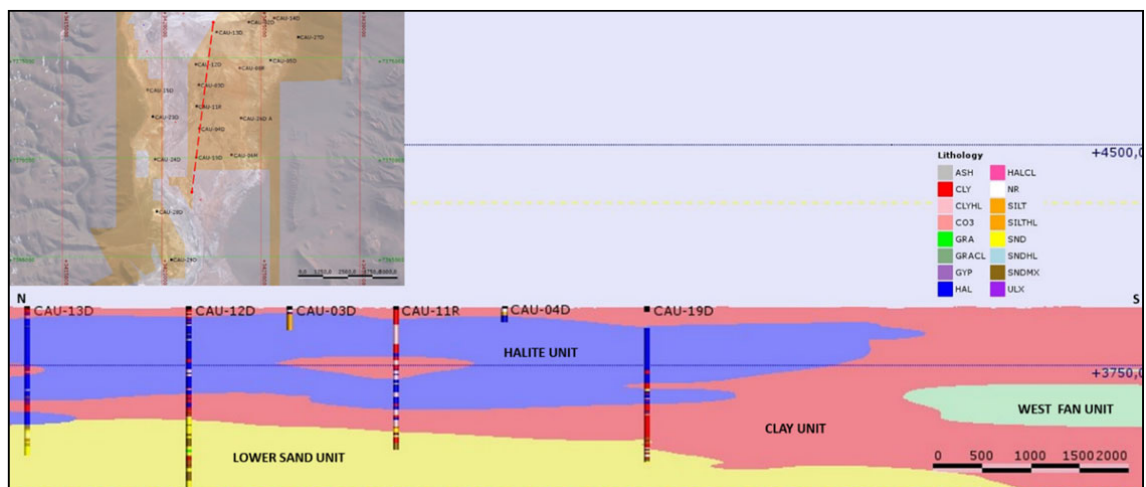


#### 7.2.4. Lower Sand unit

Boreholes CAU11R, CAU12D A, CAU13D A and CAU19D intersected a sand dominant unit at approx. 400 m depth. The bottom of this sand dominant unit was not defined in these boreholes (drilled up to 610 m depth) as shown in Figure 7.11. CAU15D on the western margin of the Salar shows sand levels with similar features to those observed in the sands before-mentioned boreholes.

With the additional borehole information, the geometry of this deep unit is still not fully defined; however the source of the sands is interpreted to be from the north.

Figure 7.11 Section with the interpreted geometry of the Lower Sand unit





The Lower Sand unit is characterized by medium, greenish gray to dark gray sand with abundant presence of friable gypsum (selenite) and lesser dark lithic and quartz crystals with some biotite (Figure 7.12). Some irregular layers with cemented carbonates or halite are also observed and that are interbedded with occasional thin reddish-brown sandy, silty and clayey layers.

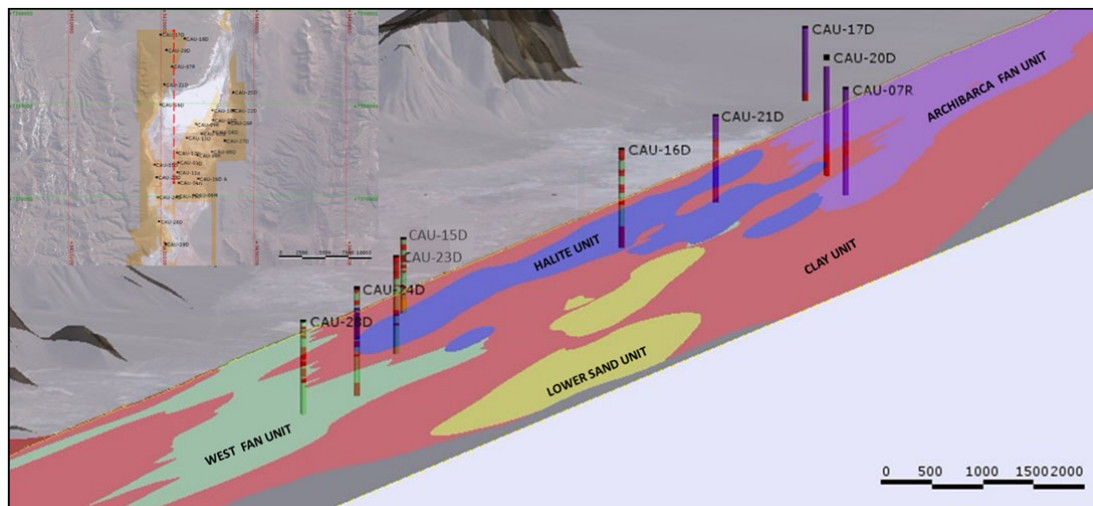
Figure 7.12 Example of the Lower Sand unit (CAU12D: 389 m)



### 7.2.5. Clay unit

The Clay unit is widely distributed throughout Salar de Cauchari and was intersected in all boreholes in the SE Sector of the Project. The Clay unit is an irregular N-S elongated body and in some boreholes (CAU08R and CAU09R) can extend to below 300 m depth. It is mainly inter-fingered with the Halite unit. The Clay unit together with the Halite unit constitutes the saline / lacustrine sediments in the center of the Salar as shown in Figure 7.13. The Clay unit appears to thicken towards the east of the Salar.

Figure 7.13 N-S section (looking NW) showing the distributions of the Clay and Halite units



The Clay unit is mainly composed of reddish or reddish brown to brown clays (Figure 7.14), silty clays and/or limey clays, with a variable content of halite crystals and ulexite nodules. To a lesser degree, some black clayey levels with a presence of organic matter and green clays were recognized. It is commonly inter-fingered with some thin levels of fine to very fine sand. Numerous crystals of twinned gypsum (selenite) are locally present forming inter-grown polycrystalline aggregates.

Figure 7.14 Example of the Clay unit (CAU12D: 177.5-179m)

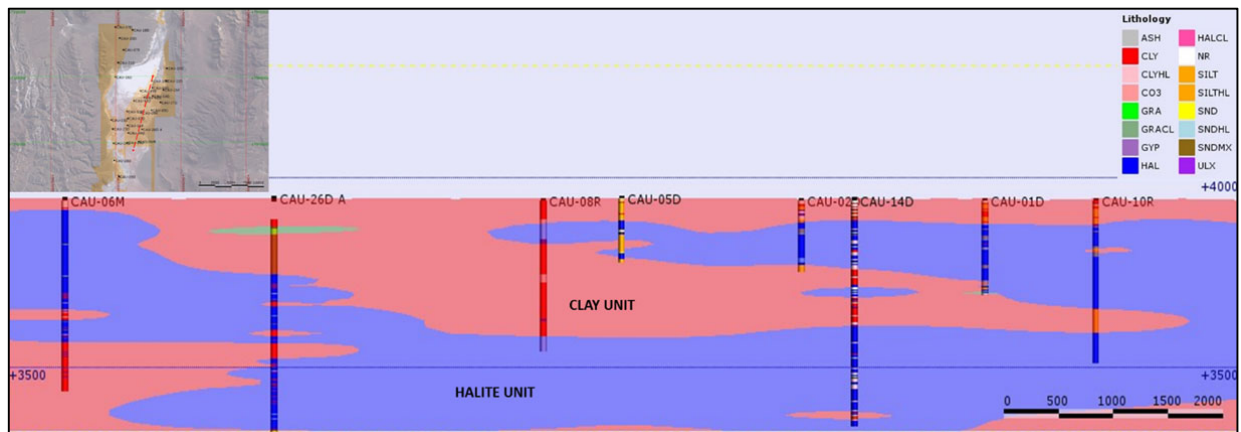


### 7.2.6. Halite unit

The boreholes in the SE Sector of the Project intersected numerous, thick and extensive levels of halite with a variable content of clastic sediments (sands and clays). These levels are interpreted as an irregular body of crystalline halite that inter-fingers with the clays (Clay unit) described above. The Halite unit thins and becomes shallower towards the western margin of the Salar.

The surface of the Salar shows a very thin halite cover (a few centimeters thick) and immediately passes to the clay core (Clay unit). The first significant halite occurs between 20 m and 35 m deep, as shown in Figure 7.15. It has an estimated thickness of 300 m in CAU13D and over 500 m in CAU14D.

Figure 7.15 NE-SW section looking west, showing the distribution of Halite and Clay units



The Halite unit is characterized by massive crystalline halite or, to a lesser extent, friable aggregates of crystals that can exceed one centimeter in size (Figure 7.16), mainly with gray to reddish brown colors, according to the associated clastic sediments (fine sands with selenite and clays and silt-clays

respectively). It is commonly inter-fingered with fine to very fine sand levels, of variable thickness, with abundant gypsum crystals (selenite) and clay layers with abundant presence of halite crystals. The halite is accompanied by crystals of mirabilite (sodium sulphate) and scarce ulexite (hydrated sodium calcium borate hydroxide). Some intervals of the halite (Figure 7.16) show enhanced permeability over the typical more compact halite material.

Figure 7.16 Example of the Halite unit



### 7.3. Mineralization

The brines from Cauchari are solutions saturated in sodium chloride with an average concentration of total dissolved solids (TDS) of 290 g/L. The average density is 1.18 g/cm<sup>3</sup>. The other components present in the Cauchari brine are: K, Li, Mg, Ca, Cl, SO<sub>4</sub> and B.

Table 7.3 shows a breakdown of the principal chemical constituents in the Cauchari brine including maximum, average, and minimum values, based on 546 brine samples used in the brine resource estimate herein that were collected from the 2011 - 2018 drilling programs.

Table 7.3 Maximum, average and minimum elemental concentrations of the Cauchari brine

| Analyte  | Li   | K     | B     | Na      | Ca    | Mg    | SO <sub>4</sub> | Density           |
|----------|------|-------|-------|---------|-------|-------|-----------------|-------------------|
| Units    | mg/L | mg/L  | mg/L  | mg/L    | mg/L  | mg/L  | mg/L            | g/cm <sup>3</sup> |
| Maximum  | 956  | 8,202 | 2,528 | 135,362 | 1,681 | 2,640 | 62,530          | 1.23              |
| Mean     | 512  | 4,349 | 941   | 105,721 | 504   | 1,323 | 18,930          | 1.19              |
| Minimum  | 157  | 101   | 62    | 101     | 174   | 314   | 101             | 1.07              |
| Std.Dev. | 144  | 1,186 | 487   | 16,033  | 212   | 412   | 8,561           | 0.03              |

Figures 14.8 and 14.9 show the kriged distribution of lithium and potassium concentrations in the Salar. Typically, concentrations of lithium and potassium show a high degree of correlation. The kriged three-dimensional distribution of lithium and potassium concentrations were used in the updated resource model as further described in Section 14.

Brine quality is evaluated through the relationship of the elements of commercial interest lithium and potassium. Components of the brine that in some respect constitute impurities, include Mg, Ca and SO<sub>4</sub>. The calculated ratios for the averaged brine chemical composition are presented in Table 7.4.

**Table 7.4 Average values (g/L) of key components and ratios for the Cauchari brine**

| K   | Li  | Mg  | Ca  | SO <sub>4</sub> | B   | Mg/Li | K/Li | (SO <sub>4</sub> +2B)/(Ca+Mg)* |
|-----|-----|-----|-----|-----------------|-----|-------|------|--------------------------------|
| 4.3 | 0.5 | 1.3 | 0.5 | 18.9            | 0.9 | 2.6   | 8.5  | 11.4                           |

\*(SO<sub>4</sub>+2B)/ (Ca+Mg) is a molar ratio

As in other natural brines in the region, such as those of the Salar de Atacama and Salar del Hombre Muerto, the Cl<sup>-</sup>, SO<sub>4</sub><sup>=</sup>, K<sup>+</sup>, Mg<sup>++</sup>, Na<sup>+</sup> ion concentrations are used to follow the crystallization of salts during the evaporation process. The known phase diagram (Janecke projection) of the aqueous quinary system (Na<sup>+</sup>, K<sup>+</sup>, Mg<sup>++</sup>, SO<sub>4</sub><sup>=</sup>, Cl<sup>-</sup>) at 25°C and saturated in sodium chloride can be used when adjusted for the presence of lithium in the brines. The Janecke projection of MgLi<sub>2</sub>-SO<sub>4</sub>-K<sub>2</sub> in mol % is used to make this adjustment. The Cauchari brine composition is represented in the Janecke Projection diagram in Figure 7.17 along with the brine compositions from other salars. The Cauchari brine composition is compared with those of Silver Peak, Salar de Atacama, Salar del Hombre Muerto, Salar de Rincon and Salar de Uyuni in Table 7.5.

**Figure 7.17 Comparison of brines from various salars in Janecke Projection**

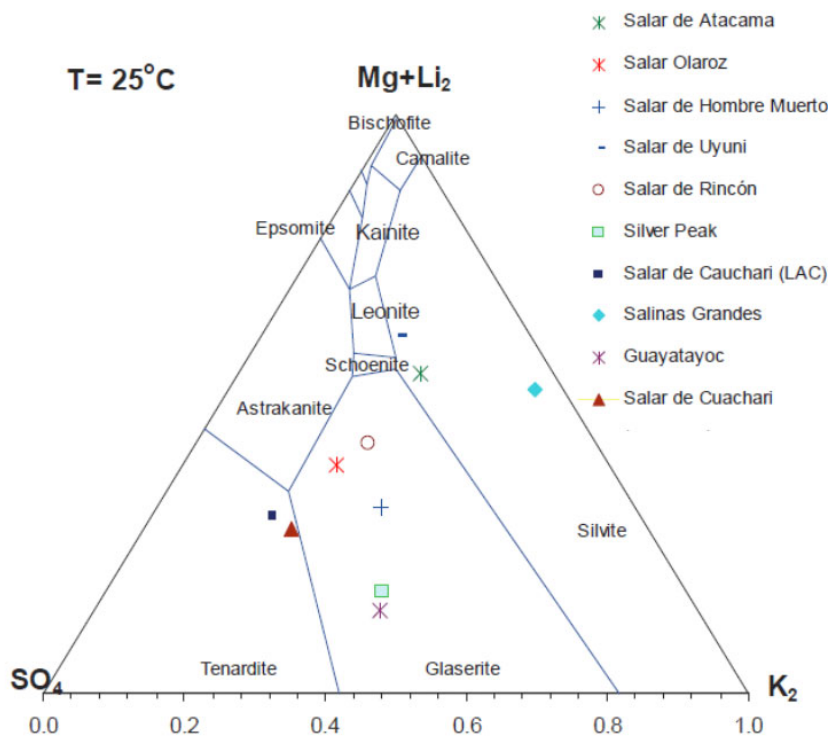


**Table 7.5 Comparison of brine composition of various salars (weight %)**

|                          | Salar de Cauchari (Argentina) | Silver Peak (USA) | Salar de Atacama (Chile) | Hombre Muerto (Argentina) | Salar de Maricunga (Chile) | Salar del Rincon (Argentina) | Salar de Uyuni (Bolivia) |
|--------------------------|-------------------------------|-------------------|--------------------------|---------------------------|----------------------------|------------------------------|--------------------------|
| <b>K</b>                 | 0.38                          | 0.53              | 1.85                     | 0.617                     | 0.686                      | 0.656                        | 0.72                     |
| <b>Li</b>                | 0.041                         | 0.023             | 0.150                    | 0.062                     | 0.094                      | 0.033                        | 0.035                    |
| <b>Mg</b>                | 0.10                          | 0.03              | 0.96                     | 0.085                     | 0.61                       | 0.303                        | 0.65                     |
| <b>Ca</b>                | 0.04                          | 0.02              | 0.031                    | 0.053                     | 1.124                      | 0.059                        | 0.046                    |
| <b>SO<sub>4</sub></b>    | 1.88                          | 0.71              | 1.65                     | 0.853                     | 0.06                       | 1.015                        | 0.85                     |
| <b>Density</b>           | 1.183                         | n.a.              | 1.223                    | 1.205                     | 1.200                      | 1.220                        | 1.211                    |
| <b>Mg/Li</b>             | 2.54                          | 1.43              | 6.40                     | 1.37                      | 6.55                       | 9.29                         | 18.6                     |
| <b>K/Li</b>              | 9.67                          | 23.04             | 12.33                    | 9.95                      | 7.35                       | 20.12                        | 20.57                    |
| <b>SO<sub>4</sub>/Li</b> | 53.04                         | 30.87             | 11.0                     | 13.76                     | 0.64                       | 31.13                        | 24.28                    |
| <b>SO<sub>4</sub>/Mg</b> | 18.78                         | 23.67             | 1.72                     | 10.04                     | 0.097                      | 3.35                         | 1.308                    |
| <b>Ca/Li</b>             | 0.382                         | 0.87              | 0.21                     | 0.86                      | 9.5                        | 1.79                         | 1.314                    |

Source: Published data from various sources

## 8 DEPOSIT TYPE

### 8.1. General

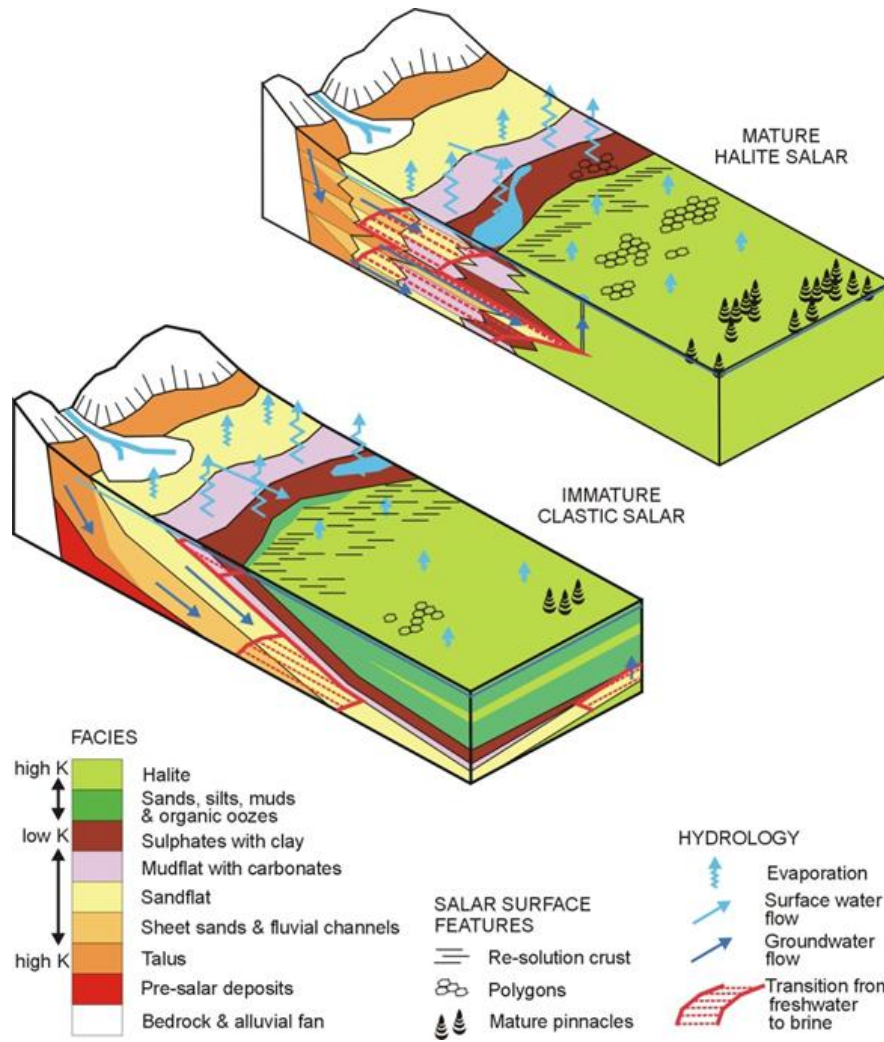
Salars occur in closed (endorheic) basins without external drainage, in dry desert regions where evaporation rates exceed stream and groundwater recharge rates, preventing lakes from reaching the size necessary to form outlet streams or rivers. Evaporative concentration of surface water over time in these basins leads to residual concentration of dissolved salts (Bradley et al., 2013) to develop saline brines enriched in one or more of the following constituents: sodium, potassium, chloride, sulfate, carbonate species, and, in some basins, metals such as boron and lithium. Salar de Cauchari is a brine deposit with enriched concentrations of lithium and potassium.

Houston et al., 2011 identified two general categories of Salars: 1) mature, halite dominant (those containing extensive thicknesses – often hundreds of meters - of halite, such as the Salar de Atacama, and the FMC Hombre Muerto operation), and 2) immature salars, which are dominated by clastic sediments with limited thicknesses of halite.

Mature salt dominated salars can have high permeability and intermediate values of specific yield near surface, with both parameters decreasing rapidly with depth. In these salars the brine resource can be within 50 m below surface.

Immature salars conversely have porosity and permeability controlled by individual layers within the salar sequence. The porosity and permeability may continue to depths of hundreds of meters in clastic salars but can be highly variable due to differences between sand and gravel units and finer grained silts and clays. The presence of different stratigraphic units in clastic salars can result in a variable distribution of the contained brine.

Figure 8.1 Model showing the difference between mature and immature salars



## 8.2. Hydrogeology

Salars generally consist of an inner nucleus of halite surrounded by marginal deposits of mixed carbonate and sulphate evaporites with fine grained clastic sediments. Coarser grained sediments generally occur on the margins of the basin, with successive inner shells of finer grained clastic units. Towards the center of the salar, sediments can show a progressive change from carbonate to sulphate and finally chloride evaporites (principally halite).

Drilling results in Cauchari to date have helped identify the following hydrogeological units:

- Alluvial fans surrounding the Salar. These are coarse grained and overall highly permeable units that drain towards the Salar. Groundwater flow is unconfined to semi-confined; specific yield (drainable porosity) is high. Water quality in the fans above the brine interface is fresh to brackish. The initial CAU07 pumping test in the NW Sector has yielded positive results and are further discussed in Section 10.4.

- A clay unit. This clay unit covers a large area over the central part of the Salar and is interpreted to extend below the alluvial fans. This clay unit has a low permeability and could locally form a hydraulic barrier. The clay contains brine in the central part of the Salar. Fresh water may sit on top of this clay unit along the edges of the Salar.
- A semi-confined to confined halite unit can be identified in the central portion of the Salar where it underlies the clay unit. Locally the halite unit is interbedded with fine grained sediment of the clay unit. Data collected to date suggest that the bulk halite unit is not very permeable, but interbedded more coarser grained clastic layer can display locally high permeabilities as seen in the CAU11 pumping test. It is host to medium- to high lithium concentration brine. The results of the CAU11 pumping test are further discussed in Section 10.4 below.
- A deep sand unit. This deep sand unit has been identified in four boreholes (CAU11, 12, 13 and 19) in the SE Sector at depths below 300 m, excluding holes that were drilled on platforms to intersect the sand at deeper levels (CAU12DA and 13DA). The unit appears to be relatively permeable based on pumping test results of CAU11 as discussed in Section 10 below. The deep sand hosts high quality lithium brine.

### 8.3. Drainable Porosity

Porosity is highly dependent on lithology. Total porosity is generally higher in finer grained sediments, whereas the reverse is true for drainable porosity or specific yield since finer grained sediments have a high specific retention (portion of fluid that cannot be extracted). The lithology within the Salar is variable with halite and halite mixed units, clay and gravel-sand-silt-clay sized mixes spanning the full range of sediment types.

Drainable porosity analyses were carried out on undisturbed core samples by laboratories GSA, DBSA and the BGS. Based on the results of these analyses, drainable porosity values were assigned to the specific lithological units defined in the geological model as described in Section 7.2. Table 8.1 summarizes the results of the porosity analysis. The analysis of drainable porosity is further discussed in Section 11.

**Table 8.1 Results of drainable porosity analyses**

| Geological Unit | No. Samples | Average | Declustered Average | Standard Deviations | Coefficient of Variation |
|-----------------|-------------|---------|---------------------|---------------------|--------------------------|
| Halite          | 144         | 0.05    | 0.05                | 0.06                | 1.1                      |
| East Fan        | 9           | 0.04    | 0.03                | 0.02                | 0.6                      |
| West Fan        | 30          | 0.11    | 0.11                | 0.06                | 0.5                      |
| Archibarca Fan  | 28          | 0.12    | 0.12                | 0.06                | 0.5                      |
| Clay            | 84          | 0.03    | 0.03                | 0.02                | 0.6                      |
| Lower Sand      | 6           | 0.16    | 0.14                | 0.11                | 0.7                      |



## 8.4. Permeability

Permeability (or hydraulic conductivity) is also a parameter that is highly dependent of lithology. Generally finer grained and well-graded sediments have a lower permeability than coarser grained poorly graded sediments. The permeability of halite can be enhanced though fracturing and solutions features. AAL has carried out pumping tests within the Salar and LAC has carried out other pumping tests in the adjacent mining properties. The analysis of the AAL pumping tests is further discussed in Section 10 below. Table 8.2 provides a general overview of the permeability values for the various hydrogeological units.

**Table 8.2 Summary of estimated permeability values**

| Unit           | Description         | K (m/d)  |
|----------------|---------------------|----------|
| Clay           | Local silt and sand | 0.01 - 1 |
| Halite         | Confined / massive  | 0.01 - 1 |
| Archibarca Fan | Confined            | 1-50     |
| Deep sand      | Confined            | 1-20     |

## 9 EXPLORATION

This section provides an overview of the geophysical exploration work that has been carried out on the Cauchari JV between 2009 and 2018 by the various owners.

### 9.1. Geophysical Surveys - 2009

Orocobre Ltd contracted Wellfield Service Ltda to undertake a gravity and audio-magnetotelluric (AMT) survey over the Cauchari JV. Three lines were conducted: one east-west line across the central properties in Cauchari, a second east-west line in the south, and third line aligned northwest along the Tocomar River in the south of the basin. The objective of the gravity survey was to obtain first order estimates of the geometry and depth of the basin, and if possible, to establish the main sedimentary sequences within the basin. The objective for the AMT survey was to define the limits of the brine body hosted in the basin sediments, and to define the brine-fresh water interface. The location of the geophysical survey lines are shown in Figure 9.1.

### 9.2. Gravity Survey - 2009

Gravity techniques measure the local value of acceleration which, after correction, can be used to detect variations in the gravitational field on the earth's surface which may then be attributed to the density distribution in the subsurface. As different rock types have different densities, it is possible to infer the likely subsurface structure and lithology, although various combinations of thickness and density can produce the same measured density; resulting in multiple possible models for layers in the salar (referred to as non-unique solutions to the gravity data).

#### 9.2.1. Data acquisition

Gravity data was acquired at 200 m spaced stations which were surveyed with high precision GPS equipment. A Scintrex CG-5 gravimeter (the most up-to-date equipment available) was used, and measurements were taken over an average 15 minute period in order to minimise noise. A base station was established with readings taken at the beginning and end of each day's activities in order to establish and subsequently correct for the effects of instrument drift and barometric pressure changes. The daily base stations were referred to the absolute gravity point PF-90N, close to Salta, where a relative gravity of 2,149.14 mGal was obtained. Since this point is distant from Cauchari, intermediate stations were used to transfer the absolute gravity to Pastos Chicos where a relative gravity base station was established with a value of 1,425.31 mGal.

A differential GPS was used to survey the x, y, and z coordinates of the gravity stations (Trimble 5700). This methodology allows centimeter accuracies with observation times comparable to or less than the corresponding gravity observation. The gravity station position data was recorded using a mobile GPS (Rover). Another GPS (Fixed) at the fixed base station recorded data simultaneously to correct the Rover GPS. The Fixed and Rover GPS units were located within a radius of 10 to 20 km of each other. Both data sets were post-processed to obtain a vertical accuracy of 1 cm.

#### 9.2.2. Data processing

In order to arrive at the complete Bouguer anomaly which can be used to interpret the subsurface the following corrections to the acquired data must be made:

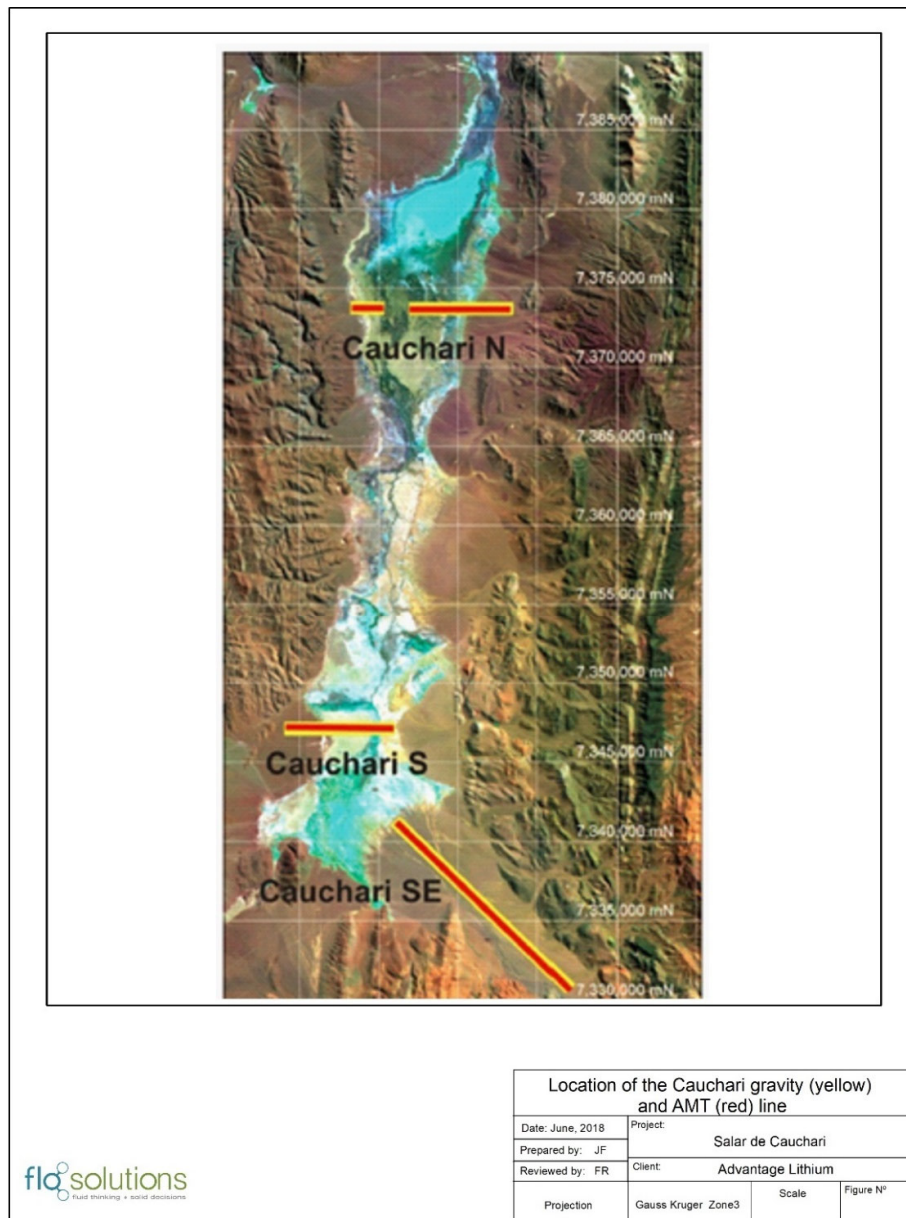
- Tidal correction.

- Drift, instrumental height and ellipsoid corrections.
- Free air, latitude, Bouguer and topographic corrections.

The tidal correction compensates for variations in gravity caused by the sun and moon. Using TIDES software, the acceleration due to gravity for these effects can be determined corresponding to the location and time of measurements. The data acquired in the survey were translated to UTC time to facilitate data handling. The exported data were converted from  $\mu\text{Gal}$  to  $\text{mGal}$  and used to correct the acquired data.

Instrument drift was calculated from the difference in gravity measured at the base station. This difference was then linearly distributed with respect to time of each reading and used to correct the acquired data.

Figure 9.1 Location of the Cauchari gravity (yellow) and AMT (red) lines



Each reading was corrected for the height of the instrument using the following formula:

$$r_h = r_t + 0.308596 h_i$$

where  $r_h$  is the corrected instrument height,  $r_t$  is the tidal correction, and  $h_i$  is the observed instrument height.

The formula employed to correct variations in gravity associated with the ellipsoidal shape of the earth corresponds to the 1980 model:

$$g_l = 978032.7 [ 1 + 0.0053024 \sin^2(l) - 0.0000058 \sin^2(2l) ]$$

where  $g_l$  is the theoretical gravity in milligals and  $l$  is latitude

The free air anomaly is calculated as:

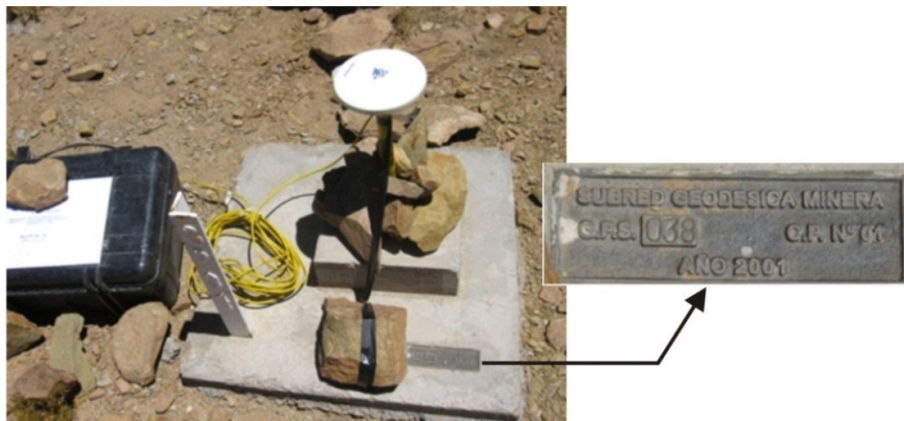
$$g_{\text{free air}} = -0.3086 (\Delta h)$$

where  $g_{\text{free air}}$  is the correction factor and  $\Delta h$  refers to the difference in altitude of the station with respect to the base.

Figure 9.2 Gravimeter base station



Figure 9.3 GPS base station



To eliminate the effect of the rock masses between the reference level and observation station, the Bouguer correction was employed.

$$g_{\text{CB}} = 0.04191(\Delta h) \rho$$

where  $g_{\text{CB}}$  is the correction factor, the value  $\Delta h$  refers to the difference in altitude between the observation point and the base station, and  $\rho$  is the mean rock mass density in the area calculated using the graphical Nettleton method to be  $2.07 \text{ gm cm}^{-3}$ .

The topographic correction is used to compensate the effects of the relief in the gravity measurements. It takes into account the topography at different levels of accuracy and importance, according to its distance from the gravimetric station to correct. Centered areas are considered at the station with radii of 100 m, 2.5 km and 150 km respectively.

The result of applying all corrections is the Bouguer anomaly.

### 9.2.3. Gravity data modelling

The Bouguer anomaly can be modeled to represent the subsurface geology. However, any model is non-unique and it is essential to take into account the known geology and rock density. Subsequent to the gravity survey, drilling was carried out 2011 and density measurements were made on 18 core samples. This information (Table 9.1) was used to remodel the gravity profile across the central part of the Salar. The interpretation is provided in Figure 9.4.

**Table 9.1 Bulk rock density values used in the gravity interpretation**

| Salar Unit        | Density used in modelling (g/cc) | Density measured from Cauchari samples (g/cc) |
|-------------------|----------------------------------|---|
| Salar deposits    | 1.6                              |   |
| Clastic sediments | 1.8                              | 1.8   |
| Compact halite    |                                  | 1.7   |
| Porous halite     |                                  | 1.4   |
| Basement 2        | 2.6                              |   |
| Basement 1        | 2.7                              |   |

The gravity interpretation extends the asymmetric nature of the Salar de Cauchari towards the south (Figure 9.4), although the maximum basin depth was interpreted to be greater than 450 m along the eastern boundary in the southern gravity line. Recent drilling by the company, with Rotary hole CAU11 completed to 480 m and other holes such as CAU14 to 600 m, suggests that the gravity modelling substantially underestimates the thickness of the salar sediments and the depth to underlying basement. Drilling by neighboring property owner Lithium Americas Corp (LAC) supports this interpretation, with the deepest historical hole drilled by LAC to 650 m (Burga et. al, 2017).

## 9.3. Audio Magnetotelluric Survey - 2009

### 9.3.1. Data acquisition

AMT measures temporary variations in the electromagnetic field caused by electrical storms (high frequencies >1 Hz), and the interaction between the solar wind and the terrestrial magnetic field (low frequencies <1 Hz), which allows variations in the electrical subsurface to depths of 2 km or more.

The electrical properties of the subsurface depend on Archie's Law:  $R_t = a R_w / P^m$  where  $R_t$  is the measured total resistivity,  $R_w$  is the resistivity of the fluid in the rock pores and  $P$  is the rock porosity,  $a$  and  $m$  are constants. Hence, it is possible to infer the subsurface variations in fluid resistivity and porosity, although it is important to note that once again the problem of a non-unique solution always exists.

Data at 250 m spaced stations was acquired using Phoenix Geophysics equipment within a range of 10,000-1 Hz, using up to 7 GPS synchronized receptors. The equipment includes a V8 receptor with 3 electrical channels and 3 magnetic channels which also serves as a radio controller of auxiliary RXU-3E acquisition units. Three magnetic coils of different size and hence frequency were used at each station,

and non-polarizable electrodes that improve signal to noise ratios. The natural geomagnetic signal during the acquisition period remained low (the Planetary A Index was  $\leq 5$  for 95% of the acquisition time) requiring 18-20 hours of recording at each station.

All stations were surveyed in using differential GPS to allow for subsequent topographic corrections.

AMT requires a Remote Station, far from the surveyed area, in a low level noise location to act as a baseline for the acquired data.

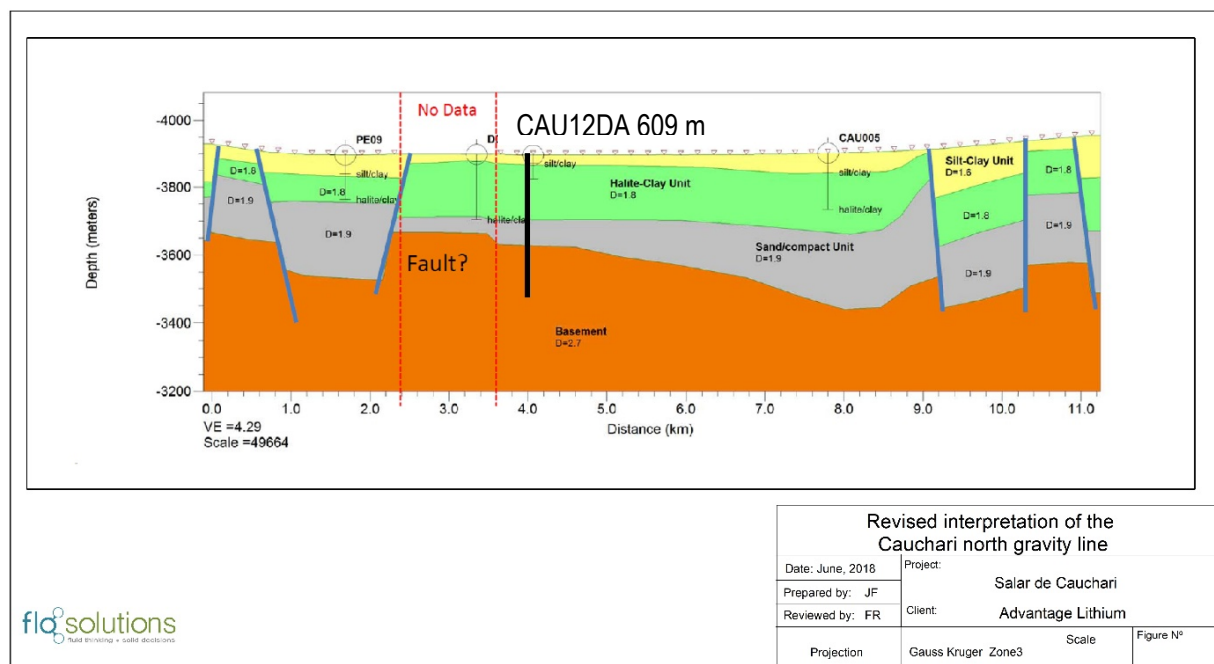
### 9.3.2. Data processing and modelling

Processing of the AMT data requires the following stages:

- Filtering and impedance inversion of each station
- 1D inversion for each station
- Development of a resistivity pseudo-section
- 2D profile inversion (including topographic 3D net)

The WinGlink software package was used for filtering, inversion and development of the pseudo-section and eventually the 2D model output.

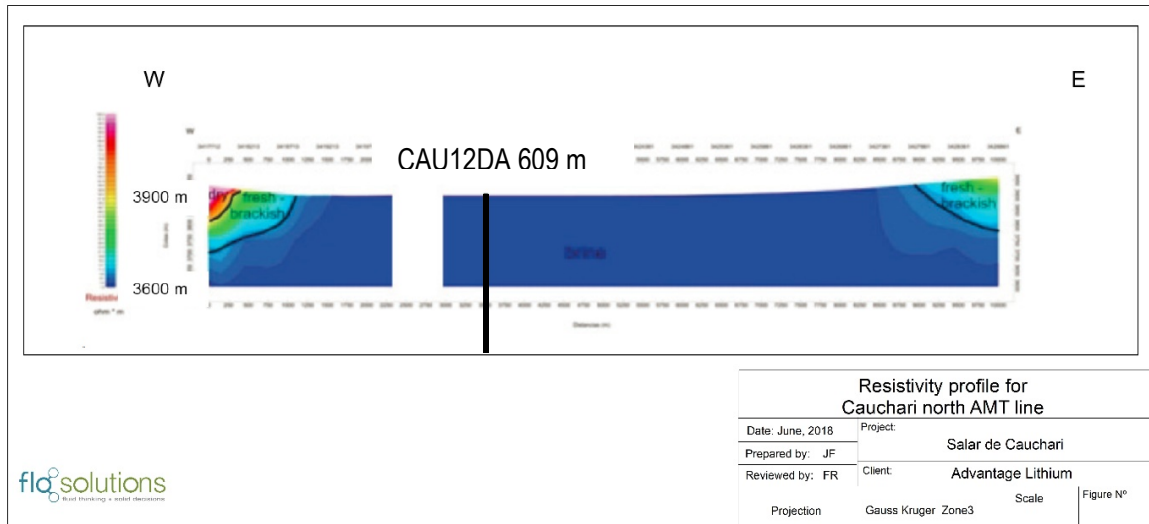
Figure 9.4 Interpretation of the Cauchari north gravity line (looking north)



### 9.3.3. Model output and interpretation

The 2D AMT model results for the northern section at Cauchari are presented below in Figures 9.5. The drill hole CAU12DA is located within 1 km of the geophysical profile. In the Cauchari north AMT line the darkest blue on the AMT line is interpreted to represent brine, which extends across the salar between bounding reverse faults which thrust older sediments and unsaturated units over the salar sediments on the margins of the salar basin. This interpretation is supported by TEM (King, 2010b) and electrical soundings (Vazques, 2011) conducted by LAC in the adjacent tenements.

Figure 9.5 Resistivity profile for Cauchari north AMT line



## 9.4. Gravity Survey - 2016

In late 2016 additional gravity data was collected on a quasi-grid basis across the NW Sector and SE Sectors of the Cauchari salar. The work was carried out by staff from the Seismology and Geophysics institute at the University of San Juan using Scintrex CG-3 and CG-5 gravimeters and digital GPS equipment to precisely locate each gravity station. A series of regional gravity points were measured in the surrounding area and a residual bouguer map was generated from the available information. Lines were on a nominal 1 km spacing north-south, with gravity stations measured every 200 m along the lines. Process of gravity data is consistent with the activities described above in the section discussing processing of the earlier acquired geophysical data.

The gravity survey confirmed the geometry of the Cauchari basin is similar to that presented in Figure 9.4, with the deepest part of the basin on the eastern side.

## 9.5. TEM Survey - 2018

In 2018 a TEM survey was undertaken in the NW Sector to assist mapping of the brine body. The TEM survey was conducted with a Geonics Protem 20 channel transmitter, with 195 stations read across five lines, using 200 x 200 m loops transmitting at 25 and 2.5 Hz with 100 V output. The receiver was configured to automatically make 3 readings, each with an integration period of 30 seconds. To evaluate the coherency of the data a comparison of the graphical display of the Z component resistivity with time was made on the three recorded measurements. If noise was detected a repeat set of 3 measurements was made.

Further quality control was made when data was downloaded from the Protem device. The data was then presented as profiles, which clearly identified the unsaturated zone, fresh to brackish water, the transition to brine and the brine body itself, as well as basement features on the margins of the survey area, near outcropping rocks. This information has been incorporated into the geological and resource model for the project, as diamond drilling has provided useful information to validate the TEM profiles.



## 10 DRILLING

### 10.1. Overview

Three drilling campaigns have been carried out for the Project since 2011. The first program in 2011 by SAS (Phase I) covered the SE Sector of the Project area; the second and third campaigns (Phases II and III) by AAL covered both the NW and SE Sectors of the Project area. The objectives of the drilling can be broken down into three general categories:

1. Exploration drilling on a general grid basis to allow the estimation of “in-situ” brine resources. The drilling methods were selected to allow for 1) the collection of continuous core to prepare “undisturbed” samples from specified depth intervals for laboratory porosity analyses and 2) the collection of depth-representative brine samples at specified intervals. The 2011 campaign included five (5) diamond core holes CAU01 through CAU05 and one rotary hole (CAU06). The Phase II and III programs included 20 diamond core holes (CAU12 through CAU29). Figure 10.1 shows the location of the exploration boreholes.
2. Test well installations. The Phase II campaign included five rotary holes (CAU07 through CAU11) which were drilled and completed as test production wells to carry out pumping tests and additional selective brine sampling. Monitoring wells were installed adjacent to these test production wells for use during the pumping tests as part of the Phase III program.
3. Pumping tests. Initial short-term (48 hour) pumping tests were carried out on CAU07 through CAU11 during 2017. Two long-term (30-day) pumping tests were carried out on CAU07 and CAU11 as part of the Phase III program. Three nested monitoring wells were completed immediately adjacent to each CAU07 and CAU11 to observe water levels in distinct hydrogeological units throughout the 30-day tests.

### 10.2. Exploration drilling

Five HQ and NQ core holes (CAU01 through CAU05) were drilled for a total of 721 m by Falcon Drilling using a Longyear 38 trailer mounted rig in 2011. CAU06R was drilled as a rotary hole to 150 m depth. 20 HQ core holes were drilled for a total of 9,376.5 m by Falcon-AGV and Major Drilling in 2017/8. Core recovery averaged 76% and 70% in the 2011 and 2017/8 programs, respectively. Table 10.1 shows the details of the drilling depths that varied from 46.5 m in CAU04D to 619 m in CAU12D. All holes were drilled vertical.

Diamond drilling was carried out in 1.5 m core runs with lexan (plastic) tubes in the core barrel in place of a split triple tube. Core recovery was measured for each run. The retrieved core was subsampled by cutting off the bottom 15 cm of alternating 1.5 m length plastic core tubes (nominal 3 m intervals) for porosity analysis. Thereafter, cores were split and the lithology was described by the on-site geological team.

Brine samples were collected using a bailer and following protocols developed by Orocobre for resource drilling at the Olaroz Project. Brine samples were taken at 3 m intervals during the 2011 program and at 6 m to 12 m intervals (due to deeper holes) during the 2017/18 program. Up to 3 well volumes of brine were bailed from the hole prior to sampling. The bailed brine volume was adjusted based on the height of the brine column at each sampling depth.

Core drilling was carried out using brackish water from the margins of the Salar as drilling fluid. This fluid has a Li concentration of less than 20 mg/l. Fluorescein, an organic tracer dye was added to the drilling fluid to distinguish between drilling fluid and natural formation brine. Detection of this bright red dye in samples provided evidence of contamination from drilling fluid and these samples were discarded.

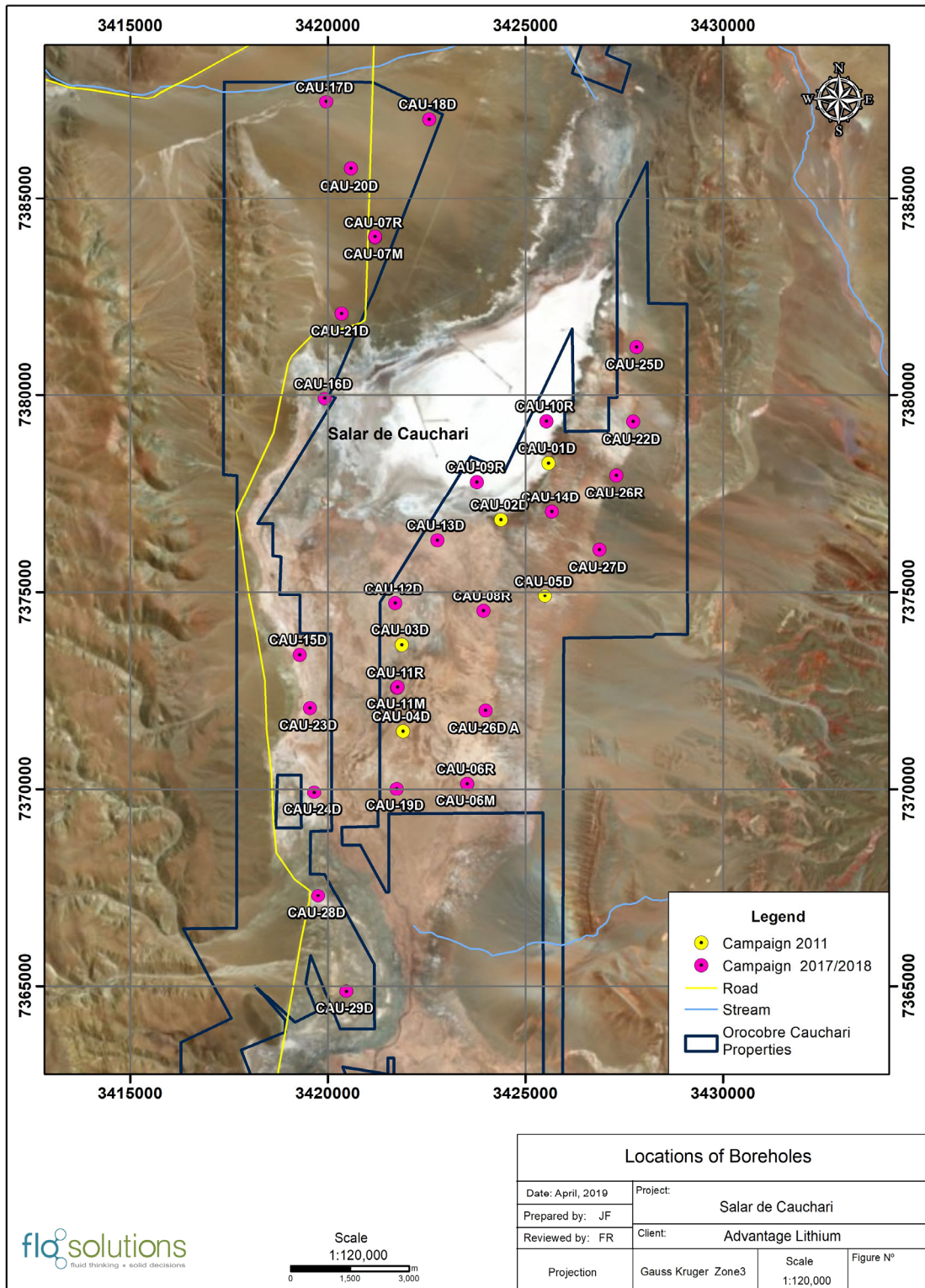
Brine sample recovery from halite and clay units was low due to the low permeability and brine samples were not obtained in a number of intervals in various holes. Double packer brine sampling equipment was used to obtain check samples from selected depth intervals. On completion of the drilling and sampling, each diamond hole was completed as a monitoring well by the installation of 3-inch diameter schedule slotted PVC.

**Table 10.1 Cauchari summary borehole information (2011-2018)**

| Hole ID  | UTM mE*   | UTM mN*   | Elev. (masl) | TD (m) | Type   | Year | Drilling Co. | Rec. (%) | SWL (m) | Screened Interval | CasingDia (in) |
|----------|-----------|-----------|--------------|--------|--------|------|--------------|----------|---------|-------------------|----------------|
| CAU01D   | 3,425,589 | 7,378,259 | 3940.42      | 249    | DDH    | 2011 | Falcon       | 76       | 0.00    | 0-249 m           | 2              |
| CAU02D   | 3,424,385 | 7,376,814 | 3940.41      | 189    | DDH    | 2011 | Falcon       | 69       | 2.15    | 0-189 m           | 2              |
| CAU03D   | 3,421,874 | 7,373,649 | 3941.06      | 71.5   | DDH    | 2011 | Falcon       | 80       | 4.16    | 0-71.5 m          | 2              |
| CAU04D   | 3,421,903 | 7,371,452 | 3941.53      | 46.5   | DDH    | 2011 | Falcon       | 77       | 5.50    | 0-46.5 m          | 2              |
| CAU05D   | 3,425,500 | 7,374,882 | 3945.57      | 168    | DDH    | 2011 | Falcon       | 82       | 0.00    | 0-168 m           | 2              |
| CAU06R   | 3,423,531 | 7,370,126 | 3941.95      | 150    | Rotary | 2011 | Valle        | NA       | 3.97    | -                 | -              |
| CAU07R   | 3,421,200 | 7,383,987 | 3964.13      | 348    | Rotary | 2017 | Andina       | NA       | -       | 134-326 m         | 6              |
| CAU08R   | 3,423,938 | 7,374,503 | 3940.95      | 400    | Rotary | 2017 | Andina       | NA       | 2.82    | 60-396 m          | 8 & 6          |
| CAU09R   | 3,423,778 | 7,377,785 | 3939.96      | 400    | Rotary | 2017 | Andina       | NA       | 5.04    | 65-394 m          | 8 & 6          |
| CAU10R   | 3,425,532 | 7,379,306 | 3940.19      | 429    | Rotary | 2017 | Andina       | NA       | 6.84    | 60-418 m          | 8 & 6          |
| CAU11R   | 3,421,752 | 7,372,571 | 3941.22      | 480    | Rotary | 2017 | Andina       | NA       | 12.20   | 50-471 m          | 8 & 6          |
| CAU12D   | 3,421,708 | 7,374,690 | 3940.56      | 413    | DDH    | 2017 | Falcon       | 64       | 1.73    | 3-201 m           | 3              |
| CAU12D A | 3,421,679 | 7,374,669 | 3940.56      | 609    | DDH    | 2018 | Falcon       | -        | -       | -                 | -              |
| CAU13D   | 3,422,774 | 7,376,298 | 3940.16      | 449    | DDH    | 2018 | Falcon       | 73       | 1.78    | 0-252 m           | 3              |
| CAU13D A | 3,422,747 | 7,376,293 | 3940.16      | 497    | DDH    | 2018 | Falcon       | -        | -       | -                 | -              |
| CAU14D   | 3,425,670 | 7,377,021 | 3942.09      | 600    | DDH    | 2018 | Falcon       | 78       | -       | 0-454.5 m         | 3 & 2          |
| CAU15D   | 3,419,292 | 7,373,396 | 3941.34      | 243.5  | DDH    | 2017 | Falcon       | 39       | 0.00    | 6-204 m           | 3              |
| CAU16D   | 3,419,924 | 7,379,892 | 3940.83      | 321.5  | DDH    | 2017 | Falcon       | 63       | 0.77    | 3-249 m           | 3              |
| CAU17D   | 3,419,965 | 7,387,430 | 3990.59      | 237.5  | DDH    | 2018 | Falcon       | 48       | 42.07   | 3.5-238 m         | 3              |
| CAU18D   | 3,422,571 | 7,386,977 | 3964.07      | 359    | DDH    | 2018 | Falcon       | 86       | 18.57   | 0-353 m           | 3              |
| CAU19D   | 3,421,745 | 7,369,998 | 3941.00      | 519.5  | DDH    | 2018 | Major        | 66.7     | -       |                   | 3              |
| CAU20D   | 3,420,585 | 7,385,750 | 3982.00      | 390    | DDH    | 2018 | Major        |          | 42.87   |                   | 3              |
| CAU21D   | 3,420,351 | 7,382,047 | 3956.00      | 283    | DDH    | 2018 | Major        |          | 16.58   |                   | 3              |
| CAU22D   | 3,427,728 | 7,379,299 | 3953.00      | 418    | DDH    | 2018 | Falcon       | 88.95    | 5.51    |                   | 3              |
| CAU23D   | 3,419,549 | 7,372,041 | 3948.00      | 319    | DDH    | 2018 | Falcon       |          | 0.56    |                   | 3              |
| CAU24D   | 3,419,658 | 7,369,902 | 3944.00      | 352.5  | DDH    | 2018 | Major        | 55.5     | 1.21    |                   | 3              |
| CAU25D   | 3,427,810 | 7,381,196 | 3955.00      | 427    | DDH    | 2018 | Falcon       | 80.55    | 9.66    |                   | 3              |
| CAU26D   | 3,423,997 | 7,371,974 | 3946.00      | 619    | DDH    | 2018 | Major        | 64.67    | -       |                   | 3              |
| CAU27D   | 3,426,874 | 7,376,061 | 3959.00      | 473    | DDH    | 2018 | Falcon       | 72.94    | 17.06   |                   | 3              |
| CAU28D   | 3,419,760 | 7,367,270 | 3959.00      | 303.5  | DDH    | 2018 | Major        | 46.46    | -       |                   | -              |
| CAU29D   | 3,420,475 | 7,364,855 | 3959.00      | 404    | DDH    | 2018 | Major        | 35.80    | -       |                   | 3              |

\*Note: Coordinates are in Zone 3 of the Argentine Gauss Kruger System with the Posgar Datum

Figure 10.1 Location map of boreholes



### 10.3. Production well drilling

Five test production wells (CAU07 through CAU11) was drilled and completed by Andina Perforaciones using a Speedstar SS-3 table drive rotary rig in 2017. The rotary holes were drilled at a first pass in 7<sup>7/8</sup>-inch diameter and subsequently reamed to 15-inch diameter in the upper part of the hole and to 12-inch diameter in the lower part of the hole. Drilling depths varied between 343 m (CAU07) and 480 m (CAU11). A total of 2,052 m was drilled with the rotary method during which cutting samples were collected at 2 m intervals for geological logging using a hand lens and binocular microscope. Cuttings were stored in chip trays. The holes were completed with 8-inch (upper section) and 6-inch diameter (lower section) blank and screened stainless steel production casing. The completion details of the test wells are provided in Table 10.1. The annulus space was completed with a gravel pack and a cement surface seal. The wells were developed by pumping over a minimum 72 hour period with a submersible pump.

### 10.4. Pumping tests

#### 10.4.1. 48-hr pumping tests

Preliminary pumping tests were carried out on the five test production wells CAU07 through CAU11 during the Phase II program in 2017. These pumping tests were carried out over a period of 48 hours after the well development was completed. In each well the pump was installed within the upper 8 inch section of the wells. The pumping test in CAU07 (completed in the coarser grained units of the NW Sector) was carried out at a rate of 17 l/s. The test in CAU11 (completed in the deep sand unit of the SE Sector) was carried out at a constant rate of 19 l/s. The tests in CAU08, CAU09, and CAU10 (all completed in the fined grained and halite units in the SE Sector) were carried out a constant rate of 4 l/s.

#### 10.4.2. 30-day pumping tests

Two long-term (30-day) pumping tests were carried out on CAU07 in the Northwest Sector and CAU11 in the SE Sector as part of the Phase III program. Three nested monitoring wells were completed immediately adjacent to CAU07 in three distinct hydrogeological units as follows: the upper Archibarca fan material (fresh water aquifer); the intermediate low permeability clay and a third in the lower brine aquifer of the NW Sector. The 30 day CAU7 test was started on December 11, 2018 and stopped on January 10, 2019. The average flow during the test was 22 l/s and the observed drawdown in the pumping well stabilized at 40.2 m. Brine produced during the pumping test was discharged through a 0.80 km length pipeline into a LAC evaporation pond. Water level recovery was observed over a 15 day period after completion of the pumping cycle. Table 10.2 shows the results of the CAU7 pumping test.

Three nested monitoring wells were also completed immediately adjacent to CAU11 units as follows: in the upper clay / halite unit, the intermediate depth halite unit and in the Lower Sand unit. The 30 day CAU11 test was started on October 25, 2018 and stopped on November 23, 2018. The average flow during the test was 18 l/s and the observed drawdown in the pumping well stabilized at 26 m. Brine produced during the pumping test was discharged away from the wellhead through an 1,0 km length pipeline into a suitable depression in the Salar. Water level recovery was observed over a 30 day period after completion of the pumping cycle. Table 10.2 shows the results of the CAU11 pumping test.

**Table 10.2 CAU07 and CAU11 pumping test results**

| Obs. Well  | Unit              | Max drawdown (m) | Method | T (m <sup>2</sup> /d) | S(-)                    | K (m/d)   | S <sub>s</sub> (m <sup>-1</sup> ) |
|------------|-------------------|------------------|--------|-----------------------|-------------------------|-----------|-----------------------------------|
| CAU07 M350 | Archibarca Fan    | 3,67             | Theis  | 477,2                 | 0,018                   | 3,4       | 1,28E-4                           |
| CAU11 MA   | Lower sand        | 1,79             | Theis  | 96 - 253              | 1,18                    | 2,4 – 6,3 | 0,03                              |
| CAU11 MB   | Halite-clay       | 26,91            | Theis  | 62 - 100              | 2,07 x 10 <sup>-4</sup> | 6 - 10    | 2,07 x 10 <sup>-5</sup>           |
| CAU11MC    | Clay, Fan, Halite | 1,3              | Theis  | 112-373               | 0,22                    | 0,7 - 2,5 | 1,4 x 10 <sup>-3</sup>            |

# 11 SAMPLE PREPARATION, ANALYSES AND SECURITY

## 11.1. Sampling methods

### 11.1.1. Core sample collection, handling and transportation

Diamond drilling took place in HQ or NQ sizes with lexan tubes inside the core barrel to facilitate recovery and preparation of the porosity sub samples. When cores were recovered to surface the lexan tube was pumped from the core barrel using water and a plug separating tube and water. Upon release from the core barrel tight fitting caps were applied to both ends of the lexan tube. The tube was then cleaned, dried and labeled.

### 11.1.2. Drainable porosity sample preparation, handling and security

The 2011 samples were prepared for drainable porosity testing and brine extraction by the BGS and consisted of a 20 cm sub-section of core cut from the bottom section of each lexan liner. The samples prepared for total porosity testing by the Company's laboratory in Salta consisted of a 10 cm sub-section of the core. Both sample types were sealed with end-caps and taped. All samples were labelled with the borehole number and depth interval. Each day the porosity samples were transferred to the workshop in the onsite camp where the samples were labelled with a unique sample number. Prior to shipping each sample was wrapped in bubble plastic to prevent disturbance during shipping. A register of samples was compiled at the camp site to control transportation of samples to the Company's Salta office. Porosity samples prepared from the HQ core collected during the 2017/8 Program followed the same procedures as outlined above.

The following test work has been carried out on the on undisturbed core samples:

- 123 samples were analyzed by the BGS laboratory for total porosity and specific yield from the 5 core holes CAU1 through CAU5 drilled in 2011. 13 samples were rejected on arrival in the BGS due to damage occurred during the shipping and handling.
- 164 samples were analyzed in 2011 by the Company's Salta laboratory for total porosity.
- 292 samples were analyzed by GSA in 2017/8 for drainable porosity and other physical parameters.
- 30 samples (subsamples from the 2017/18 GSA samples) were analyzed as QA/QC analyses by Corelabs in Houston TX in 2018, with a further 26 samples were analyzed by DBSA.

### 11.1.3. Brine sample preparation, handling and security

Brine samples were taken using bailer, packer and drive point methods. In addition, a second sampling was carried out once drilling was finished using Low Flow Sampling (LFS) equipment inside the 3-inch diameter PVC slotted casing installed in each of the DD borehole. Prior to bottling, the sample was transferred to a bucket, which had been rinsed with the same brine as the sample. When necessary fine sediment was allowed to settle in the bucket before the brine sample was transferred from the bucket to two 1 liter plastic bottles. The bottles were rinsed with the brine and then filled to the top of the bottle removing any airspace and capped. Bottles were labeled with the borehole number and sample depth with permanent marker pens, and labels were covered with transparent tape, to prevent labels

being smudged or removed. Samples with fluorescein contamination were noted at this point and except in specific circumstances these were not sent for laboratory analysis, due to the interpreted sample contamination.

A volume of the same brine as the bottled sample was used to measure the physical parameters: density (with a picnometer), temperature, pH, Eh and in some samples dissolved oxygen. Details of field parameters were recorded on paper tags, which were stuck to the bottle with transparent tape when completed with sample information.

Samples were transferred from the drill site to the field camp where they were stored in an office out of direct sunlight. Samples with suspended material were filtered to produce a final 150 ml sample for the laboratory. Before being sent to the laboratory the 150 ml bottles of fluid were sealed with tape and labeled with a unique sample ticket number from a printed book of sample tickets. The hole number, depth, date of collection, and physical parameters of each sample number were recorded on the respective pages of the sample ticket book and in a spreadsheet control of samples. Photographs were taken of the original 1 liter sample bottles and the 150 ml bottles of filtered brine to document the relationship of sample numbers, drill holes and depths.

Brine chemistry analyses were carried out as follows:

- 268 brine samples including (QA/QC samples: duplicates, standards and blanks) were analysed by Alex Steward Assayers (ASA) in Mendoza Argentina as the primary laboratory for the 2011 campaign.
- 15 brine samples were analyzed by the University of Antofagasta as the external secondary laboratory for QA/QC analyses during the 2011 campaign.
- 1,565 brine samples including (QA/QC samples: duplicates, standards and blanks) were analysed by Norlabs in Jujuy, Argentina as the primary laboratory for the 2017/8 campaign.
- 42 brine samples were analyzed by Alex Steward Assayers (ASA) in Mendoza Argentina as the secondary laboratory for QA/QC analyses during the 2017/8 campaign.
- 35 brine samples were analyzed by the University of Antofagasta as the external secondary laboratory for QA/QC analyses during the 2017/8 campaign

## 11.2. Drainable porosity analysis and quality control results

### 11.2.1. British Geological Survey - 2011

The BGS was used during the 2011 campaign to analyze drainable porosity. Specific yield (or drainable porosity) is defined as the volume of water released from storage by an unconfined aquifer per unit surface area of aquifer per unit decline of the water table. Bear (1979) relates specific yield to total porosity as follows:  $n = S_y + S_r$ ; where  $S_r$  is specific retention.

The BGS determines drainable porosity using a centrifugation technique where samples are saturated with simulated formation brine and weighed. They are then placed in a low-speed refrigerated centrifuge with swing out rotor cups and centrifuged at 1,200 rpm for two hours and afterwards weighed a second time. A centrifuge speed is selected to produce a suction on the samples equivalent



to 3,430 mm H<sub>2</sub>O. This suction is chosen as it had previously been used by Lovelock (1972) and Lawrence (1977) and taken to be characteristic of gravitational drainage.

### 11.2.2. GeoSystems Analyses – 2017/8

GSA was selected as the main laboratory for the Phase II and III drainable porosity (Sy) and other physical parameter analyses. GSA utilized the Rapid Brine Release method (Yao et al., 2018) to measure drainable porosity and the total porosity. The Rapid Brine Release (RBR) method is based on the moisture retention characteristics (MRC) method for direct measurement of total porosity (Pt, MOSA Part 4 Ch. 2, 2.3.2.1), specific retention (Sr, MOSA Part 4 Ch3, 3.3.3.5), and specific yield (Sy, Cassel and Nielson, 1986). A simplified Tempe cell design (Modified ASTM D6836-16) was used to test the core samples. Brine release was measured at 120 mbar and 330 mbar of pressure for reference (Nwankwor et al., 1984, Cassel and Nielsen, 1986).

In addition to drainable porosity, bulk density, particle size analyses and specific gravity were determined on selected core samples. Table 11.1 provides an overview of the test work carried out by GSA. Figure 11.2 shows the results of the test work by lithology type.

**Table 11.1 Physical and hydraulic test work on core samples – 2017/8**

| Test Type                 | Sample Type and Number   | Test Method                                     | Testing Laboratory                                      | Standard <sup>1,2</sup>                   |
|---------------------------|--|---|---|---|
| Physical                  | 292 core samples   | Bulk Density                                    | GSA Laboratory, (Tucson, AZ)                            | ASTM D2937-17e2 <sup>1</sup>              |
|                           | 64 core samples  | Particle Size Distribution with #200 brine wash | GSA Laboratory, (Tucson, AZ)                            | ASTM D6913-17 / ASTM C136-14 <sup>1</sup> |
|                           | 160 core samples   | Specific Gravity of Soils                       | GSA Laboratory, (Tucson, AZ)                            | ASTM D854-14 <sup>1</sup>                 |
| Hydraulic                 | 26 core samples  | Relative Brine Release Capacity (RBRC)          | Daniel B. Stephens & Associates, Inc. (Albuquerque, NM) | Stormont et. al., 2011                    |
|                           | 30 core samples  | Centrifuge Moisture Equivalent of Soils         | Core Laboratories (Houston, TX)                         | Modified ASTM D425-17 <sup>1</sup>        |
|                           | 292 core samples   | Estimated Total Porosity                        | GSA Laboratory (Tucson, AZ)                             | MOSA Part 4 Ch. 2, 2.3.2.1 <sup>2</sup>   |
|                           |  | Estimated Field Water Capacity                  |   | MOSA Part 4 Ch. 3, 3.3.3.2 <sup>2</sup>   |
| Rapid Brine Release (RBR) | Modified ASTM D6836-16 <sup>1</sup><br>MOSA Part 4 Ch. 3, 3.3.3.5 <sup>2</sup> |   |   |   |

### 11.2.3 Drainable porosity quality control - 2017/8

For quality control, a subset of paired samples representative of the range in lithology types were selected by AAL and GSA for testing using the Relative Brine Release Capacity (RBRC, Stormont et. al., 2011) method by DBSA, or the Centrifuge Moisture Equivalent of Soils (Centrifuge, ASTM D 6836-16) method by Core Laboratories (Houston, TX). Table 11.2 shows a summary of the comparison by laboratory for each method derived for paired core samples using the RBR, RBRC, and Centrifuge methods. A comparison is provided in Table 11.2.

Correlations between GSA and external laboratory measured values are provided in Figure 11.3. There is a lower correlation between the specific yield data ( $R^2 = 0.44$ ). Correlation was slightly higher ( $R^2 = 0.45$ ) between  $S_y$  (RBRC and Centrifuge) and drainable porosity at 120 mbar (RBR, Figure 11.4). Most of the samples tested for  $S_y$  fall below the 1:1 line, indicating that GSA measured  $S_y$  values were often higher than external laboratory measured  $S_y$  values, particularly those from Core Laboratories. Differences are likely attributable to testing equilibration time and testing method, with GSA testing the samples for a longer period than the DBSA laboratory using the RBRC method.

**Table 11.2 Summary of the drainable porosity statistics by laboratory methods**

| Lithological Group  | RBR Drainable Porosity<br>@330 mbar (GSA) |      |        | RBR Drainable Porosity<br>@120 mbar (GSA) |      |        | Centrifuge $S_y$<br>(Core Laboratories) |      |        | RBRC $S_y$<br>(DBS&A) |      |        |
|---------------------|---|------|--------|---|------|--------|---|------|--------|-----------------------|------|--------|
|                     | n   | Mean | StdDev | n   | Mean | StdDev | n                                       | Mean | StdDev | n                     | Mean | StdDev |
|                     | Clay dominated                            | 34   | 0.03   | 0.02                                      | 32   | 0.02   | 0.02                                    | 4    | 0.02   | 0.02                  | 0    | --     |
| Halite dominated    | 63  | 0.04 | 0.03   | 58  | 0.03 | 0.03   | 0                                       | --   | --     | 21                    | 0.05 | 0.02   |
| Sand/Clay dominated | 48  | 0.07 | 0.04   | 46  | 0.04 | 0.03   | 15                                      | 0.05 | 0.04   | 0                     | --   | --     |
| Sand dominated      | 38  | 0.19 | 0.06   | 44  | 0.13 | 0.06   | 13                                      | 0.12 | 0.05   | 3                     | 0.08 | 0.05   |

Figure 11.1 Comparison between GSA RBR and Core Labs Centrifuge by lithology

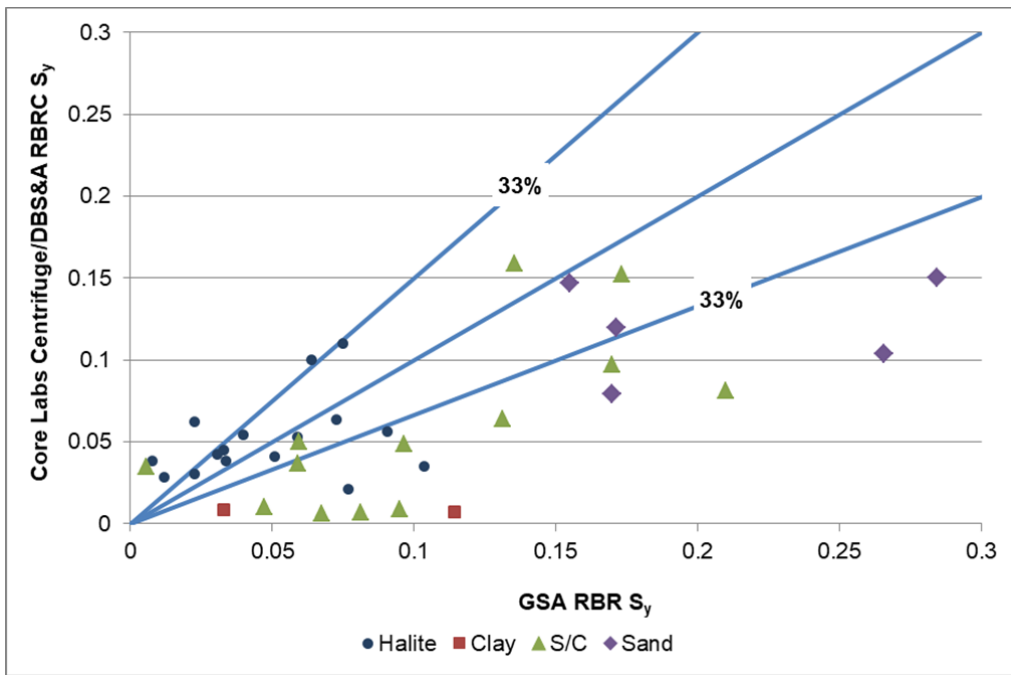
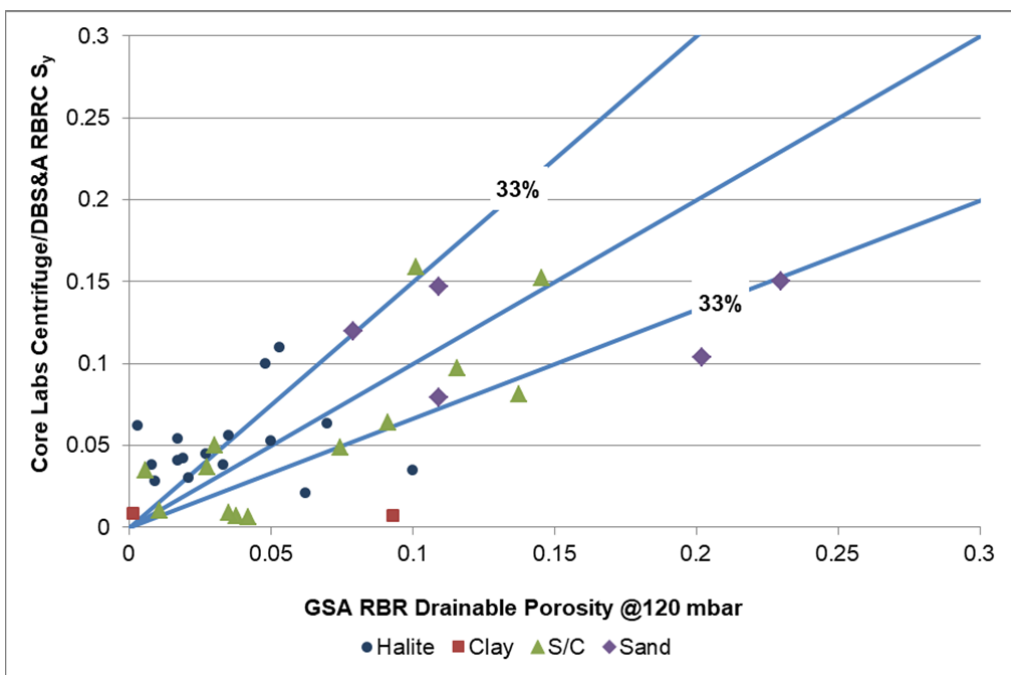


Figure 11.2 Comparison between GSA RBR @120 mbar and Core Labs centrifuge by lithology



## 11.3. Brine analysis and quality control results

### 11.3.1. Analytical methods

Alex Stewart Argentina in Jujuy, Argentina (NorLab) was selected as the primary laboratory to conduct the assaying of the brine samples collected as part of the 2017/18 drilling program. This laboratory is ISO 9001 accredited and operates according to Alex Stewart Group standards consistent with ISO 17025 methods at other laboratories.

Alex Stewart Argentina in Mendoza, Argentina (ASAMen) was used for the analysis of external check samples during the 2017/18 drilling campaign and as primary laboratory during the 2011 drilling campaign. The laboratory of the University of Antofagasta in northern Chile was also used for external check samples during the 2017/18 and 2011 campaign. This laboratory is not ISO certified, but it is specialized in the chemical analysis of brines and inorganic salts, with extensive experience in this field since the 1980s, when the main development studies of the Salar de Atacama were begun. Other clients include SQM, FMC, LAC and Orocobre.

Table 11.3 lists the basic suite of analyses requested from the laboratories. The labs used the same analytical methods based on the Standard Methods for the Examination of Water and Wastewater, published by American Public Health Association (APHA) and the American Water Works Association (AWWA), 21<sup>st</sup> edition, 2005, Washington DC.

**Table 11.3 List of analyses requested from the University of Antofagasta and Alex Stewart  
Argentina SA Laboratories**

| ANALYSIS                    | ALEX STEWART ARGENTINA                        | UNIVERSITY OF ANTOFAGASTA                   | METHODS                               |
|-----------------------------|---|---|---------------------------------------|
| Total Dissolved Solids      | SM 2540-C                                     | SM 2540-C                                   | Total Dissolved Solids Dried at 180°C |
| PH                          | SM 4500-H+B                                   | SM 4500-H+B                                 | Electrometric Method                  |
| Density                     | IMA-28  | CAQ – 001DS                                 | Pycnometer                            |
| Alkalinity                  | SM 2320-B                                     | SM 2320-B                                   | Acid-Base Titration                   |
| Boron (B)                   | ICP - OES                                     | CAQ – 005 BS                                | Acid-Base Titration                   |
| Chlorides (Cl)              | SM 4500-Cl-B                                  | SM 4500-Cl-B                                | Argentometric Method                  |
| Sulfates (SO <sub>4</sub> ) | SM 4500 <sup>2</sup> -C (Ignition of Residue) | SM 4500 <sup>2</sup> -D (Drying of Residue) | Gravimetric Method                    |
| Sodium (Na)                 | ICP-OES 10                                    | SM 3111 B                                   | Direct Aspiration-AA or ICP Finish    |
| Potassium (K)               | ICP-OES 10                                    | SM 3111 B                                   | Direct Aspiration-AA or ICP Finish    |
| Lithium (Li)                | ICP-OES 10                                    | SM 3111 B                                   | Direct Aspiration-AA or ICP Finish    |
| Magnesium (Mg)              | ICP-OES 10                                    | SM 3111 B                                   | Direct Aspiration-AA or ICP Finish    |
| Calcium (Ca)                | ICP-OES 10                                    | SM 3111 D                                   | Direct Aspiration-AA or ICP Finish    |

### 11.3.2. Analytical quality control - 2011 Program

A full QA/QC program for monitoring accuracy, precision and potential contamination of the entire brine sampling and analytical process was implemented. Accuracy, the closeness of measurements to the “true” or accepted value, was monitored by the insertion of standards, or reference samples, and by check analysis at an independent secondary laboratory.

Precision of the sampling and analytical program, which is the ability to consistently reproduce a measurement in similar conditions, was monitored by submitting blind field duplicates to the primary laboratory. Contamination, the transference of material from one sample to another, was measured by inserting blank samples into the sample stream at site. Blanks were barren samples on which the presence of the main elements undergoing analysis has been confirmed to be below the detection limit.

The results of the analyses of the standards are summarized in Table 11.4. The analyses showed little systematic drift in the results relative to the standard values over the period of analyzed. Results are generally within 10% of stated standard values, with a small number of exceptions for each element. However, boron values were consistently below the standard value for standards 4G, 5G and SG2.

**Table 11.4 Standards analysis results from ASA Mendoza (2011)**

|                               | B mg/l     | Ca mg/l      | K mg/l       | Li mg/l      | Mg mg/l      | Na mg/l       | Chlorides mg/l | Sulfates mg/l |
|-------------------------------|------------|--------------|--------------|--------------|--------------|---------------|----------------|---------------|
| <b>Field standard CJ 1314</b> |            |              |              |              |              |               |                |               |
| # Samples                     | 11         | 11           | 11           | 11           | 11           | 11            | 11             | 11            |
| Average                       | 392        | 2,189        | 17,235       | 1,547        | 4,159        | 93,338        | 184,782        | 4,335         |
| StdDev                        | 23         | 157          | 1,017        | 68           | 318          | 6,147         | 3,987          | 382           |
| RSD%                          | 6.0%       | 7.2%         | 5.9%         | 4.4%         | 7.6%         | 6.6%          | 2.2%           | 8.8%          |
| Max                           | 430        | 2,316        | 18,904       | 1,658        | 4,474        | 103,728       | 193,035        | 4,989         |
| Min                           | 364        | 1,875        | 16,042       | 1,467        | 3,571        | 83,569        | 177,210        | 3,787         |
| RPD %                         | 16.7%      | 20.1%        | 16.6%        | 12.3%        | 21.7%        | 21.6%         | 8.6%           | 27.7%         |
| <b>STD SG1</b>                | <b>20</b>  | <b>1,000</b> | <b>9,000</b> | <b>1,000</b> | <b>1,735</b> | <b>80,000</b> | <b>143,556</b> |               |
| # Samples                     | 7          | 7            | 7            | 7            | 7            | 7             | 7              | 7             |
| Average                       | 21         | 1,176        | 8,494        | 942          | 1,695        | 87,485        | 131,680        | 22,270        |
| StdDev                        | 4          | 31           | 210          | 35           | 17           | 4,985         | 833            | 809           |
| RSD%                          | 18.7%      | 2.7%         | 2.5%         | 3.8%         | 1.0%         | 5.7%          | 0.6%           | 3.6%          |
| Max                           | 30         | 1,224        | 8,908        | 1,018        | 1,714        | 92,383        | 132,246        | 23,799        |
| Min                           | 18         | 1,143        | 8,304        | 912          | 1,672        | 78,016        | 130,483        | 21,387        |
| RPD %                         | 54.2%      | 6.9%         | 7.1%         | 11.2%        | 2.5%         | 16.4%         | 1.3%           | 10.8%         |
| <b>STD SG2</b>                | <b>80</b>  | <b>200</b>   | <b>6,000</b> | <b>600</b>   | <b>1,301</b> | <b>90,000</b> | <b>149,289</b> |               |
| # Samples                     | 7          | 7            | 7            | 7            | 7            | 7             | 7              | 7             |
| Average                       | 69         | 363          | 6,121        | 584          | 1,133        | 121,435       | 142,596        | 61,823        |
| StdDev                        | 4          | 11           | 313          | 30           | 78           | 1,588         | 988            | 1,362         |
| RSD%                          | 5.4%       | 2.9%         | 5.1%         | 5.2%         | 6.9%         | 1.3%          | 0.7%           | 2.2%          |
| Max                           | 73         | 374          | 6,307        | 645          | 1,301        | 123,709       | 144,036        | 63,526        |
| Min                           | 62         | 347          | 5,418        | 561          | 1,071        | 118,365       | 141,329        | 59,838        |
| RPD %                         | 16.4%      | 7.4%         | 14.5%        | 14.3%        | 20.3%        | 4.4%          | 1.9%           | 6.0%          |
| <b>STD-4G</b>                 | <b>400</b> | <b>200</b>   | <b>4,000</b> | <b>400</b>   | <b>1,820</b> | <b>80,000</b> | <b>129,446</b> | <b>7,500</b>  |
| # Samples                     | 12         | 12           | 12           | 12           | 12           | 12            | 12             | 12            |
| Average                       | 349.5      | 252.1        | 3943.7       | 401.7        | 1841.8       | 80544.9       | 126666.2       | 8688.2        |
| StdDev                        | 14.9       | 10.0         | 184.0        | 18.5         | 134.1        | 3766.8        | 1662.4         | 380.9         |
| RSD%                          | 4.3%       | 4.0%         | 4.7%         | 4.6%         | 7.3%         | 4.7%          | 1.3%           | 4.4%          |
| Max                           | 369.7      | 265.5        | 4171.5       | 438.4        | 2019.6       | 87279.7       | 129195.9       | 9203.4        |
| Min                           | 320.7      | 236.3        | 3618.1       | 385.0        | 1644.2       | 75146.4       | 124093.8       | 8092.1        |
| RPD %                         | 14.0%      | 11.6%        | 14.0%        | 13.3%        | 20.4%        | 15.1%         | 4.0%           | 12.8%         |
| <b>STD-5G</b>                 | <b>800</b> | <b>100</b>   | <b>7,500</b> | <b>800</b>   | <b>2,707</b> | <b>85,000</b> | <b>142,200</b> | <b>11,000</b> |
| # Samples                     | 6          | 6            | 6            | 6            | 6            | 6             | 6              | 6             |
| Average                       | 707        | 197          | 7,318        | 802          | 2,632        | 83,219        | 137,497        | 12,469        |
| StdDev                        | 20         | 4            | 144          | 19           | 81           | 4,572         | 3,119          | 640           |
| RSD%                          | 2.8%       | 2.2%         | 2.0%         | 2.3%         | 3.1%         | 5.5%          | 2.3%           | 5.1%          |
| Max                           | 734        | 202          | 7,451        | 820          | 2,716        | 87,768        | 141,417        | 13,295        |
| Min                           | 677        | 191          | 7,121        | 772          | 2,544        | 76,549        | 134,435        | 11,607        |
| RPD %                         | 7.9%       | 5.8%         | 4.5%         | 6.0%         | 6.8%         | 13.4%         | 5.1%           | 13.8%         |

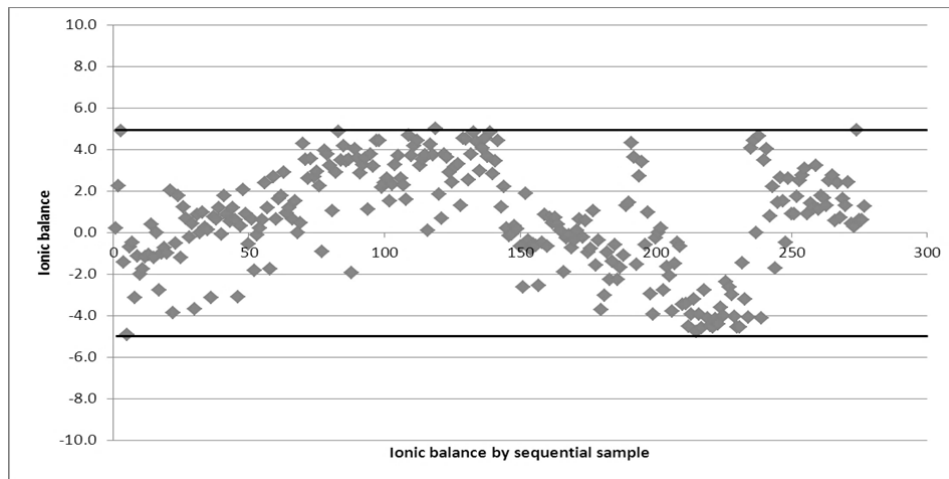
Table 11.5 shows a summary of the duplicate samples analysis. The duplicates show there is a high level of analytical repeatability and precision in the bailed samples analyzed by ASAMen, with duplicates generally well within +/-10.

**Table 11.5 Duplicate analysis results (2011)**

|              | B        |           | K        |           | Li       |           | Mg       |           |
|--------------|----------|-----------|----------|-----------|----------|-----------|----------|-----------|
|              | Original | Duplicate | Original | Duplicate | Original | Duplicate | Original | Duplicate |
| # Samples    | 19       | 19        | 19       | 19        | 19       | 19        | 19       | 19        |
| Average mg/l | 646      | 650       | 4283     | 4317      | 458      | 463       | 1143     | 1158      |
| Std Dev      | 314      | 309       | 2292     | 2306      | 288      | 285       | 795      | 795       |
| Graph $r^2$  | 0.992    |           | 0.996    |           | 0.994    |           | 0.997    |           |
| RPD%         | 0.6%     |           | 0.8%     |           | 1.0%     |           | 1.3%     |           |
|              | SO4      |           | Cl       |           | TDS      |           | Density  |           |
| # Samples    | 19       | 19        | 19       | 19        | 19       | 19        | 19       | 19        |
| Average mg/l | 21,499   | 21,372    | 165,287  | 165,283   | 303,932  | 303,917   | 1.2      | 1.2       |
| Std Dev      | 7,284    | 7,309     | 16,503   | 16,712    | 32,315   | 32,140    | 0.0      | 0.0       |
| Graph $r^2$  | 0.934    |           | 0.980    |           | 0.985    |           | 0.977    |           |
| RPD%         | 0.6%     |           | 0.0%     |           | 0.0%     |           | 0.0%     |           |

Ionic balances shown in Figure 11.5 demonstrate that the analyses are of good quality.

Figure 11.3 Results of ionic balance analyses (2011)



A suite of inter-laboratory check samples was analyzed at the University of Antofagasta. These samples showed generally low RPD values between the ASAMen and University of Antofagasta laboratory, suggesting ASAMen analyses have an acceptable level of accuracy as well as precision. Overall the ASAMen results are considered of acceptable accuracy and precision.

### 11.3.3. Analytical quality control - 2017/18 program

A total of 841 primary brine samples were analyzed from the 2017/18 drilling campaign. An additional 338 brine samples from pumping tests and baseline monitoring were analyzed. These primary analyses were supported by a total 386 QA/QC (24.7%) analyses consisting of:

- 152 standard samples (10%) with 8 different standards.
- 130 duplicates (8%) by external laboratory (ASA Mendoza).
- 104 blank samples (7%).

The results of the standards analyses are summarized in Table 11.6. This table lists the statistics, number of samples exceeding the acceptable failure criteria of the mean  $\pm$  2 standard deviations, and the relative standard deviation (RSD) for each standard. Standard analyses at NorLab indicate very acceptable accuracy.

**Table 11.6 Results of standards analysis by NorLab (2017/18)**

|                | Li mg/l | Ca mg/l | Mg mg/l | B mg/l | Na mg/l | K mg/l | Cl <sup>-</sup> mg/l | SO <sub>4</sub> mg/l |
|----------------|---------|---------|---------|--------|---------|--------|----------------------|----------------------|
| <b>STD SG1</b> |         |         |         |        |         |        |                      |                      |
| # Samples      | 4       | 4       | 4       | 4      | 4       | 4      | 4                    | 4                    |
| Average        | 521     | 213     | 1316    | 568    | 76497   | 4000   | 122461               | 4970                 |
| StdDev         | 12      | 13      | 146     | 6      | 213     | 57     | 267                  | 64                   |
| RSD%           | 2.39%   | 6.21%   | 11.09%  | 1.01%  | 0.28%   | 1.42%  | 0.22%                | 1.29%                |
| Max            | 539     | 228     | 1530    | 577    | 76715   | 4078   | 122808               | 5049                 |
| Min            | 510     | 201     | 1201    | 565    | 76213   | 3949   | 122166               | 4893                 |
| RPD %          | 5.39%   | 13.01%  | 25.01%  | 2.14%  | 0.66%   | 3.23%  | 0.52%                | 3.14%                |
| <b>STD SG2</b> |         |         |         |        |         |        |                      |                      |
| # Samples      | 6       | 6       | 6       | 6      | 6       | 6      | 3                    | 3                    |
| Average        | 601     | 363     | 1375    | 79     | 115875  | 5795   | 140429               | 65132                |
| StdDev         | 10      | 30      | 15      | 2      | 875     | 54     | 1274                 | 548                  |
| RSD%           | 1.71%   | 8.21%   | 1.12%   | 1.90%  | 0.76%   | 0.94%  | 0.91%                | 0.84%                |
| Max            | 610     | 396     | 1389    | 80     | 117191  | 5903   | 141794               | 65730                |
| Min            | 588     | 334     | 1347    | 76     | 114837  | 5759   | 139271               | 64656                |
| RPD %          | 3.68%   | 17.22%  | 3.05%   | 5.05%  | 2.03%   | 2.49%  | 1.80%                | 1.65%                |
| <b>STD SG4</b> |         |         |         |        |         |        |                      |                      |
| # Samples      | 25      | 25      | 25      | 25     | 25      | 25     | 23                   | 23                   |
| Average        | 575     | 499     | 1866    | 561    | 71278   | 5587   | 117085               | 7625                 |
| StdDev         | 10      | 8       | 53      | 17     | 533     | 173    | 575                  | 134                  |
| RSD%           | 1.72%   | 1.69%   | 2.85%   | 2.95%  | 0.75%   | 3.10%  | 0.49%                | 1.76%                |
| Max            | 593     | 509     | 1924    | 596    | 72200   | 5770   | 117801               | 7730                 |
| Min            | 546     | 474     | 1760    | 520    | 69996   | 5024   | 115060               | 7079                 |
| RPD %          | 8.05%   | 7.06%   | 8.83%   | 13.61% | 3.09%   | 13.36% | 2.34%                | 8.53%                |
| <b>STD SG5</b> |         |         |         |        |         |        |                      |                      |
| # Samples      | 3       | 3       | 3       | 3      | 3       | 3      | 3                    | 3                    |
| Average        | 755     | 233     | 2741    | 763    | 84638   | 7090   | 135282               | 11817                |
| StdDev         | 3       | 7       | 27      | 11     | 176     | 41     | 329                  | 287                  |
| RSD%           | 0.37%   | 3.11%   | 0.97%   | 1.38%  | 0.21%   | 0.58%  | 0.24%                | 2.43%                |
| Max            | 758     | 242     | 2771    | 775    | 84841   | 7114   | 135653               | 12065                |
| Min            | 752     | 229     | 2720    | 755    | 84534   | 7042   | 135023               | 11503                |
| RPD %          | 0.70%   | 5.68%   | 1.84%   | 2.56%  | 0.36%   | 1.02%  | 0.47%                | 4.75%                |



| STD SG7   |        |        |        |        |       |        |        |        |
|-----------|--------|--------|--------|--------|-------|--------|--------|--------|
| # Samples | 16     | 16     | 16     | 16     | 16    | 16     | 15     | 15     |
| Average   | 294    | 249    | 924    | 282    | 36598 | 2827   | 60187  | 3609   |
| StdDev    | 4      | 5      | 11     | 9      | 640   | 170    | 837    | 145    |
| RSD%      | 1.30%  | 1.84%  | 1.24%  | 3.13%  | 1.75% | 6.03%  | 1.39%  | 4.02%  |
| Max       | 301    | 260    | 946    | 301    | 37346 | 3034   | 61881  | 3927   |
| Min       | 285    | 244    | 906    | 263    | 35484 | 2456   | 59175  | 3317   |
| RPD %     | 5.48%  | 6.70%  | 4.28%  | 13.21% | 5.09% | 20.44% | 4.50%  | 16.89% |
| STD 200   |        |        |        |        |       |        |        |        |
| # Samples | 30     | 30     | 30     | 30     | 30    | 30     | 24     | 24     |
| Average   | 214    | 82     | 506    | 246    | 32131 | 1648   | 50646  | 2062   |
| StdDev    | 6      | 2      | 12     | 4      | 509   | 42     | 971    | 52     |
| RSD%      | 2.75%  | 2.56%  | 2.36%  | 1.75%  | 1.58% | 2.56%  | 1.92%  | 2.53%  |
| Max       | 226    | 84     | 527    | 255    | 32975 | 1737   | 52768  | 2153   |
| Min       | 199    | 78     | 483    | 237    | 31181 | 1591   | 48311  | 1962   |
| RPD %     | 12.52% | 7.68%  | 8.63%  | 7.52%  | 5.58% | 8.87%  | 8.80%  | 9.23%  |
| STD 400   |        |        |        |        |       |        |        |        |
| # Samples | 29     | 29     | 29     | 29     | 29    | 29     | 24     | 24     |
| Average   | 375    | 39     | 864    | 413    | 32518 | 2964   | 52330  | 3415   |
| StdDev    | 9      | 2      | 26     | 6      | 440   | 57     | 947    | 94     |
| RSD%      | 2.45%  | 4.68%  | 2.95%  | 1.37%  | 1.35% | 1.92%  | 1.81%  | 2.76%  |
| Max       | 391    | 44     | 902    | 422    | 33380 | 3100   | 53673  | 3581   |
| Min       | 350    | 35     | 805    | 397    | 31349 | 2875   | 50609  | 3284   |
| RPD %     | 10.88% | 21.59% | 11.29% | 6.11%  | 6.24% | 7.59%  | 5.86%  | 8.69%  |
| STD 500   |        |        |        |        |       |        |        |        |
| # Samples | 29     | 29     | 29     | 29     | 29    | 29     | 20     | 20     |
| Average   | 519    | 483    | 1413   | 826    | 84261 | 4543   | 134535 | 8521   |
| StdDev    | 11     | 9      | 43     | 14     | 1451  | 129    | 1005   | 258    |
| RSD%      | 2.15%  | 1.78%  | 3.05%  | 1.70%  | 1.72% | 2.85%  | 0.75%  | 3.02%  |
| Max       | 538    | 497    | 1569   | 846    | 86919 | 4812   | 136191 | 9343   |
| Min       | 500    | 462    | 1338   | 786    | 81592 | 4177   | 132233 | 8163   |
| RPD %     | 7.21%  | 7.35%  | 16.34% | 7.27%  | 6.32% | 13.99% | 2.94%  | 13.84% |

Checks analyses were conducted at ASAMen on 5% of the primary brine samples consisting of 42 external duplicate samples. In addition, some blanks and standard control samples were inserted to monitor accuracy and potential laboratory bias. No bias was found in relation to the blanks and standard control samples. Table 11.7 summarizes the results of the duplicate analyses and lists the statistics, number of samples exceeding the acceptable failure criteria of a 5% bias between duplicates. An important bias for the ASAMen laboratory was found for medium to high potassium concentrations.

**Table 11.7 Results of duplicate analyses by ASAMen (2017/18)**

|                      | B        |           | K        |           | Li       |           | Mg       |           |
|----------------------|----------|-----------|----------|-----------|----------|-----------|----------|-----------|
|                      | Original | Duplicate | Original | Duplicate | Original | Duplicate | Original | Duplicate |
| # Samples            | 42       | 42        | 42       | 42        | 42       | 42        | 42       | 42        |
| Average mg/l         | 688      | 686       | 3898     | 3901      | 433      | 434       | 1070     | 1072      |
| Std Dev              | 373      | 370       | 2283     | 2276      | 249      | 250       | 562      | 563       |
| Graph r <sup>2</sup> | 0.9977   |           | 0.9991   |           | 0.9996   |           | 0.9992   |           |
| RPD%                 | 0.29%    |           | 0.07%    |           | 0.33%    |           | 0.18%    |           |
|                      | Na       |           | SO4      |           | Cl       |           | TDS      |           |
|                      | Original | Duplicate | Original | Original  | Original | Duplicate | Original | Duplicate |
| # Samples            | 42       | 42        | 32       | 32        | 32       | 32        | 26       | 26        |
| Average mg/l         | 88245    | 88402     | 19355    | 19211     | 136025   | 135889    | 242194   | 241118    |
| Std Dev              | 45205    | 45363     | 11252    | 11080     | 58920    | 58900     | 120174   | 120184    |
| Graph r <sup>2</sup> | 0.9989   |           | 0.9911   |           | 0.9992   |           | 0.9964   |           |
| RPD%                 | 0.18%    |           | 0.75%    |           | 0.10%    |           | 0.44%    |           |

In addition to evaluation of standards, field duplicates and blanks, the ionic balances (the difference between the sum of the cations and the anions) were reviewed for to evaluate the quality of the laboratory analyses. Balances are generally considered to be acceptable if the difference is <5% and were generally <1%. No samples were rejected as having > 5% balances. The results of standard duplicate and blank samples analyses are considered to be adequate and appropriate for use in the resource estimation described herein.

#### 11.3.4. Precision (Duplicates)

During the 2017/18 drilling campaigns a total of 127 duplicate samples were inserted (Table 11.8). The elements for this analysis were Li, Ca, Mg, B, Na and K (Annex QAQC). A tolerance limit of 5% error was established.

**Table 11.8 Results of duplicate analyses by Norlab (2017/18)**

| Sample Type | Element | No. Of Samples | No. Errors | Error Rate (%) | "Mix Up" |
|-------------|---------|----------------|------------|----------------|----------|
| Duplicates  | Li      | 122            | 0          | 0,00%          | 5        |
|             | Ca      | 121            | 3          | 2,48%          | 6        |
|             | Mg      | 121            | 5          | 4,13%          | 6        |
|             | B       | 122            | 1          | 0,82%          | 5        |
|             | Na      | 122            | 4          | 3,28%          | 5        |
|             | K       | 119            | 3          | 2,52%          | 8        |

#### 11.3.5. Accuracy (Standards)

The project has two groups of standards. The first group was inserted in lot 1 to 39, and the second group was inserted from lot 40 to 71. As a result of inconsistency in the composition of the first standard group in the last few batches in which they were used, a second group of standards was prepared and used throughout the remainder of the drilling and sampling program. The deterioration of the first

standard group was detected in batch 34, 35 and then reanalyzed and confirmed in batch 36, so the standard samples of these batches (34, 35 and 36) were discarded for this analysis.

The first group of standards consisted of six different standards of which only two were submitted to three inter-laboratories tests (RRA): standards STD-4G and STD-7G. Only these two standards were used for the analysis.

The second group of standards was prepared from a locally available brine source provided by the Sales de Jujuy laboratory with approximate Li concentrations of 900 mg/l and 500 mg/l. In order to have representative standards and enough quantities for the continuity of the drilling program, a series of dilutions were carried out under controlled conditions to yield three final standards with approximate lithium concentrations of 500 mg/l, 400 mg/l and 200 mg/l and named (STD-500, STD-400 and STD-200). These standards were subjected to a round robin analysis (RRA) of pre-selected laboratories (Norlab, ASA Mendoza, SGS in Argentina and Universidad Católica del Norte and Universidad de Antofagasta in Chile).

Control and accuracy charts were prepared for each standard (Annex QAQC). The values reported for the standards were plotted in a time sequence, the lines corresponding to:

- B (Best Value)
- 1.05 \* BV (Best Value) + CI (Confidence Interval)
- 0.95 \* BV (Best Value) - CI (Confidence Interval)
- AV (Average) ± 2 \*SD (standard deviation)

The Best Value (BV) and the Confidence Interval (CI) at 95 percent were calculated for the results of the different laboratories; the average (AV) and the standard deviation (SD) were calculated with the results of the analysis of the inserted standards. As a rule, the standards that fall within the limits defined by the mean ± two standard deviations are accepted, values that fall beyond these limits are qualified as outliers. The analytical bias  $S_a$  is calculated by the following formula:

$$S_a (\%) = (AV/BV) - 1$$

Where AV represents the average of the values obtained after excluding the erratic values and BV represents the best value of the standard for the element in question. The bias is considered acceptable if its absolute value is less than 5%, questionable if it is between 5% and 10%, and unacceptable when it exceeds 10%.

The general bias of each element is calculated with the following formula:

$$S_g (\%) = SRL - 1$$

Where SRL is the slope of the linear regression of the plotted line of the Average versus the Best Value of each standard and element. A summary of the characteristics and performance of the standards of the first group are presented in Table 11.9 and of the second group in Table 11.10. For all the elements considered of the standards analyzed, good accuracy is observed (Bias <5%).

**Table 11.9 Performance of STD-4G and STD-7G Standards. Norlab (2017/18)**

| Element | N  | R2      | m        | b         | General Bias | Atypical Values |
|---------|----|---------|----------|-----------|--------------|-----------------|
| Li      | 42 | 1.00000 | 1.006091 | -2.3608   | 0.61%        | 2               |
| Ca      | 42 | 1.00000 | 1.008086 | -2.7492   | 0.81%        | 2               |
| Mg      | 42 | 1.00000 | 1.007522 | -6.9485   | 0.75%        | 1               |
| B       | 42 | 1.00000 | 1.009221 | -18.4657  | 0.92%        | 6               |
| Na      | 42 | 1.00000 | 1.003473 | -127.1128 | 0.35%        | 1               |
| K       | 42 | 1.00000 | 0.989959 | -159.7059 | -1.00%       | 4               |

**Table 11.10 Performance of STD-500, STD-400 and STD-200 Standards. Norlab (2017/18)**

| Element | N  | R2      | m        | b        | General Bias | Atypical Values |
|---------|----|---------|----------|----------|--------------|-----------------|
| Li      | 88 | 0.99965 | 1.006091 | 10.2693  | -3.13%       | 5               |
| Ca      | 88 | 1.00000 | 1.002345 | -0.3551  | 0.23%        | 4               |
| Mg      | 88 | 0.99875 | 0.994037 | 20.2245  | -0.60%       | 3               |
| B       | 88 | 1.00000 | 0.996055 | 6.3056   | -0.39%       | 6               |
| Na      | 88 | 0.99998 | 0.978342 | -72.0559 | -2.17%       | 1               |
| K       | 88 | 0.99836 | 0.964586 | -9.3029  | -3.54%       | 6               |

### 11.3.6. Contamination (Blanks)

A total of 106 blanks were inserted to analyze for potential sample contamination. Some batches showed values of Ca and Na that exceeded the quantification limit (Annex QAQC). Nevertheless, the correlation between these samples and their respective consecutives allows to establish that there is no clear analytical contamination but a variation in the source of distilled water used in the preparation of the blanks.

## 12 DATA VERIFICATION

The author reviewed the protocols for drilling, sampling and testing procedures at the initial planning stage as well as the execution of the 2017/18 drilling and testing programs in Salar de Cauchari. The author spent a significant amount of time in the field during the 2017/18 field campaign overlooking the implementation and execution of drilling, testing, and sampling protocols.

The author was responsible for the oversight and analysis of the QA/QC programs related to brine sampling and laboratory brine chemistry analysis as well as the laboratory porosity analysis. A significant amount of QA/QC protocols were implemented for the brine chemistry and drainable porosity analysis programs that allowed continuous verification of the accuracy and reliability of the results obtained. As described in Section 11 no significant issues were found with the results of the brine and porosity laboratory analysis. It is the opinion of the author that the information developed and used for the brine resource estimate herein is adequate, accurate and reliable.

## 13 MINERAL PROCESSING AND METALLURGICAL TESTING

The brines from Salar de Cauchari are solutions nearly saturated in sodium chloride with an average concentration of total dissolved solids (TDS) of 290 g/L. The average density is 1.18 g/cm<sup>3</sup>. Components present in the Cauchari brine are: K, Li, Mg, Ca, Na, Cl, SO<sub>4</sub>, HCO<sub>3</sub> and B. Table 7.3 shows a breakdown of the principal chemical constituents in the brine including maximum, average, and minimum values, based on the 546 brine samples that were collected and analyzed from the exploration boreholes during the 2011 and 2018 drilling programs.

The Cauchari brine chemistry is very similar to the brine of Salar de Olaroz that is being processed successfully by Orocobre in the Olaroz lithium carbonate facility, 20 km north of the Project area. The Cauchari brine can be processed using a similar process technology to that which is applied by Orocobre at the Olaroz plant, which is further discussed in Chapter 17.

## 14 MINERAL RESOURCE ESTIMATES

### 14.1 Overview

The essential elements of a brine resource determination for a salar are:

- Definition of the aquifer geometry,
- Determination of the drainable porosity or specific yield (Sy), and
- Determination of the concentration of the elements of interest.

Resources may be defined as the product of the first three parameters. The use of specific yield allows the direct comparison of brine resources from the widest range of environments.

Aquifer geometry is a function of both the shape of the aquifer, the internal structure and the boundary conditions (brine / fresh water interface). Aquifer geometry and boundary conditions can be established by drilling and geophysical methods. Hydrogeological analyses are required to establish catchment characteristics such as surface and groundwater inflows, evaporation rates, water chemistry and other factors potentially affecting the brine reservoir volume and composition in-situ. Drilling is required to obtain samples to estimate the salar lithology, specific yield and grade variations both laterally and vertically.

### 14.2 Resource model boundary and domains

The Cauchari JV resource model domain covers an area of 117.7 km<sup>2</sup> and is limited to the Cauchari JV roject area and further constrained by the following factors:

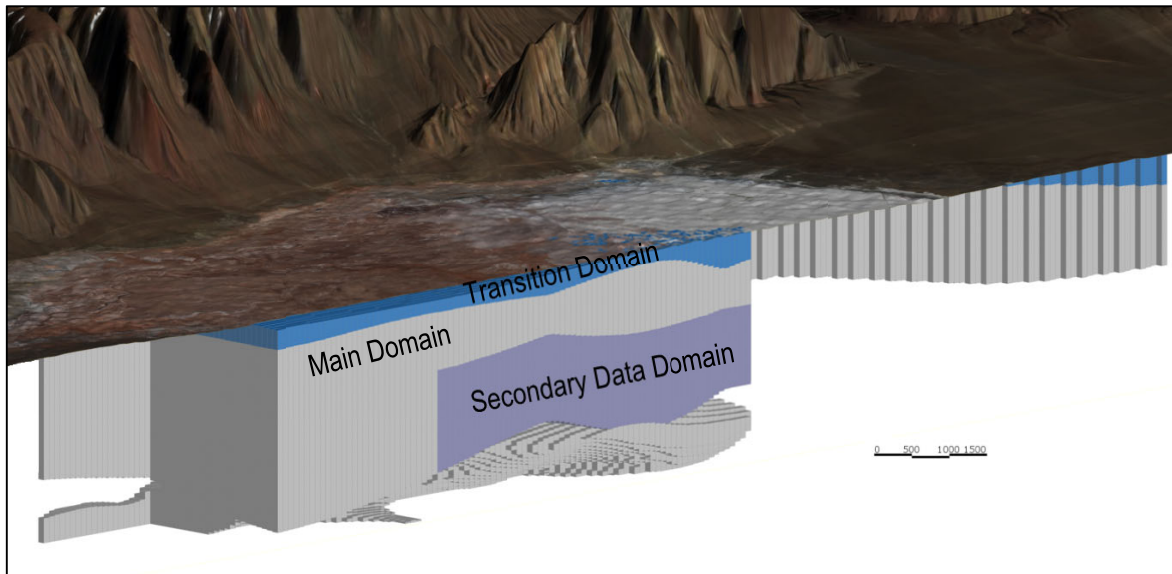
- The top of the model coincides with the brine level in the Salar as measured in a number of monitoring wells and further interpreted by TEM and SEV geophysical profiles.
- The lateral boundaries of the model domain are limited to the area of the Cauchari tenements where they flank the neighboring LAC concessions and by the brine / fresh water interface along the eastern and western limits of the Salar as interpreted from boreholes information and TEM and SEV profiles.
- The bottom of the model coincides with a surface created from the bottom of the boreholes. Locally, a deeper resource volume has been defined in the Lower Sand as defined by boreholes CAU11R, CAU12DA, CAU13DA and CAU19D.

The resource model has been divided in three domains to account for the different data availability, geological knowledge and sample support. The domains are shown in figure 14.1 and are described as follow:

- **Transition Domain:** Accounts for five percent of the total resources and is defined as the volume in the upper part of the Salar that includes fresher water and transition into pure brine. The lithium concentrations in the transition zone increase with depth. The number of brine samples in the transition domain is low because the surface casing installations for the exploration boreholes (mostly in the transition domain) was generally carried out using rotary mud drilling that is not suitable for reliable brine sample collection. A regression approach was adapted to estimate the lithium concentrations within this domain due to the good correlation with depth and the lack of samples.

- Main Domain: Accounts for 83% of the total resources and have normal and reliable sample data obtained during the drilling. A kriging approach was selected for this domain due to the number of samples available.
- Secondary Data Domain: Accounts for 12% of the total resources and its lithium content was defined mostly by brine chemistry analysis on samples derived during pumping tests on CAU8, CAU9, CAU10, and CAU11. An inverse distance approach was selected because of the amount of information available.

**Figure 14.1 Schematic showing the block model domains**

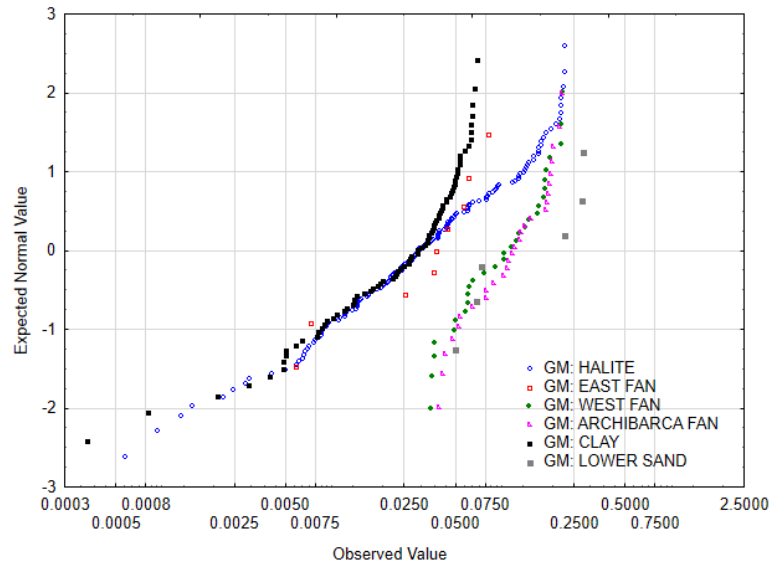


### 14.3 Specific yield

Specific yield is defined as the volume of water released from storage by an unconfined aquifer per unit surface area of aquifer per unit decline of the water table.

The specific yield values used to develop the resources model are based on analyses of 301 undisturbed valid samples from diamond drill core by GSA, Core Laboratories, and DBSA. Figure 14.2 shows the normal distribution of the specific yield grouped by lithology.





A cell de-clustering approach was used to account for spatial sample density. The de-clustered average was assigned to each geological unit. Table 14.1 shows the general statistics and the de-clustered average for each geological unit.

**Table 14.1 Distribution of specific yield (Sy) in the resource model**

| Geological Unit | No. Samples | Average | Declustered Average | Standard Deviations | Coefficient of Variation |
|-----------------|-------------|---------|---------------------|---------------------|--------------------------|
| Halite          | 144         | 0.05    | 0.05                | 0.06                | 1.1                      |
| East Fan        | 9           | 0.04    | 0.03                | 0.02                | 0.6                      |
| West Fan        | 30          | 0.11    | 0.11                | 0.06                | 0.5                      |
| Archibarca Fan  | 28          | 0.12    | 0.12                | 0.06                | 0.5                      |
| Clay            | 84          | 0.03    | 0.03                | 0.02                | 0.6                      |
| Lower Sand      | 6           | 0.16    | 0.14                | 0.11                | 0.7                      |

## 14.4 Brine Concentration

The distributions of lithium and potassium concentrations in the model domain are based on a total of 546 brine analyses (not including QA/QC analyses and contaminated samples). Table 7.3 shows a summary of the brine chemical composition.

## 14.5 Resource Category

### 14.5.1 CIM definitions

The CIM Council (May 10, 2014) adopted the following definition standards for minerals resources:

#### Inferred Mineral Resource

An Inferred Mineral Resource is that part of a Mineral Resource for which quantity and grade or quality are estimated on the basis of limited geological evidence and sampling. Geological evidence is sufficient to imply but not verify geological and grade or quality continuity.

An Inferred Mineral Resource has a lower level of confidence than that applying to an Indicated Mineral Resource and must not be converted to a Mineral Reserve. It is reasonably expected that the majority of Inferred Mineral Resources could be upgraded to Indicated Mineral Resources with continued exploration.

An Inferred Mineral Resource is based on limited information and sampling gathered through appropriate sampling techniques from locations such as outcrops, trenches, pits, workings and drill holes. Inferred Mineral Resources must not be included in the economic analysis, production schedules, or estimated mine life in publicly disclosed Pre- Feasibility or Feasibility Studies, or in the Life of Mine plans and cash flow models of developed mines. Inferred Mineral Resources can only be used in economic studies as provided under NI 43-101.

There may be circumstances, where appropriate sampling, testing, and other measurements are sufficient to demonstrate data integrity, geological and grade/quality continuity of a Measured or Indicated Mineral Resource, however, quality assurance and quality control, or other information may not meet all industry norms for the disclosure of an Indicated or Measured Mineral Resource. Under these circumstances, it may be reasonable for the Qualified Person to report an Inferred Mineral Resource if the Qualified Person has taken steps to verify the information meets the requirements of an Inferred Mineral Resource.

#### Indicated Mineral Resource

An Indicated Mineral Resource is that part of a Mineral Resource for which quantity, grade or quality, densities, shape and physical characteristics are estimated with sufficient confidence to allow the application of Modifying Factors in sufficient detail to support mine planning and evaluation of the economic viability of the deposit.

Geological evidence is derived from adequately detailed and reliable exploration, sampling and testing and is sufficient to assume geological and grade or quality continuity between points of observation.

An Indicated Mineral Resource has a lower level of confidence than that applying to a Measured Mineral Resource and may only be converted to a Probable Mineral Reserve.

Mineralization may be classified as an Indicated Mineral Resource by the Qualified Person when the nature, quality, quantity and distribution of data are such as to allow confident interpretation of the geological framework and to reasonably assume the continuity of mineralization. The Qualified Person must recognize the importance of the Indicated Mineral Resource category to the advancement of the feasibility of the project. An Indicated Mineral Resource estimate is of sufficient quality to support a Pre-Feasibility Study which can serve as the basis for major development decisions.

## Measured Mineral Resource

A Measured Mineral Resource is that part of a Mineral Resource for which quantity, grade or quality, densities, shape, and physical characteristics are estimated with confidence sufficient to allow the application of Modifying Factors to support detailed mine planning and final evaluation of the economic viability of the deposit.

Geological evidence is derived from detailed and reliable exploration, sampling and testing and is sufficient to confirm geological and grade or quality continuity between points of observation.

A Measured Mineral Resource has a higher level of confidence than that applying to either an Indicated Mineral Resource or an Inferred Mineral Resource. It may be converted to a Proven Mineral Reserve or to a Probable Mineral Reserve.

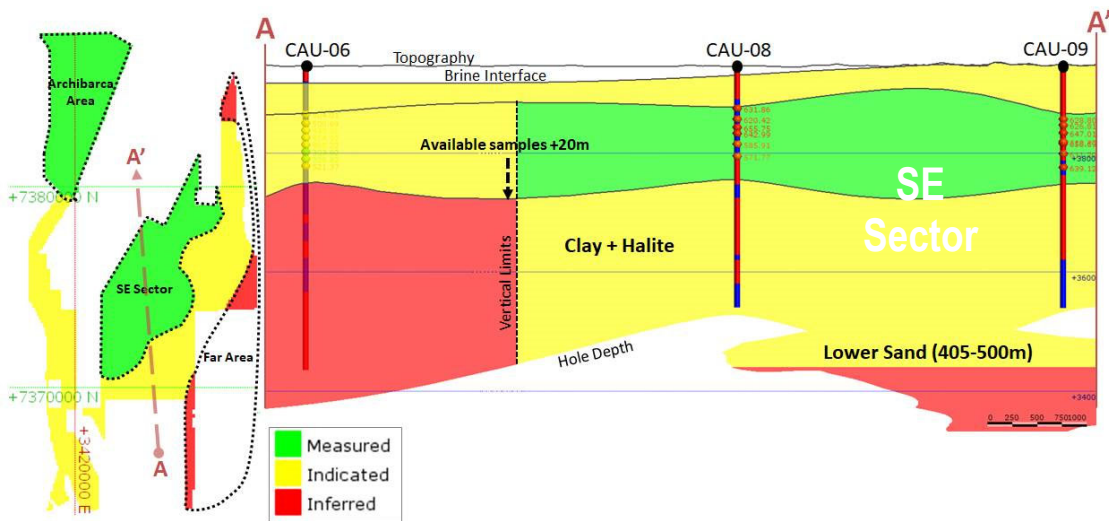
Mineralization or other natural material of economic interest may be classified as a Measured Mineral Resource by the Qualified Person when the nature, quality, quantity and distribution of data are such that the tonnage and grade or quality of the mineralization can be estimated to within close limits and that variation from the estimate would not significantly affect potential economic viability of the deposit. This category requires a high level of confidence in, and understanding of, the geology and controls of the mineral deposit.

### 14.5.2 Resource category definition

The resources category for the project has been assigned according to the CIM guidelines described above and reflect level of hydrogeological knowledge, sample availability and quality. The category classification is shown in figure 14.3 and is described as follow:

- Measured Resources include the majority of Archibarca Fan area and the Clay and Halite units to a variable depth of up to approximately 400 m (based on core and brine sample availability) within the SE Sector of the project.
- Indicated Resources include the West Fan, the deeper portions of the Clay and Halite Units, the upper part of the East Fan (within the transitions domain) and the Lower Sand to a depth of 500 m.
- Inferred Resources include outlying deeper pockets of the Archibarca Fan area, the Lower Sand below 500 m depth, the limits of the property in the East and the East Fan below the transition domain.

Figure 14.3 Resources category classification



## 14.6 Resource modeling methodology and construction

### 14.6.1 Overview

The Stanford Geostatistical Modeling Software (SGeMS) was used for the Cauchari JV brine resource estimation. SGeMS has been used in the past for the estimation of brine resources in other areas of the Central Andes. Geostatistics is a branch of statistics specifically developed to estimate ore grades for mining operations from spatiotemporal datasets. Geostatistics goes far beyond simple interpolation methods such as nearest neighbor or inverse distance as it accounts for the spatial correlation and continuity of geological properties typically observed in the field. Based on this, the following steps were carried out to estimate the lithium and potassium resources.

- The block model geometry was adapted to represent the geological model with an appropriate block size (x=100 m, y=100 m, z=1 m).
- Generation of histograms, probability plots and box plots was conducted for the Exploratory Data Analysis (EDA) for lithium and potassium.
- Calculation of the experimental variograms with their respective variogram models for lithium and potassium in three orthogonal directions.
- Definition of the random function model and selection of the kriging method.
- Interpolation of lithium and potassium for each block in mg/L using ordinary kriging with the variogram models shown in Figure 14.12 and Figure 14.13.
- Calculation of total resources using the de-clustered porosity average value for each geological unit, based on the boreholes data. Each geological unit will represent a particular porosity value as shown in Table 14.1. The total resources are shown in Table 14.5.

### 14.6.2 Exploratory data analysis

The Exploratory Data Analysis (EDA) of lithium (Li) and potassium (K) concentrations consisted of a univariate statistical description using histograms, probability plots and box plots, and a spatial description based on data posting and trend analysis. This information is used to define the random function models and the type of kriging method.

Exploratory data results show significant differences in both the statistical properties of the concentration of ions and the patterns of spatial continuity across the different lithological units defined in the study area. To illustrate this, Figure 14.4 and 14.5 show the box-plot of Li and K, respectively. The box-plots depict the quartiles (the second quartile is the median) as well as the minimum and maximum values of the data analyzed separately by lithological units. In addition, Tables 14.2 and 14.3 summarize the main univariate statistics of Li and K for the different lithological units.

Li in the Archibarca unit renders less variability than the Halite and West Fan units, and that the mean value of the West Fan is significantly smaller (more than 100 mg/L) than that of the Archibarca unit. Based on this, data within each lithological unit is treated as a separate population. The spatial patterns of Li and K in the different lithological units are also significantly different, suggesting the existence of different statistical populations. This is shown in the next section.

Figure 14.4 Lithium Box-plot

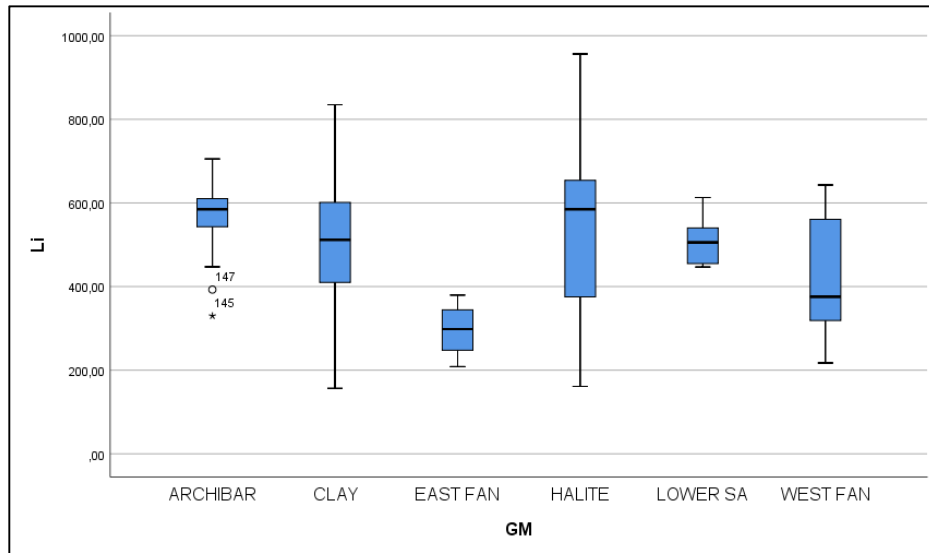


Figure 14.5 Potassium Box-plot

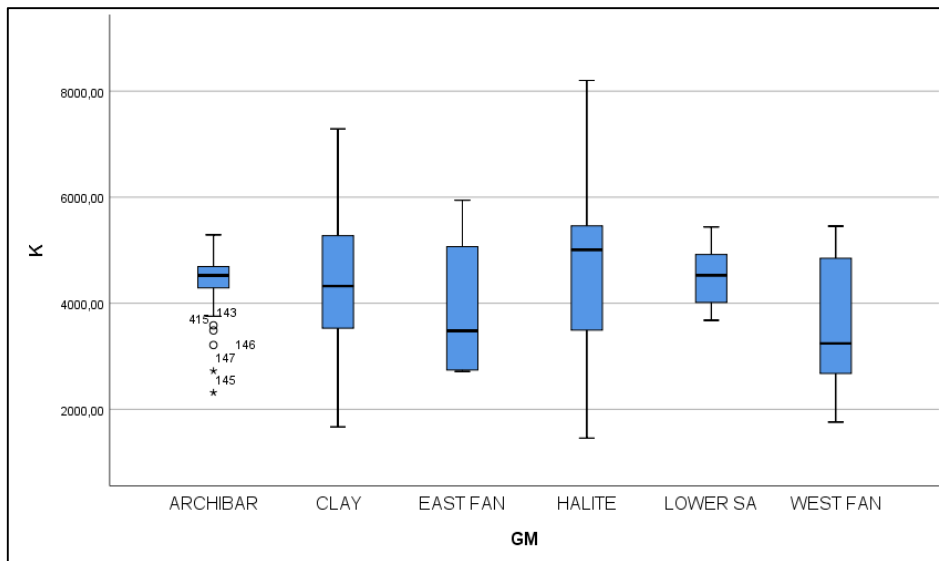


Table 14.2 Univariate statistics of Li concentrations (mg/L) for each lithological unit

| GM             | Sample Number | Li Mean | Li Standard Deviation | Li Minimum | Li Maximum |
|----------------|---------------|---------|-----------------------|------------|------------|
| Archibarca Fan | 93            | 578     | 59                    | 330        | 705        |
| Clay           | 185           | 495     | 138                   | 157        | 835        |
| East Fan       | 4             | 296     | 70                    | 209        | 379        |
| Halite         | 188           | 530     | 165                   | 161        | 956        |
| Lower Sand     | 14            | 506     | 55                    | 447        | 613        |
| West Fan       | 62            | 417     | 127                   | 217        | 643        |

**Table 14.3 Univariate statistics of K concentrations (mg/L) for each lithological unit**

| GM             | Sample Number | K Mean | K Standard Deviation | K Minimum | K Maximum |
|----------------|---------------|--------|----------------------|-----------|-----------|
| Archibarca Fan | 93            | 4,471  | 459                  | 2,316     | 5,290     |
| Clay           | 185           | 4,352  | 1,169                | 1,668     | 7,287     |
| East Fan       | 4             | 3,904  | 1,522                | 2,715     | 5,942     |
| Halite         | 188           | 4,578  | 1,352                | 1,457     | 8,202     |
| Lower Sand     | 14            | 4,525  | 554                  | 3,679     | 5,439     |
| West Fan       | 62            | 3,525  | 1,089                | 1,758     | 5,454     |

### 14.6.3 Variography

The spatial variability of Li and K concentrations were characterized by the semivariogram,  $\gamma(\mathbf{h})$ . The semivariogram is a function that measures the variability between pairs of variables separated by a distance  $\mathbf{h}$ . Very often, the correlation between two variables separated by a certain distance disappears when  $|\mathbf{h}|$  becomes too large. At this instant,  $\gamma(\mathbf{h})$  approaches a constant value. The distance beyond which  $\gamma(\mathbf{h})$  can be considered to be a constant value is known as the range, which represents the transition of the variable to the state of negligible correlation. Experimental semivariograms obtained along multiple directions revealed that the random function model of the selected ions can be characterized with an axisymmetric random function model; and symmetric semivariogram with respect to the z-direction. This type of correlation function model is typically observed in sedimentary geological formations such as an evaporitic system.

#### Variogram models of potassium

The experimental semivariograms of K or the different units were fitted with a theoretical model consisting of two correlation structures, i.e., the combination of an exponential model with a Gaussian model. This composite structure is necessary in this case to properly represent the small-scale correlation observed along the z-direction compared to a larger correlation observed in the xy plane directions.

$$\text{Clay-Halite } \gamma_K(h) = 9 \times 10^5 + 5 \times 10^5 \gamma_{Exp}(a_x = a_y = 3300, a_z = 60) + 8 \times 10^5 \gamma_{Gauss}(a_x = a_y = 3300, a_z = 300)$$

$$\text{Archibarca } \gamma_K(h) = 80800 \gamma_{Exp}(a_x = a_y = 4320, a_z = 20) + 140000 \gamma_{Gauss}(a_x = a_y = 4320, a_z = 350)$$

$$\text{West Fan } \gamma_K(h) = 2 \times 10^5 \gamma_{Exp}(a_x = a_y = 3300, a_z = 60) + 1.8 \times 10^6 \gamma_{Gauss}(a_x = a_y = 12000, a_z = 580)$$

The semivariogram is expressed in units of  $\text{mg}^2/\text{L}^2$ , and the range in units of meters. Thus, the correlation structure in the xy plane has a range between 3,300 and 4,320 meters, whereas the correlation structure in the z-direction has a range between 300 and 580 meters. This means that in overall the system is stratified with lenses that extend laterally several kilometers but with limited thickness of few hundreds of meters. The variogram models shown below were fitted to experimental semivariograms. Only the semivariogram point estimates with sufficient pair samples were considered. The experimental variograms of lithium and potassium are shown in the following figures with their respective variogram models

Figure 14.6 Archibarca variogram model fitted with the corresponding experimental variogram

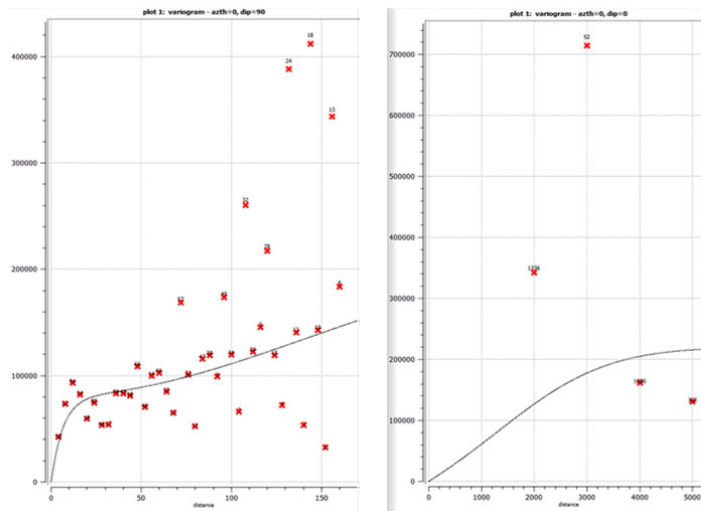


Figure 14.7 Clay-Halite variogram model fitted with the corresponding experimental variogram

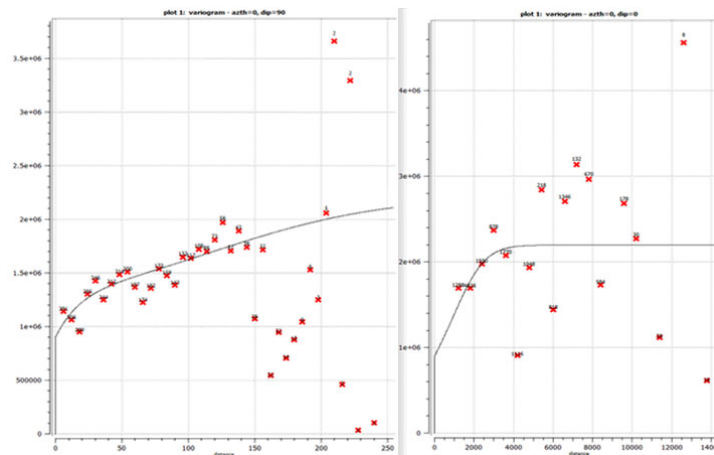
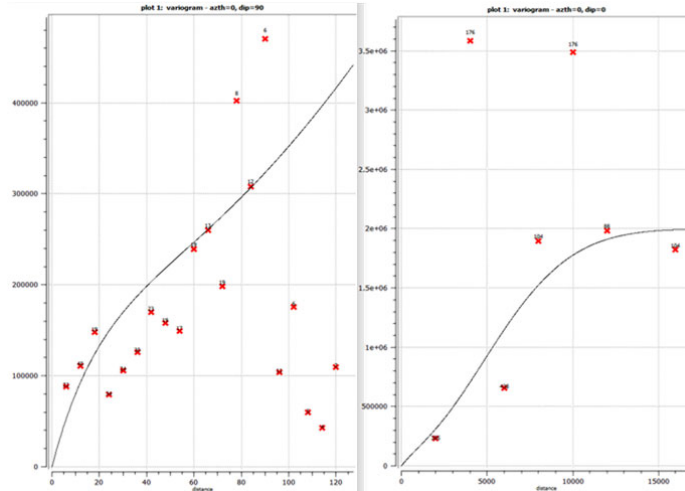




Figure 14.8 West Fan variogram model fitted with the corresponding experimental variogram



### Variogram models of lithium

The experimental semivariograms were fitted with a theoretical model consisting of only one correlation structure and a nugget coefficient. The experimental variograms for Li with their respective variogram models are shown in the following figures.

Clay-Halite  $\gamma_{Li}(h) = 9000 + 18000\gamma_{sph}(a_x = a_y = 3835, a_z = 150)$

Archibarca  $\gamma_{Li}(h) = 2800 \gamma_{Exp}(a_x = a_y = 4320, a_z = 40)$

West Fan  $\gamma_{Li}(h) = 3000 \gamma_{Exp}(a_x = a_y = 5800, a_z = 50)$

The semivariogram is expressed in units of  $mg^2/L^2$ , and the range in units of meters. In this case, the correlation structure in the xy plane has a range that varies between 3,835 and 5,800 metres, whereas the correlation structure in the z-direction has one structure with a range that oscillates between 40 and 150 meters. Results show that Li is more stratified than K with similar spatial continuity in the xy plane.

Figure 14.9 Archibarca variogram model fitted with the corresponding experimental variogram

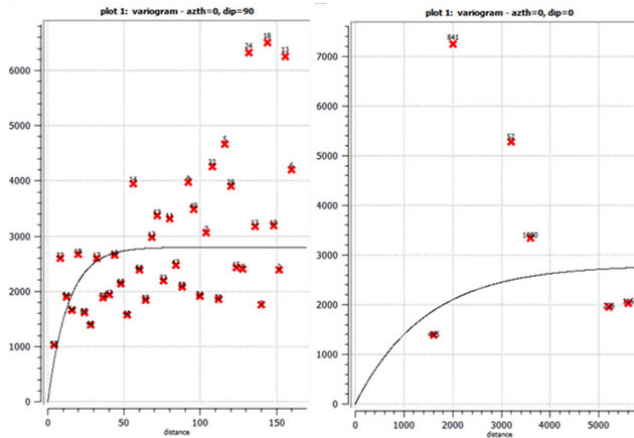


Figure 14.10 Clay-Halite variogram model fitted with the corresponding experimental variogram

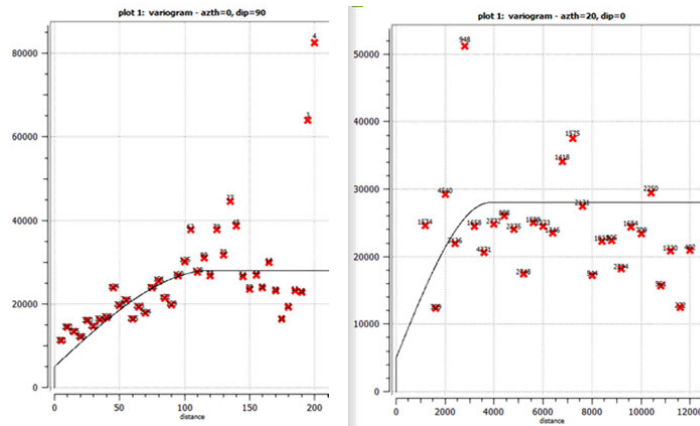
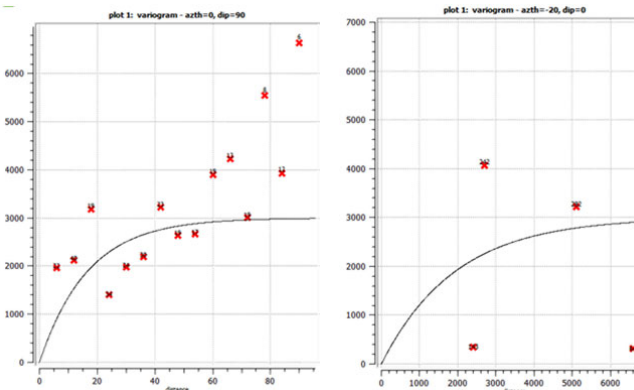


Figure 14.11 West Fan variogram model fitted with the corresponding experimental variogram



**Table 14.4 Parameters for the calculation of the experimental variograms**

| Variogram Parameters |                  |             |         | Tolerance     |             |
|----------------------|------------------|-------------|---------|---------------|-------------|
| Lag (m)              | Max. No. Of Lags | Azimuth (°) | Dip (°) | Bandwidth (m) | Angular (°) |
| 200                  | 50               | 20          | 0       | 500           | 45          |
| 10                   | 70               | 0           | 90      | 500           | 89          |

#### 14.6.4 Kriging estimation of Li and K concentrations

The estimation procedure follows the method known as kriging within strata (KWS). The estimation within each unit is performed with the data associated with that unit and the corresponding variogram model. In some units, the semivariogram is poorly estimated because the number of data pairs is insufficient. This is the case of Lower Sand and East Fan. In those cases, the proportional effect correction suggested by Journel and Huijbregts (1978) is used to estimate the variogram.

The results of the EDA indicate that even though the structure of heterogeneity (random function model) is different for each unit, ordinary kriging is an appropriate technique for the estimation of Li and K concentrations in each unit. The ordinary kriging method is the most commonly used kriging method. It assumes that the mean is an unknown constant dictated by neighborhood data. Essentially, ordinary kriging re-estimates, at each estimation location, the mean value by only using the data within the search neighborhood. Hence, ordinary kriging can represent a random function with varying mean but stationary variogram. As previously, in accordance to this random function model, all experimental variograms were properly fitted with a combination of stationary theoretical variograms characterized by a well-defined sill. Figure 14.12 and 14.13 show the results from the kriging estimation.

Figure 14.12 Li concentration distribution

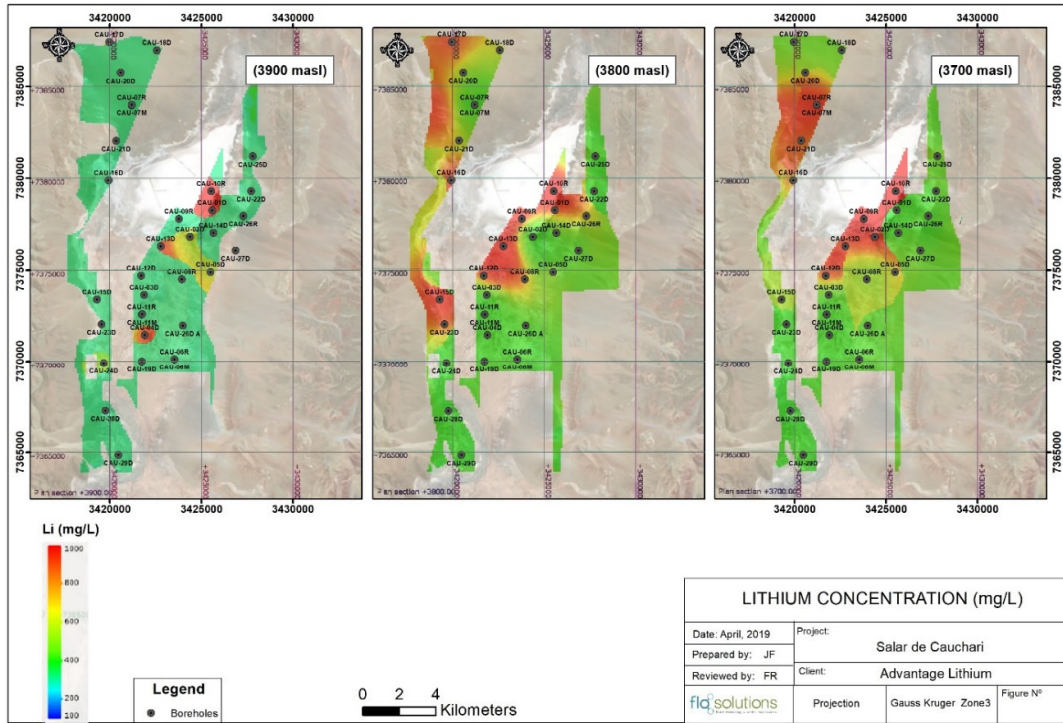
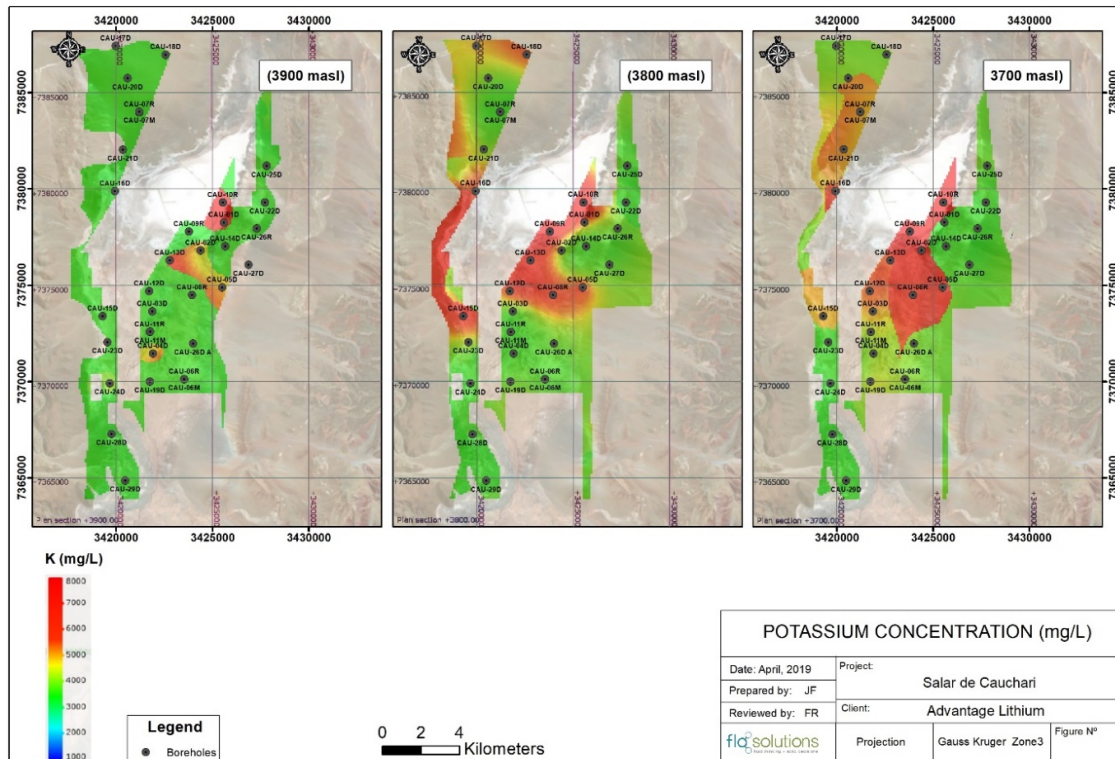


Figure 14.13 K concentration distribution



## 14.7 Grade estimate

The grade of lithium and potassium in each model block was calculated applying the following operation:

$$R_i = C_i \cdot S_{y_i} \cdot V_i$$

Where:  $i$  is the indice of the block, going from 1 to 4,138,515

$R_i$ : Grade value to be assigned (g)

$C_i$ : Concentration value assigned from the estimation (mg/L)

$S_{y_i}$ : Porosity value assigned from the estimation (%)

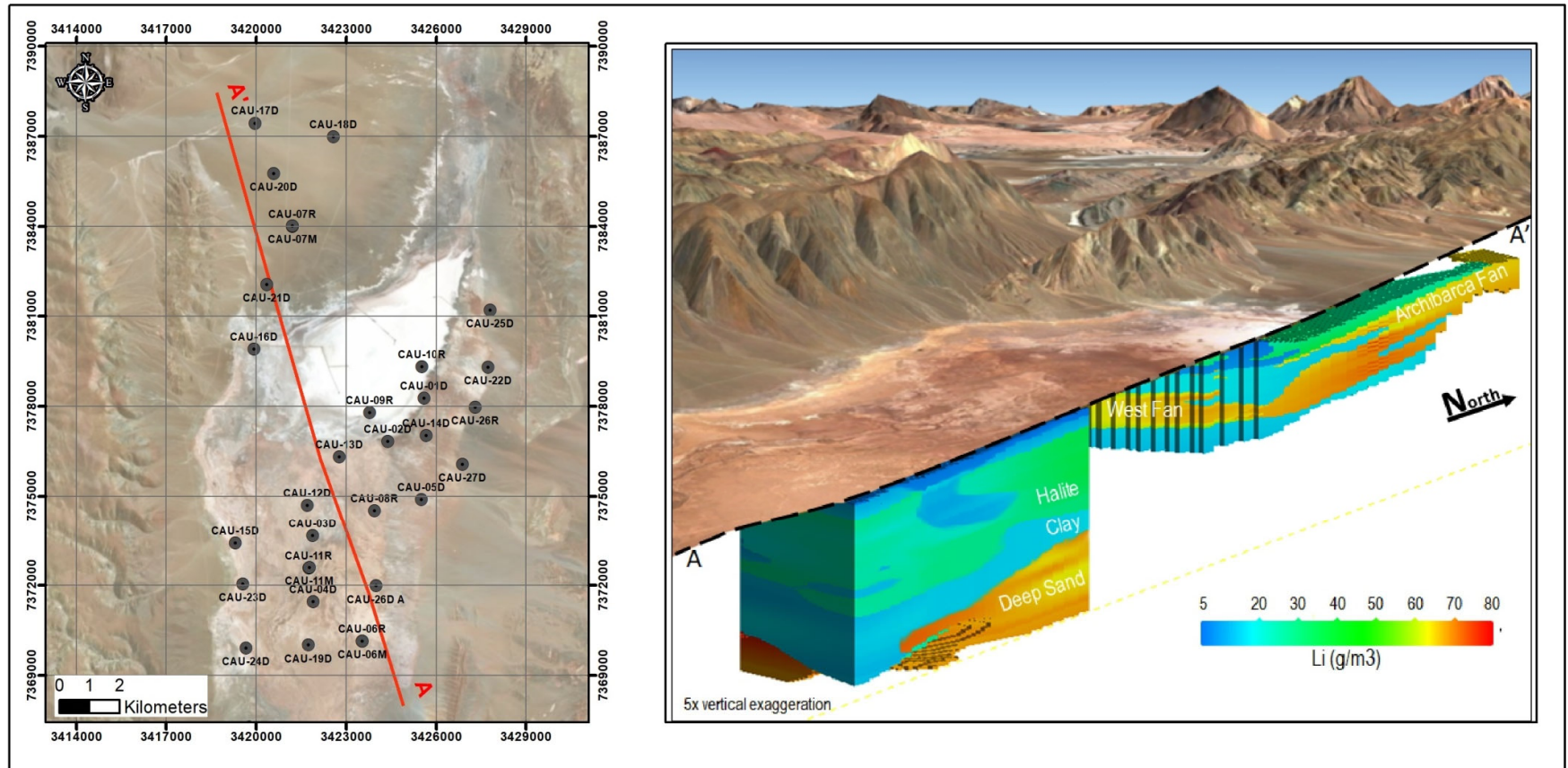
$V_i$ : Block volume (m<sup>3</sup>)

The total resource in the reservoir is estimated as the sum of all blocks in the model,

$$R_T = \sum_i R_i$$

Figure 14.14 shows lithium grade distributions along a NW-SE section across the project.

Figure 14.14 NW-SE section looking West through the resource model showing the lithium grade



## 14.8 Resource estimate

The resource estimate was prepared in accordance with the guidelines of National Instrument 43-101 and uses best practice methods specific to brine resources, including a reliance on core drilling and sampling methods that yield depth-specific chemistry and drainable porosity measurements.

The lithium and potassium brine resources are summarized in Table 14.5.

**Table 14.5 Cauchari JV Project Lithium and Potassium Resources estimate (April 19, 2019)**

|  | Measured (M)   |                  | Indicated (I)  |                  | M+I            |                  | Inferred       |                  |
|--|----------------|------------------|----------------|------------------|----------------|------------------|----------------|------------------|
| <b>Aquifer volume (km<sup>3</sup>)</b> | 10             |                  | 21             |                  | 31             |                  | 11             |                  |
| <b>Mean specific yield</b>             | 6.6%           |                  | 5.9%           |                  | 6.1%           |                  | 5.6%           |                  |
| <b>Brine volume (km<sup>3</sup>)</b>   | 0.6            |                  | 1.2            |                  | 1.9            |                  | 0.6            |                  |
| <b>Brine volume (km<sup>3</sup>)</b>   | <b>Li</b>      | <b>K</b>         | <b>Li</b>      | <b>K</b>         | <b>Li</b>      | <b>K</b>         | <b>Li</b>      | <b>K</b>         |
| <b>Mean grade (g/m<sup>3</sup>)</b>    | 35             | 291              | 26             | 238              | 29             | 255              | 27             | 225              |
| <b>Mean concentration (mg/l)</b>       | 527            | 4,438            | 452            | 4,145            | 476            | 4,238            | 473            | 3,867            |
| <b>Resource (tonnes)</b>               | <b>345,000</b> | <b>2,800,000</b> | <b>550,000</b> | <b>5,000,000</b> | <b>900,000</b> | <b>7,800,000</b> | <b>290,000</b> | <b>2,400,000</b> |

Notes to Table 14.5:

- CIM definitions were followed for mineral resources.
- The Qualified Person for this Mineral Resource estimate is Frits Reidel, CPG.
- No cut-off concentrations have been applied to the resource estimate
- Numbers may not add due to rounding.

Table 14.4 shows the Mineral Resource of the Cauchari JV expressed as lithium carbonate equivalent (LCE) and potash (KCl).

**Table 14.6 Cauchari JV Project Mineral Resources expressed as LCE and potash**

|                         | Measured (M) | Indicated (I) | M+I        | Inferred  |
|-------------------------|--------------|---------------|------------|-----------|
| Lithium Carbonate (LCE) | 1,850,000    | 2,950,000     | 4,800,000  | 1,500,000 |
| Potash (KCl)            | 5,400,000    | 9,600,000     | 14,900,000 | 4,600,000 |

Notes to Table 14.6:

- Lithium is converted to lithium carbonate (Li<sub>2</sub>CO<sub>3</sub>) with a conversion factor of 5.32.
- Potassium is converted to potash with a conversion factor of 1.91.
- Numbers may not add due to rounding.

It is the opinion of the author that the Salar geometry, brine chemistry composition and the specific yield of the Salar sediments have been adequately characterized to support the resource estimates for the Project herein.

## 15 MINERAL RESERVE ESTIMATES

No mineral reserve estimate has been prepared for the Project.



## 16 MINING METHODS

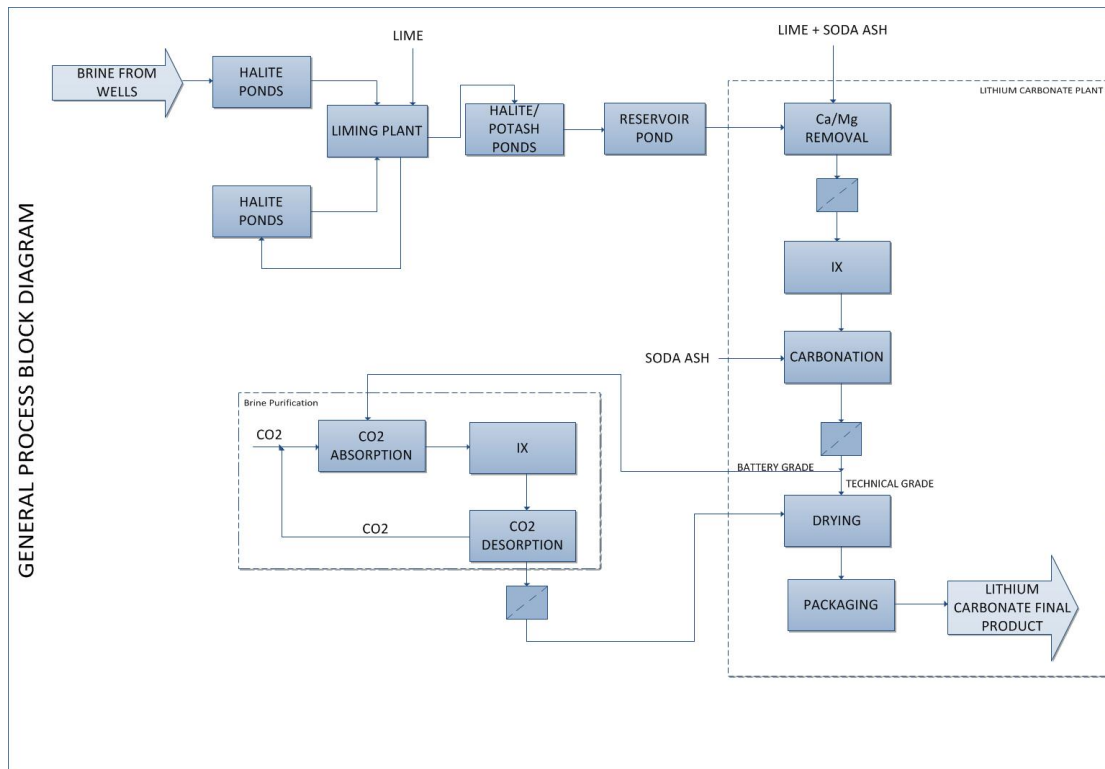
Based on the results of the pumping tests carried out on the project it is most likely that brine abstraction from the Salar will take place by installing and operating conventional production wellfields. Pumping rates of individual wells could be in the range between 10 l/s and 25 l/s. Well completion depths will depend on locations in the NW or SE Sectors. Additional information about mining methods was provided in the Project's Preliminary Economic Assessment (PEA) prepared by Worley Parsons and dated 31 August, 2018.

## 17 RECOVERY METHODS

Recovery methods were described in the PEA prepared by Worley Parsons and dated 31 August, 2018. This section provides a brief summary of the recovery methods considered in the PEA.

The Project considers the design of production wells, evaporation ponds and processing plant to obtain up to 25,000 TPY of battery and technical grade lithium carbonate ( $\text{Li}_2\text{CO}_3$ ), maximising the production of technical battery grade when possible. A general block diagram of the process may be seen in Figure 17.1.

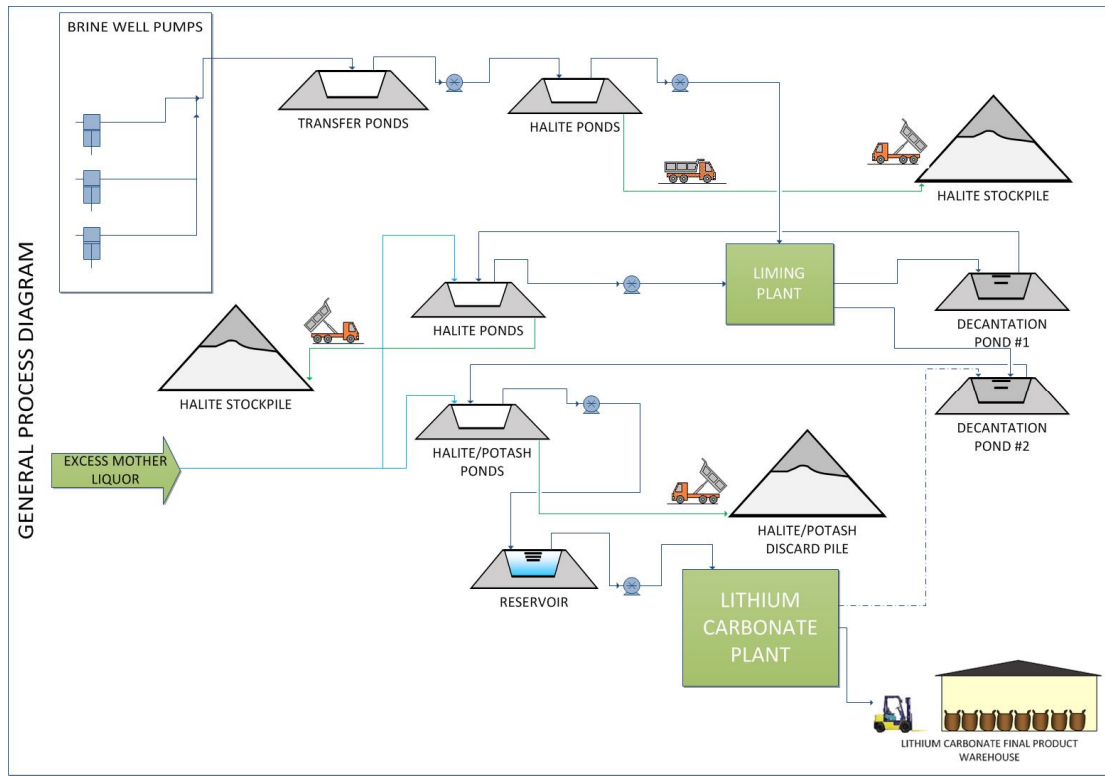
Figure 17.1 Schematic of the lithium recovery process for the Cauchari JV Project



As a general overview of the process, the brine that feeds the Lithium Carbonate ( $\text{Li}_2\text{CO}_3$ ) Plant is produced from the brine wellfield which is divided in two zones, the NW Sector wells and the SE Sector wells. The brine is pumped to the evaporation ponds, designed to precipitate halite and halite/potash salts. This occurs through solar evaporation, aided with the liming of the brine, which precipitates most of the magnesium (Mg), as magnesium hydroxide, present in the brine. The calcium from the lime is precipitated as gypsum. After the evaporation ponds, the brine is fed to the  $\text{Li}_2\text{CO}_3$  plant, where, through a series of processes, solid technical grade or battery grade lithium carbonate is obtained, to be shipped, according to each client's requirements. A general process flow diagram is shown in

Figure 17.2 .

Figure 17.2 General process diagram



Evaporation of the water in the brine results in the crystallization of mainly halite salts, while lithium (Li) concentrates in the remaining brine. At a defined point in the process, the brine is sent to a liming plant, where, through the reaction between calcium hydroxide ( $\text{Ca}(\text{OH})_2$ ) and the Mg and sulphates ( $\text{SO}_4$ ) in the brine, in a specific reactor, magnesium hydroxide and calcium sulphate precipitate. The pulp is then sent to a decantation pond. Subsequently, the brine is transferred to the next group of solar evaporation ponds for further concentration. A back-up stage liming plant is installed to ensure the removal of some remaining magnesium from the brine. After decantation the concentrated brine is then pumped to the final ponds, where halite and some potassium salts crystallize. When the brine reaches a suitable lithium concentration for lithium carbonate processing, it is then stored in reservoir ponds, which feed the Lithium Carbonate Plant.

The Lithium Carbonate Plant is a chemical facility that receives brine concentrate from the solar ponds and through specific processes removes the final impurities, in order to obtain lithium carbonate meeting the required specifications.

In the  $\text{Li}_2\text{CO}_3$  plant, the remaining Mg and Ca in the brine are removed through precipitation, by reacting the brine with a mixture of mother liquor (solution recovered from the belt filtration stage), soda ash and slaked lime. These impurities precipitate in the form of calcium carbonate ( $\text{CaCO}_3$ ) and magnesium hydroxide ( $\text{Mg}(\text{OH})_2$ ), and are pumped to a re-pulping tank, and then to a discard pond.

The brine with low levels of impurities is pumped to an ion exchange (IX) stage, which, through adsorption of some of the minor impurities in the brine, delivers purified brine to the carbonation stage.

In the carbonation stage, lithium carbonate precipitates, through the addition of soda ash. This reaction occurs at high temperatures. The precipitated lithium carbonate is then separated from the solution through a belt filter.

From here there are 2 options: the precipitated lithium carbonate may be transferred directly to the drying/packaging stage and sold as technical grade lithium carbonate or further processed to battery grade.

For the latter, the lithium carbonate is re-pulped with water and then reacted with carbon dioxide in order to produce a more soluble lithium bicarbonate solution. The solution is filtered, removing insoluble impurities. The filtered solution goes through an ion exchange stage where all di and tri valent metals and boron are removed. The solution is heated in order to release and recover the carbon dioxide and crystalize pure lithium carbonate. The solids are thickened and filtered, and then dried, micronized and packaged.

## 18 PROJECT INFRASTRUCTURE

Project infrastructure was described in detail in the PEA prepared by Worley Parsons and dated 31 August, 2018. Infrastructure requirements can be summarized as two brine production wellfields and pipelines, evaporation ponds, power plant, water supply, accommodation facilities, sewage system, laboratory, office facilities, equipment storage and maintenance facilities, roads, waste salt storage facility, and chemical raw material storage facility.

## 19 MARKETING STUDIES AND CONTRACTS

No updated marketing studies have been prepared as part of this mineral resource estimate for the Project. Detailed marketing information was provided in the project PEA prepared by Worley Parsons dated 31 August, 2018.

## 20 ENVIRONMENTAL STUDIES, PERMITTING, AND SOCIAL OR COMMUNITY IMPACT

### 20.1. Environmental studies

AAL has completed various environmental studies required to support its exploration programs between 2011 and the present. AAL has initiated baseline environmental, hydrogeological, hydrological and other studies in support of the Project EIA and the PFS planned for 2019.

The EIA will be required prior to approval for construction of any lithium brine extraction and processing plant. It is expected that the EIA for the future brine operation will be completed in parallel with the PFS.

### 20.2. Project permitting

Relevant permissions and permits for future construction and operation activities will be obtained once the EIA approval is obtained and before construction is initiated.

### 20.3. Social and community requirements

The company has been very actively involved in community relations since the properties were acquired by SAS. Although there is minimal habitation in the area of the Salar, AAL has consulted extensively with the local aboriginal communities and employs members of these communities in the current exploration activities. The EIA permitting process will address community and socio-economic issues; it is expected the project will have a positive impact through the creation of new employment opportunities and investment in the region.

## 21 CAPITAL AND OPERATING COSTS

No capital and operating costs have been prepared as part of this mineral resource estimate. AAL is currently undertaking a PFS that will be completed during 2019. Initial estimates of capital and operating costs were provided in the Project PEA prepared by Worley Parsons and dated 31 August, 2018.



## 22 ECONOMIC ANALYSIS

No economic analysis has been carried out as part of this updated mineral resource estimate. AAL is currently undertaking a PFS that will be completed during 2019. An initial economic analysis was provided in the Project PEA prepared by Worley Parsons and dated 31 August, 2018.

## 23 ADJACENT PROPERTIES

### 23.1. General comments

The Cauchari JV is located directly adjacent to two other lithium projects, the producing Olaroz lithium project (Sales de Jujuy, owned by Orocobre) and the development project owned by Lithium Americas Corp, in joint venture with major Chinese lithium producer Ganfeng.

### 23.2. Salas de Jujuy – Olaroz lithium project

The Sales de Jujuy project to the north in the Olaroz salar has a reported resource of 6.4 million tonnes of lithium carbonate equivalent and 19.3 million tonnes of potash (KCL) (Houston and Gunn, 2011). Further exploration by Sales de Jujuy (announced on 23 October 2014) also defined a significant exploration target of between 1.6 and 7.5 mt LCE underlying the resource that was defined to a depth of 200 m. That exploration target requires additional drilling to determine what can be converted into project resources and subsequently reserves. The Cauchari NW Sector discussed in this report is immediately adjacent to, and continues south from the Olaroz properties.

### 23.3. LAC exploration and development work in Salar de Cauchari

Lithium Americas Corp (LAC) owns mineral properties immediately adjacent to the AAL mineral properties in Salar de Cauchari. LAC announced (in 2018) a strategic investment and increased ownership by Ganfeng to advance its Cauchari-Olaroz Project in Jujuy. Ganfeng and LAC created a Joint Venture with equal shareholder interests. Development work is underway to construct the project with planned production of 25,000 ktpa of LCE and evaluation of an expansion to 40 ktpa. In March 2019 LAC announced an expansion of resources. M+I Resources amount to 3.38million t of lithium metal equivalent (LME) and Probable and Proven Reserves are estimated at approximately 1,499,000t of LME.

## 24 ADDITIONAL RELEVANT INFORMATION

There is no other relevant information to present as part of this updated mineral resource estimate for the Project.

## 25 INTERPRETATION AND CONCLUSIONS

Based on the analyses and interpretation of the results of the exploration work carried out on the Cauchari JV between 2011 and December 2018, the following concluding statements are prepared:

- The entire Cauchari JV area has been covered by exploratory drilling between 2011 and December 2018 at an approximate borehole density of one exploration borehole per 4 km<sup>2</sup>; it is the opinion of the author that such borehole density is appropriate for the mineral resource estimate described herein.
- The results of the drilling (25 diamond core holes and 6 rotary boreholes), 8 pumping tests and the analysis of 546 primary brine samples identify distinct brine composition and grade at specific depth intervals, showing a relatively uniform distribution of lithium bearing brines throughout the Project area to a depth of 600 m. Table 25.1 provides an overview of the Cauchari brine composition.

**Table 25.1 Average values of key components of the Cauchari brine composition (g/L)**

| K   | Li  | Mg  | Ca  | SO <sub>4</sub> | B   | Mg/Li | K/Li | (SO <sub>4</sub> +2B)/(Ca+Mg)* |
|-----|-----|-----|-----|-----------------|-----|-------|------|--------------------------------|
| 4.3 | 0.5 | 1.3 | 0.5 | 18.9            | 0.9 | 2.6   | 8.5  | 11.4                           |

\*(SO<sub>4</sub>+2B)/(Ca+Mg) is a molar ratio

- The geology of the Cauchari JV consists of permeable alluvial fan material in the NW Sector of the Project and along the eastern and western external property boundaries. This fan material grades into finer grained materials towards the center of the Salar. In the center of the Salar a clay unit has been identified near surface that overlies a thick halite unit. Deep drilling intersections in the SE Sector of the Project have identified a relatively permeable Lower Sand unit between 400 m and 600 m depth that underlies the central halite.
- The positive results of laboratory analyses suggest specific yield (or drainable porosity) values as follows: the halite unit: 0.05; fan sediments: 0.04 – 0.12; the clay unit: 0.03; and the lower sand: 0.14.
- It is the opinion of the author that the Salar geometry, brine chemistry composition and the specific yield of the Salar sediments have been adequately defined to support the Measured, Indicated and Inferred Resource estimate described in Table 25.2 and summarized in terms of mineral products in Table 25.3.
- It is recommended that further development work is carried out on the Cauchari JV Project as outlined in Section 26.

**Table 25.2 Cauchari JV Project Lithium and Potassium Resources estimate (April 19, 2019)**

|  | Measured (M)   |                  | Indicated (I)  |                  | M+I            |                  | Inferred       |                  |
|--|----------------|------------------|----------------|------------------|----------------|------------------|----------------|------------------|
| <b>Aquifer volume (km<sup>3</sup>)</b> | 10             |                  | 21             |                  | 31             |                  | 11             |                  |
| <b>Mean specific yield</b>             | 6.6%           |                  | 5.9%           |                  | 6.1%           |                  | 5.6%           |                  |
| <b>Brine volume (km<sup>3</sup>)</b>   | 0.6            |                  | 1.2            |                  | 1.9            |                  | 0.6            |                  |
| <b>Brine volume (km<sup>3</sup>)</b>   | Li             | K                | Li             | K                | Li             | K                | Li             | K                |
| <b>Mean grade (g/m<sup>3</sup>)</b>    | 35             | 291              | 26             | 238              | 29             | 255              | 27             | 225              |
| <b>Mean concentration (mg/l)</b>       | 527            | 4,438            | 452            | 4,145            | 476            | 4,238            | 473            | 3,867            |
| <b>Resource (tonnes)</b>               | <b>345,000</b> | <b>2,800,000</b> | <b>550,000</b> | <b>5,000,000</b> | <b>900,000</b> | <b>7,800,000</b> | <b>290,000</b> | <b>2,400,000</b> |

Notes to Table 25.2:

- CIM definitions were followed for mineral resources.
- The Qualified Person for this Mineral Resource estimate is Frits Reidel, CPG.
- No cut-off concentrations have been applied to the resource estimate
- Numbers may not add due to rounding.

Table 25.3 shows the Mineral Resources of the Cauchari JV Project expressed as lithium carbonate equivalent (LCE) and potash (KCl).

**Table 25.3 Cauchari JV Project Mineral Resources expressed as LCE and potash (tonnes)**

|                         | Measured (M) | Indicated (I) | M+I        | Inferred  |
|-------------------------|--------------|---------------|------------|-----------|
| Lithium Carbonate (LCE) | 1,850,000    | 2,950,000     | 4,800,000  | 1,500,000 |
| Potash (KCl)            | 5,400,000    | 9,600,000     | 14,900,000 | 4,600,000 |

Notes to Table 25.3:

- Lithium is converted to lithium carbonate (Li<sub>2</sub>CO<sub>3</sub>) with a conversion factor of 5.32.
- Potassium is converted to potash with a conversion factor of 1.91.
- Numbers may not add due to rounding.

## 26 RECOMMENDATIONS

- It is recommended that the PFS for the Cauchari JV Project is completed as planned during 2019
- It is recommended that a three-dimensional groundwater flow and transport model is constructed and calibrated for Salar de Cauchari to carry out simulations of future brine production scenarios and prepare a brine reserve estimate.
- Environmental baseline monitoring should be continued during 2019 as well as the completion of the EIA by Q3 2019.

## 27 REFERENCES

Allmendinger, R.W., Jordan, T.E., Kay, S.M., and Isacks, B.L., 1997, The Evolution of the Altiplano-Puna Plateau of the Central Andes: *Annual Review of Earth and Planetary Science*, v. 25, p. 139-174.

Alonso, R.N., Jordan, T.E., Tabbutt, K.T. and Vandevoort, D.S. 1991. Giant evaporate belts of the Neogene central Andes. *Geology*, 19: 401-404.

Burga, D., Burga, E., Genk, W., Weber, D. NI 43 – 101 Technical Report Updated Mineral Resource Estimate for the Cauchari-Olaroz Project, Jujuy Province, Argentina. Public report, March 31, 2019.

Chernicoff, C.J., Richards, J.P., and Zappettini, E.O., 2002, Crustal lineament control on magmatism and mineralization in northwestern Argentina: geological, geophysical, and remote sensing evidence: *Ore Geology Reviews*, v. 21, p. 127-155.

Coira, B., Davidson, J., Mpodozis, C., and Ramos, V., 1982, Tectonic and Magmatic Evolution of the Andes of Northern Argentina and Chile: *Earth Science Reviews*, v. 18, p. 303-332.

de Silva, S.L., 1989, Altiplano-Puna volcanic complex of the central Andes: *Geology*, v. 17, p. 1102-1106.

de Silva, S.L., Zandt, G., Trumbull, R., Viramonte, J.G., Salas, G., and Jiménez, N., 2006, Large ignimbrite eruptions and volcano-tectonic depressions in the Central Andes: a thermomechanical perspective, *in* Troise, C., De Natale, G., and Kilburn, C.R.J., eds., 2006, *Mechanisms of Activity and Unrest at Large Calderas*: Geological Society, London, Special Publication 269, p. 47-63.

Garzzone, C.N., Molnar, P., Libarkin, J.C., and MacFadden, B.J., 2006, Rapid late Miocene rise of the Bolivian Altiplano: Evidence for removal of mantle lithosphere: *Earth and Planetary Science Letters*, v. 241, p. 543-556.

Gregory-Wodzicki, K.M., 2000, Uplift history of the Central and Northern Andes: A review: *Geological Society of America Bulletin*, v. 112, p. 1091-1105.

Hartley, A.J., Chong, G., Houston, J., and Mather, A. 2005. 150 million years of climatic stability: evidence from the Atacama Desert, northern Chile. *Journal of the Geological Society, London*, 162: 421-424.

Houston, J. 2006a. Variability of Precipitation In the Atacama Desert: Its Causes and Hydrological Impact. *International Journal of Climatology* 26: 2181-2189.

Houston, J. 2006b. Evaporation in the Atacama desert: An empirical study of spatio-temporal variations and their causes. *Journal of Hydrology*, 330: 402-412.

Houston, J and Ehren, P. Technical Report on the Olaroz Project, Jujuy Province, Argentina. NI 43-101 report prepared for Orocobre Ltd, April 30, 2010a

Houston, J. Technical Report on the Cauchari Project, Jujuy-Salta Provinces, Argentina. NI 43-101 report prepared for Orocobre Ltd, April 30, 2010b

- Houston, J., Gunn, M. Technical Report on the Salar De Olaroz Lithium-Potash Project Jujuy Province, Argentina. NI 43-101 report prepared for Orocobre Ltd, May 13, 2011.
- Houston, J., Butcher, A., Ehren, P., Evans, K., and Godfrey, L. The Evaluation of Brine Prospects and the Requirement for Modifications to Filing Standards. *Economic Geology*. V 106, p 1225-1239.
- Igarzábal, A. P. 1984. Estudio geológico de los recursos mineros en salares del NOA (Puna Argentina). Proyecto de Investigación. Consejo de Investigación. Universidad Nacional de Salta
- Jordan, T.E., Alonso, R.N. 1987. Cenozoic stratigraphy and basin tectonics of the Andes Mountains, 20-28°S latitude. *American Association of Petroleum Geologists Bulletin*, 71:49-64.
- King, M. 2010. Measured, Indicated and Inferred Resource Estimation of Lithium and Potassium at the Cauchari and Olaroz Salars, Jujuy Province, Argentina. December 6, 2010.
- King, M., Kelly, R., and Abbey, D. NI 43 – 101 Technical Report Feasibility Study Reserve Estimation and Lithium Carbonate and Potash Production at the Cauchari-Olaroz Salars, Jujuy Province, Argentina. 11 July, 2012.
- Roskill Information Services. 2009. *The Economics of Lithium*. 11th ed. Roskill Information Services Ltd., 27a Leopold Road, London SW19 7BB, United Kingdom.
- Salfity, J.A., and Marquillas, R.A. 1994. Tectonic and sedimentary evolution of the Cretaceous-Eocene Salta Group basin, Argentina. In Salfity, J.A. (ed) *Cretaceous tectonics of the Andes*, Earth Evolution Series, Vieweg, Weisbaden.
- Vazques, G. L. 2011. Investigación Hidrogeológica en Salares con la Aplicación del Método Geoeléctrico Salar De Olaroz–Cauchari - Departamento Susques - Jujuy -Argentina. VII Congreso Argentino de Hidrogeología y V Seminario Hispano-Latinoamericano Sobre Temas Actuales de la Hidrología Subterránea. *Hidrogeología Regional y Exploración Hidrogeológica Salta*, Argentina, 2011.
- Worley Parsons, 2011. NI 43 - 101 Technical Report Preliminary Assessment and Economic Evaluation of the Cauchari-Olaroz Lithium Project, Jujuy Province, Argentina. 30 April, 2011.



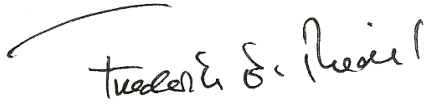
## 28 DATE AND SIGNATURE PAGE - CERTIFICATE of AUTHOR

Qualified person Frederik Reidel

I, Frederik Reidel, CPG, as author of this report entitled “NI 43-101 Technical Report: Cauchari JV Project, Updated Mineral Resource Estimate, prepared for Advantage Lithium, dated April 19, 2019 do hereby certify that:

1. I am employed as Principal Hydrogeologist and General Manager by FloSolutions-Chile, residing at: Roger de Flor 2950, Piso 5, Las Condes, Santiago, Chile.
2. I am a graduate of New Mexico Institute of Mining and Technology with a Bachelors of Science Degree in Geophysics, 1986
3. I am registered a Certified Professional Geologist (#11454) with the American Institute of Professional Geologists.
4. I have worked as hydrogeologist for a total of 31 years since my graduation. My relevant experience for the purpose of the Technical Report is:
  - Qualified Person for the Sal de los Angeles Project, Salta, Argentina for LiX Energy Corp) 2016 – to date).
  - Qualified Person and Member of the technical committees of Li3 Energy Ltd and Minera Salar Blanco for the development of the Maricunga Lithium Project in Chile (2011 – to date).
  - Co-author of the NI 43-101 Technical Reports on the lithium and potash resources in Salar de Maricunga for Li3 Energy Ltd (2012 and 2017).
  - Evaluation of lithium and potash resources in Salar de Olaroz for Orocobre Ltd. in support of the project’s DFS and NI 43-101 Technical Report (2010-2011).
  - Evaluation of lithium and potash resources in Salar de Cauchari for Lithium Americas Corporation; NI 43-101 Technical Report preparation; member of the company’s Technical Advisory Panel (2009-2010).
  - Evaluation of brine resources in Salar de Hombre Muerto for FMC (1992-1993)
  - Consulting hydrogeologist in the evaluation and development of groundwater resources for international mining companies in North- and South America (1989-2012).
5. I have read the definition of "qualified person" set out in National Instrument 43-101 (NI 43-101) and certify that by reason of my education, affiliation with a professional association (as defined in NI 43-101) and past relevant work experience, I fulfill the requirements to be a "qualified person" for the purposes of NI 43-101.
6. I have visited the Cauchari JV Project and the project area numerous times between August 2011 and to date. I was present on site on a regular basis during the 2017/8 drilling and testing programs.
7. I have been involved as a QP with the property since 2017, but have no previous involvement with Advantage Lithium Corp.
8. I am responsible for the overall preparation of this report.
9. I am independent of the Issuer applying the test set out in Section 1.4 of NI 43-101.
10. I have read NI 43-101, and the Technical Report has been prepared in compliance with NI 43-101 and Form 43-101F1.
11. To the best of my knowledge, information, and belief, the Technical Report contains all scientific and technical information that is required to be disclosed to make the technical report not misleading.

Dated this 19th day of April , 2019

A handwritten signature in black ink, reading "Frederik S. Reidel". The signature is written in a cursive style with a long, sweeping horizontal line above the first few letters.

Frederik Reidel, CPG